HEAT GAIN FROM POWER PANELBOARD

by

EMILIO C. PIESCIOROVSKY

E. E., National Technological University, Argentina, 1998
M. Mktg, National University of La Plata, Argentina, 2001

A THESIS

submitted in partial fulfillment of the requirements for the degree

MASTER OF SCIENCE

Department of Electrical and Computer Engineering
College of Engineering

KANSAS STATE UNIVERSITY
Manhattan, Kansas

2009

Approved by;

Co-Major Professor
Dr. Warren N. White

Approved by;

Co-Major Professor
Dr. Anil Pahwa

Abstract

This thesis focuses on estimating the power loss from power panelboards by means of power loss models. The model is intended to be used by HVAC engineers to help estimate building heat loss. While McDonald & Hickok (1985) did not report power losses for power panelboards, Rubin (1979) did. These publications present the power losses of electrical devices at rated loads in tables. In this thesis, the models for electrical devices are created and used, instead of tables, to estimate power losses. The use of curve fit models presents a convenience in calculation of power losses.

Breaker, fusible switch, and motor starter power losses presented by McDonald & Hickok (1985) and Rubin (1979) were updated using manufacturer published data, technical papers, industrial standards, and test samples. Test, manufacturer, and analytical model data are collected and power loss curve fit models are created for breakers, fusible switches, motor starters, and bus bars with enclosures. The panelboard power loss is calculated as the sum of partial power losses of the component electrical equipment, i.e. breakers, fusible switches, motor starters, and bus bars with enclosures used in power panelboards.

A power loss model for main breaker and fusible switch power panelboards are created based on the sum of breaker, fusible switch, motor starter, and bus bars with enclosure power loss models. The main breaker and fusible switch power panelboard power loss models are used in a heat loss example. It is shown that power panelboard power losses can be significantly overestimated when calculated with one of the methods currently used (Rubin, 1979). This can result in erroneous sizing of HVAC equipment.

Table of Contents

List of Figures

List of Tables

Acknowledgements

I would like to thank to Dr. Anil Pahwa from the Department of Electrical and Computer Engineering (ECE) and Dr. Warren N. White from the Department of Mechanical and Nuclear Engineering (MNE). Dr. Pahwa was my advisor and he opened the first door at Kansas State University (KSU) for me. Dr. White was the professor and advisor with whom I worked on heat gain from electrical equipment including power panelboards. I would also want to thank the American Society of Heating Refrigeration and Air Conditioning Engineers (ASHRAE) for funding this work, especially TC 9.2 Industrial Air Conditioning and TC 9.1 Large Building Air Conditioning Systems.

A special thanks to Dr. White because I learned important things with him during this time at KSU. I wrote my first technical paper and report in English, and I presented my first paper in a conference (2009 ASHRAE, Louisville, Kentucky). The experience gained during this time was very important for me and I will never forget the support and advice from Drs. White and Pahwa, who gave me the chance to acquire new experiences and knowledge improving my professional background. I also want to thank my wife, Dr. Maria S. Ferrer, for supporting me during my masters program when I studied for some courses or worked on my research during long nights and weekends at home.

CHAPTER 1 - Introduction

To size heating, ventilation, and air conditioning (HVAC) equipment, HVAC designers must estimate with certainty the amount of energy released into the environment from various heat sources and lost through various heat sinks located in a room. Heat could be released from several sources, such as the presence of many people in a classroom or office, solar radiation through windows, and electrical equipment. A sink could consist of outside doors and windows in winter or a basement floor or wall that remains at an essentially constant temperature throughout the year. Estimating the total amount of electrical power equipment rejected heat is a necessary part of sizing the heating and refrigeration equipment required for the building. By closely estimating the heat gain or loss, the HVAC equipment would not be undersized with insufficient capacity or oversized with costly, unutilized, excess capability.

Building and industrial plants make use of electrical power for many applications such as lighting, driving motorized devices, HVAC, and energy transmission and distribution throughout the structure. The electrical equipment installed in a room is a heat source and a great variety of equipment exists such as panelboards, switchboards, motor control centers, and switchgear.

The National Electrical Code (NEC) defines a panelboard as a "single panel or group of panel units designed for assembly in the form of a single panel, including buses, automatic overcurrent devices, and equipped with or without switches for the control of light, heat, or power circuits; designed to be placed in a cabinet or cutout box placed in or against a wall, partition, or other support; and accessible only from the front," (NEC, Article 100-definitions).

Panelboards are classified according to their applications into lighting and power panelboards. Lighting panelboards are only used in light control applications and power panelboards are used not only in light but also heat or power circuits (motor applications). The ampere rating of a power panelboard is usually higher than a lighting panelboard. This thesis focuses on estimating power losses from power panelboards which distribute currents greater than those found in lighting panelboards.

The primary sources of information available for the design engineers for estimating the electrical equipment rejected power losses are the publications by McDonald & Hickok (1985) and Rubin (1979). McDonald & Hickok (1985) reported the power losses for lighting panelboards as 0.8 watts/amp, single- or three-phase buses, based on a mixture of 15, 20, and 30

amps circuits, but did not report any data for power panelboards. Rubin (1979) reported the same power losses for lighting and power panelboards based on the number of single pole circuit breakers as shown in Table 1.1.

Table 1.1: Power and Lighting Panelboards Power Losses (Rubin, 1979)

Number of Single Pole Circuit Breakers	Power Losses [watts]
12	150
24	300
36	450
42	500

Also, McDonald & Hickok (1985) and Rubin (1979) reported some power losses at rated loads for breakers, fusible switches, and National Electrical Manufacturers Association (NEMA) motor starters, which are used in power panelboards. The publications by McDonald & Hickok (1985) and Rubin (1979) are based on tables that present the power losses at rated loads for breakers, fusible switches, and NEMA motor starters. In these tables, the power loss corresponds to the ampere rating of the unit. When a rating is not listed in these tables, a linear interpolation is applied between two known power loss values. In this linear interpolation, inaccuracy can occur if the power loss does not vary linearly. Tables may not be a convenient method to estimate power losses when the devices are not operated at rated loads.

Power loss data for breakers up to 1200 amps, fusible switches up to 600 amps, and NEMA 0, 1, 2 and 3 motor starters presented by McDonald & Hickok (1985) and Rubin (1979) are dated because they used information from manufacturer publications, technical papers, industrial standards, and test data from the late 1970s to early 1980s.

The power loss models for breakers and NEMA motor starters will be created from power loss data from tests, while the power loss models for fuses and fusible switches will be created from manufacturer power loss data. A comparison between calculated power losses and the data from McDonald and Hickok (1985) and Rubin (1979) will be done for breakers, fusible switches and NEMA motor starters.

No bus bar power loss measurements will be shown in this thesis. To measure the power loss in the bars with the three phase data logging watt meter used in this study, it is necessary to attach voltage leads to either end of a section of a bus as shown in Figure 1.1. The voltage drop along the bar would be small and the voltage leads and conductor constitute a closed path that

would have a flux linkage created by the high current bus bars. The concern is that the changing magnetic field created by the bus bars would induce a voltage in the loop created by the voltage leads and the conductor, thus rendering the measured voltage and the associated power loss suspicious.

Because of these measurement difficulties, analytical models will be developed for the three phase bus bars based on White and Piesciorovsky (2009) and the enclosure based on Del Vecchio (2003). These two models will be presented in a later section. The bus bar with enclosure or enclosure-bus bar, as it will be subsequently called, will be estimated by the sum of these two models.

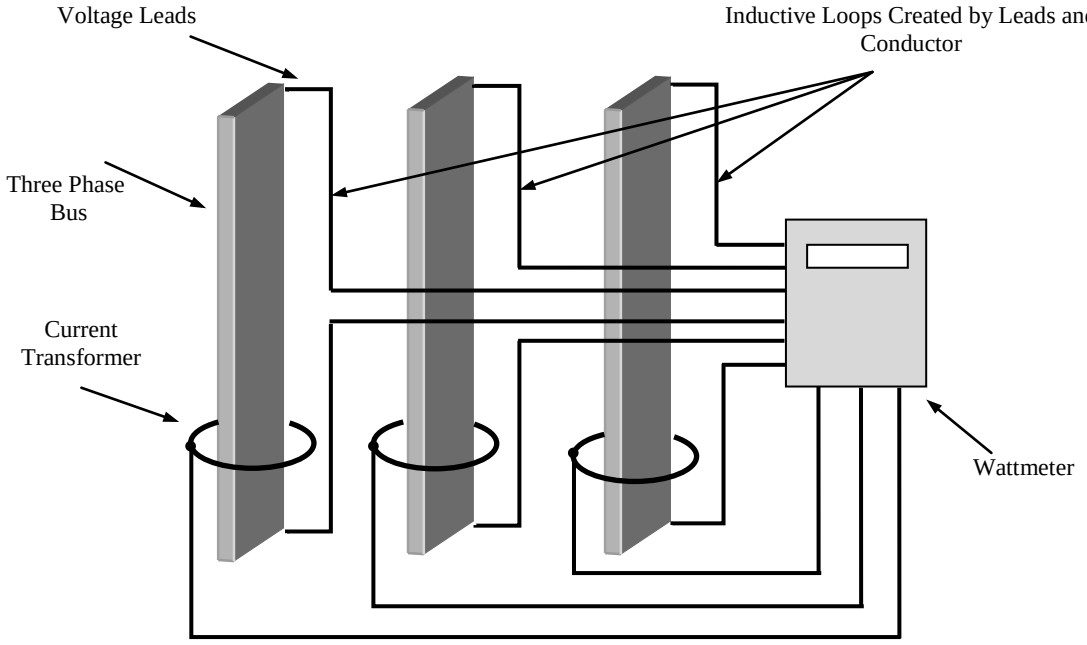

Figure 1.1: Three Phase Bus Bars with Wattmeter Connection

No enclosure-bus bar power loss data for panelboards were reported by McDonald & Hickok (1985) and Rubin (1979). However, these two papers reported power losses at rated loads for 600 volts copper bus-ways that will be compared with the calculated panelboard enclosure-bus bar power losses at rated loads.

Finally, a power loss model for main breaker and fusible switch power panelboards will be found based on the sum of the breaker, fusible switch, motor starter, and enclosure-bus bar power loss models.

A heat loss example will be presented using the main breaker and fusible switch panelboard power loss models. The result will be compared to the traditional method for estimating losses, namely the paper by Rubin (1979).

A summary of this thesis is shown in Table 1.2. The range of electrical equipment, model and non-model collected data, and power loss model equations are shown for breakers, fusible switches, motor starters, enclosure-bus bars, and power panelboards.

Table 1.2: Executive Summary. Range of Electrical Equipment, Model and Non-Model Collected Data, and Power Loss Model Equations for Electrical Equipment.

Electrical Equipment	Equipment Range	Model Collected Data	Non-Model Collected Data	Power Loss Model Equations (Balanced 3 Phase Currents)
Breakers	Maximum Voltage Rating: 600 VAC Maximum Ampere Rating: 1200 amps Three Poles	Test power losses	The calculated breaker losses are compared with McDonald & Hickok (1985), and Rubin (1979) data in Figures 2.1 and 2.2; and manufacturer data in Figure 2.3.	Equation (2.4)
Fusible Switches	**1) Fuses:** Maximum Voltage Rating: 690 VAC Maximum Ampere Rating: 630 amps Single Pole **2) Switches:** Maximum Voltage Rating: 1000 VAC Maximum Ampere Rating: 600 amps Three Poles	Manufacturer data	The calculated fuses losses are compared with the IEC-60269-2-2006 Std in Figures 3.1 and 3.2. The calculated fusible switch losses are compared with McDonald & Hickok (1985), and Rubin (1979) data in Figure 3.4; and test data in Figure 3.5.	Equations (3.9) and (3.10)
Motor Starters	Fusible Switch Motor Starters NEMA sizes: 0, 1, 2 and 3 Type : Full Voltage Non-reversing (FVNR) Maximum horsepower: 50 hp	Test power losses	The calculated motor starter losses are compared with McDonald & Hickok (1985), Rubin (1979) data in Figure 4.8; and manufacturer data in Figure 4.9.	Equations (4.5), (4.6), (4.7), and (4.8)
Enclosure and Bus bars	**1) Enclosure:** Galvanized steel sheet 1.74 and 2.74 mm box thick **2) Bus bars:** Copper (conductivity of 98.9 % IACS) 1000 amps/inch^2 (155 amps/cm^2) Ampere ratings: 250, 400, 600, 800 and 1200 amps	**1) Enclsosure:** Analytical model (Del Vecchio, 2003). **2)Three phase bus bars:** Analytical model (White, 2009)	The calculated enclosure-bus bar losses are compared with McDonald & Hickok (1985) data in Figure 5.6.	Equation (5.7)
Power Panelboard	Max. voltage rating: 600 volts Ampere ratings: 250, 400, 600, 800 and 1200 amps	Test, manufacturer and analytical model data	The calculated panelboard losses are compared with Rubin (1979) in the example of Chapter 6.	Equations (6.3) and (6.4)

VAC=Volts Alternating Current, IACS=International Annealed Copper Standar

CHAPTER 2 - Molded Case Circuit Breakers

The objective of this chapter is to create a power loss model to estimate the power losses of molded case circuit breakers (MCCBs) at a given breaker load. A description of the equipment will be given. The steps used to create the curve fit model of breaker power losses are (1) collection of test power loss data, (2) creation of a curve fit model of breaker power losses at rated loads based on collected data, (3) comparison of the curve fit model of breaker power losses at rated loads with independent data for verification, and (4) creation of the curve fit model of breaker power losses at any load. Finally, the model is used to estimate the power losses of three breakers.

Electrical Equipment Description

There are different types of low voltage circuit breakers that are used in power distribution systems. These low voltage circuit breakers can be segregated into three types, which are molded case circuit breakers (MCCB), insulated case circuit breakers (ICCB), and low voltage power circuit breakers (LVPCB). Table 2.1 shows the characteristics of low voltage circuit breakers.

Table 2.1: Low Voltage Circuit Breaker Characteristics

Characteristics	Molded case circuit breakers (MCCB)	Insulated case circuit breakers (ICCB)	Low voltage power circuit breakers (LVPCB)
Application	Panelboards Switchboards Motor Control Centers	Switchboards Motor Control Centers	Switchgears Switchboards
Mounting	Fixed Mounted	Draw out Mounted and Fixed Mounted	Draw out Mounted
Ampere Ratings	up to 2500 Amperes	400 to 5000 Amperes	800 to 5000 Amperes
Trip Mechanism	Thermal magnetic trip	Solid state trip with time current curve characteristics	Solid state trip with a great range of time current curve characteristics
Standards	UL 489-1996 IEEE- 1458-2005	UL 489-1996	UL 1066-1997

The MCCB is a control and protection device. The breakers used in power panelboards are molded case circuit breakers (MCCB) and have a maximum voltage rating of 600 VAC and an ampere rating of up to 1200 amps.

Power Loss - Collected Data and Results

In this study, test data was collected on molded case circuit breakers. These data are listed in Table 2.2. The apparatus shown in Appendix A was used to collect the data. Power measurements were sampled regularly over a period of several minutes. At each sample point, the resistance of each breaker phase was calculated and averaged. The resistance at each point in time was calculated by

$$R = (Ratio \times P_p) / (I)^2 \tag{2.1}$$

where R is the resistance per phase, *Ratio* is the potential transformer turns ratio (1/60), P_p is the power loss per phase in watts, and I is the current per phase in amperes.

The average resistance per phase was determined. These resistances are denoted by Ra_{Avg}, Rb_{Avg}, and Rc_{Avg}. The total power loss at rated load is given by

$$P = I^2 \times \left(Ra_{Avg} + Rb_{Avg} + Rb_{Avg}\right) \tag{2.2}$$

where I is the rated phase current in the panelboard circuit. The results of these calculations are listed in Table 2.2. These circuit breaker resistances included the enclosure and lug resistances of the breakers because the breakers were connected in the panelboards when the tests were made.

Table 2.2: Molded Case Circuit Breakers Tested in Panelboards at KSU

Case	Amperes Rating "I"	Test Sample Name (Excel File)	Ra_{Avg} [ohms]	Rb_{Avg} [ohms]	Rc_{Avg} [ohms]	3 Phase Resistance "R_T" [ohms]	3 Phase Power Loss [watts]
1	70	70ampbreakermeasurementsSouthElevato	0.001433	0.001516	0.001357	0.004308	21.11
2	175	175ampbreakermeasurementsA022307	0.000466	0.000647	0.000456	0.001569	48.08
3	200	200ampbreakermeasurements022307	0.000322	0.000627	0.000566	0.001515	60.63
4	225	225ampbreakermeasurementsAckert0508	0.000489	0.000582	0.000628	0.001700	86.06
5	400	400ampbreakerBmeasurementsAckert050	0.000154	0.000168	0.000288	0.000611	97.84
6	450	450ampbreakermeasurementsAckert0508	0.000187	0.000228	0.000124	0.000540	109.37
7	1000	1000ampbreakermeasurementsAckert060	0.000058	0.000079	0.000104	0.000242	242.32
8	200	200-Aampbreakermeasurements022307	0.000430	0.000836	0.000366	0.001633	65.34
9	200	200ampbreakermeasurementsA022307	0.000326	0.000624	0.000565	0.001516	60.65
10	250	250ampbreakermeasurements022307	0.000493	0.000340	0.000673	0.001507	94.20
11	300	300ampbreakerCmeasurementsAckert060	0.000369	0.000036	0.000445	0.000851	76.61
12	350	350ampbreakermeasurementsAckert0516	0.000227	0.000098	0.000333	0.000659	80.79
13	400	400ampbreakermeasurementsAckert0508	0.000129	0.000053	0.000194	0.000378	60.48
14	600	600ampbreakermeasurement081406	0.000122	0.000150	0.000122	0.000395	142.24
15	1200	1200abreakermeasurementsAckert050807	0.000073	0.000062	0.000102	0.000238	344.02
16	175	175ampbreakermeasurements022307	0.000466	0.000639	0.000458	0.001565	47.93
17	200	200-AampbreakermeasurementsA022307	0.000430	0.000834	0.000365	0.001630	65.22
18	200	200ampbreakermeasurementsAckert0525	0.000382	0.000351	0.000303	0.001037	41.50
19	250	250ampbreakermeasurementsA022307	0.000493	0.000342	0.000667	0.001503	93.98
20	400	400ampbreakerAmeasurementsAckert050	0.000465	0.000295	0.000417	0.001179	188.66
21	400	400ampbreakermeasurementsAckert0521	0.000165	0.000183	0.000210	0.000558	89.38
22	800	800ampbreakermeasurementsAckert0525	0.000060	0.000105	0.000133	0.000299	191.72

A comparison of power loss at rated loads of the tested molded case circuit breakers with those reported by McDonald & Hickok (1985) and Rubin (1979) is shown in Figure 2.1. The comparison was made for breaker frames up to 1200 amps. The test breaker power losses shown in the last column of Table 2.2 were fitted with the curve

$$P_{br} = 0.2658 \times I_{br} \tag{2.3}$$

where P_{br} is the breaker power loss at rated loads in watts and I_{br} is the breaker frame ampere rating.

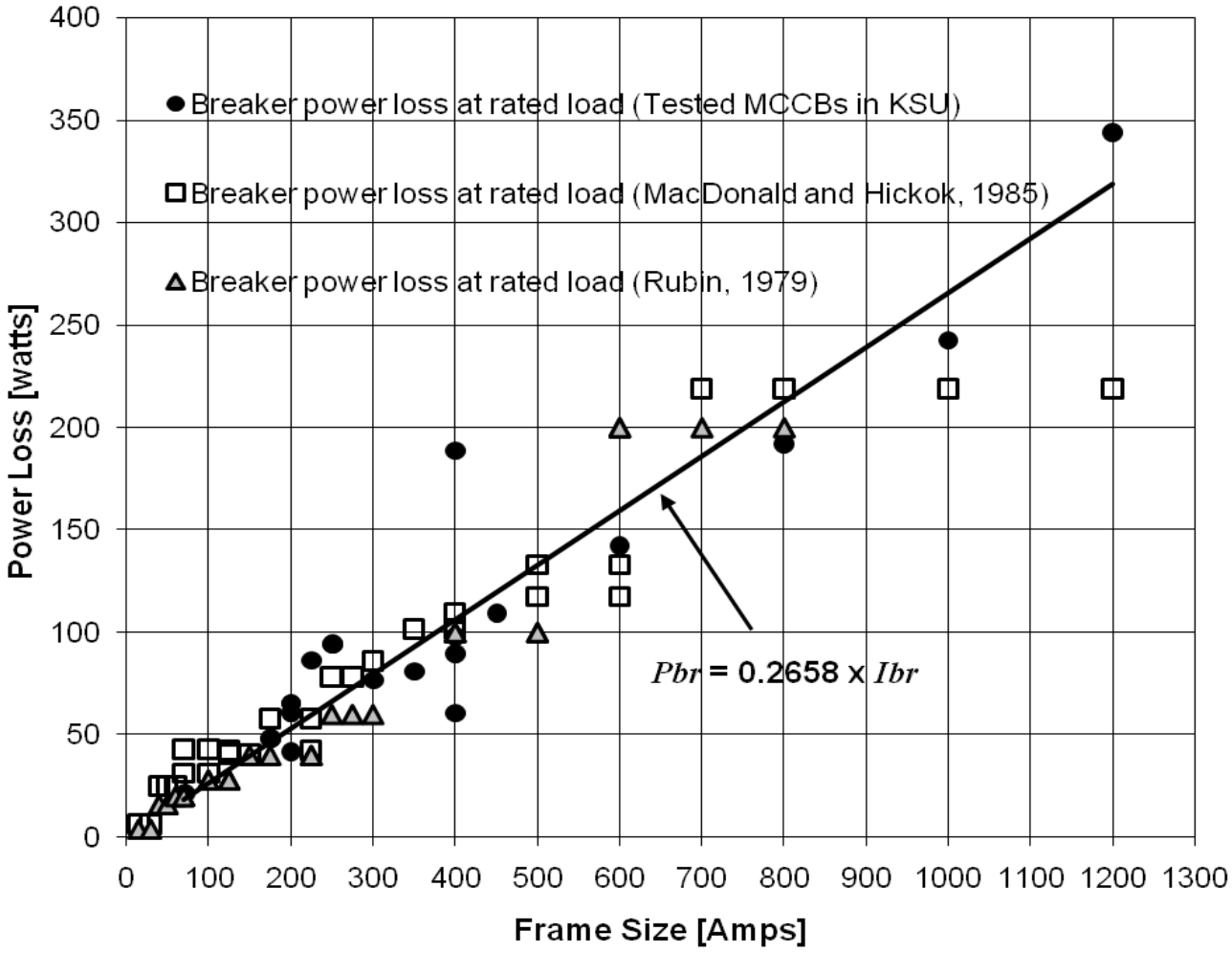

Figure 2.1: Comparison of Breaker Power Losses at Rated Loads

The power losses at rated loads of the tested breakers together with those reported by McDonald & Hickok (1985) and Rubin (1979) are shown in Figure 2.1 and each data set is fitted with a curve fit. Figure 2.2 shows the three fits. In Figure 2.2, the test data match with the published data for breaker frame sizes below 600 amps.

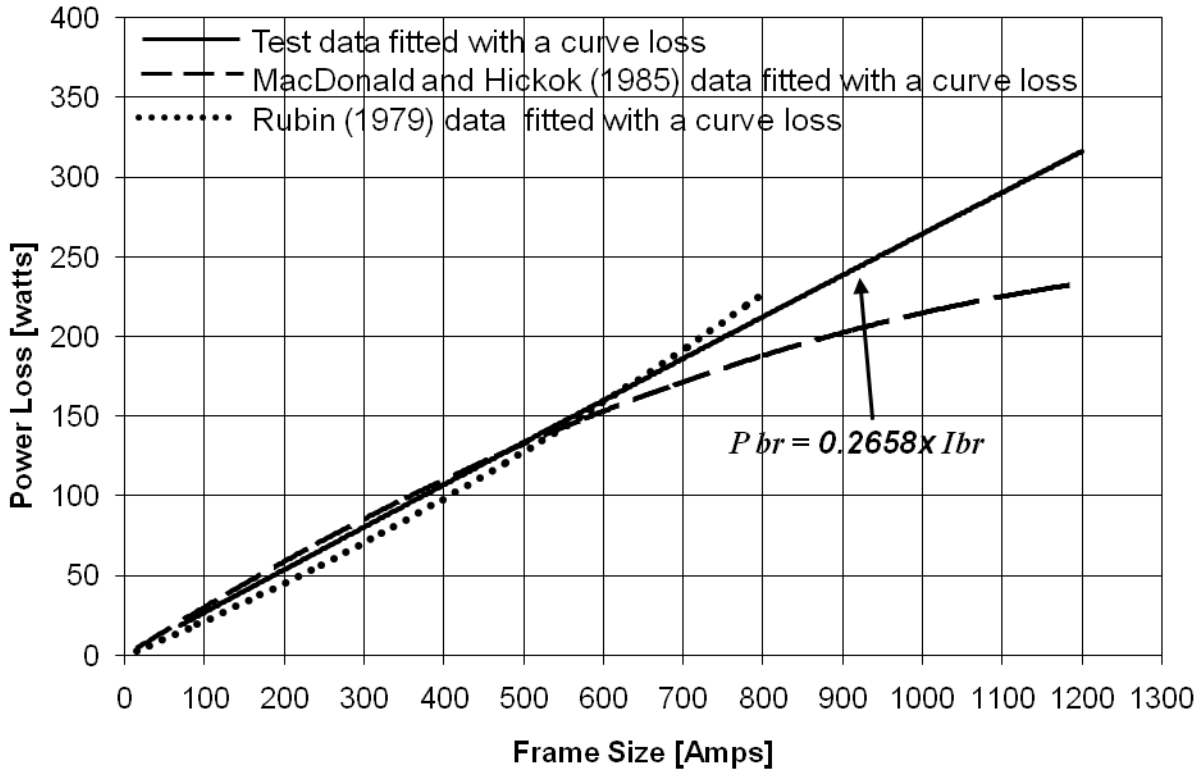

Figure 2.2: Comparison of Breaker Power Loss Curve Fits

A second comparison is made using updated data. Table 2.3 shows breaker power losses published in manufacturer literature. The comparison of the power losses at rated loads of the tested molded case circuit breakers with those published in Siemens and Asea Brown Boveri literature is shown in Figure 2.3.

Table 2.3: Breaker Power Losses from Manufacturer Literature

Manufacturer	Frame Size-Amps	Breaker Power Loss (3 Poles) [watts]	Manufacturer	Frame Size-Amps	Breaker Power Loss (3 Poles) [watts]	Manufacturer	Frame Size-Amps	Breaker Power Loss (3 Poles) [watts]
Asea Brown Boveri	15	10.8	Asea Brown Boveri	60	23.1	Asea Brown Boveri	175	27.6
	15	9.6		60	11.7		175	34.8
	15	3.9		60	13.8		200	29.7
	15	3.0		70	13.8		200	39.6
	20	10.8		70	12.6		200	29.7
	20	9.6		70	14.1		200	39.6
	20	3.9		70	15.9		220	36
	20	5.1		80	13.8		225	40.5
	25	9.9		80	18		225	45
	25	6		80	14.4		250	41.1
	25	4.8		80	16.2		300	36.9
	30	10.8		90	22.8		400	58.5
	30	10.5		90	15		600	120.3
	30	5.4		90	20.7		600	91.8
	30	7.2		90	18.3		800	93

Table 2.3 (cont.)

Manufacturer	Frame Size-Amps	Breaker Power Loss (3 Poles) [watts]	Manufacturer	Frame Size-Amps	Breaker Power Loss (3 Poles) [watts]	Manufacturer	Frame Size-Amps	Breaker Power Loss (3 Poles) [watts]
Asea Brown Boveri	35	14.4	Asea Brown Boveri	100	15.6	Siemens	150	15
	35	9		100	21		150	48
	40	11.4		100	15.9		250	32
	40	18.9		100	20.4		250	80
	40	8.4		100	23.1		400	60
	40	7.8		125	17.1		400	175
	50	11.7		125	19.8		600	85
	50	15.9		125	20.1		600	230
	50	9.6		150	20.7		800	170
	50	11.1		150	26.4		800	250
				150	22.2			

In Table 2.3, all MCCBs have thermal magnetic trip

The manufacturer data of Table 2.2 was fitted with a curve and compared with the breaker power loss model, equation (2.3). This comparison is shown in Figure 2.3.

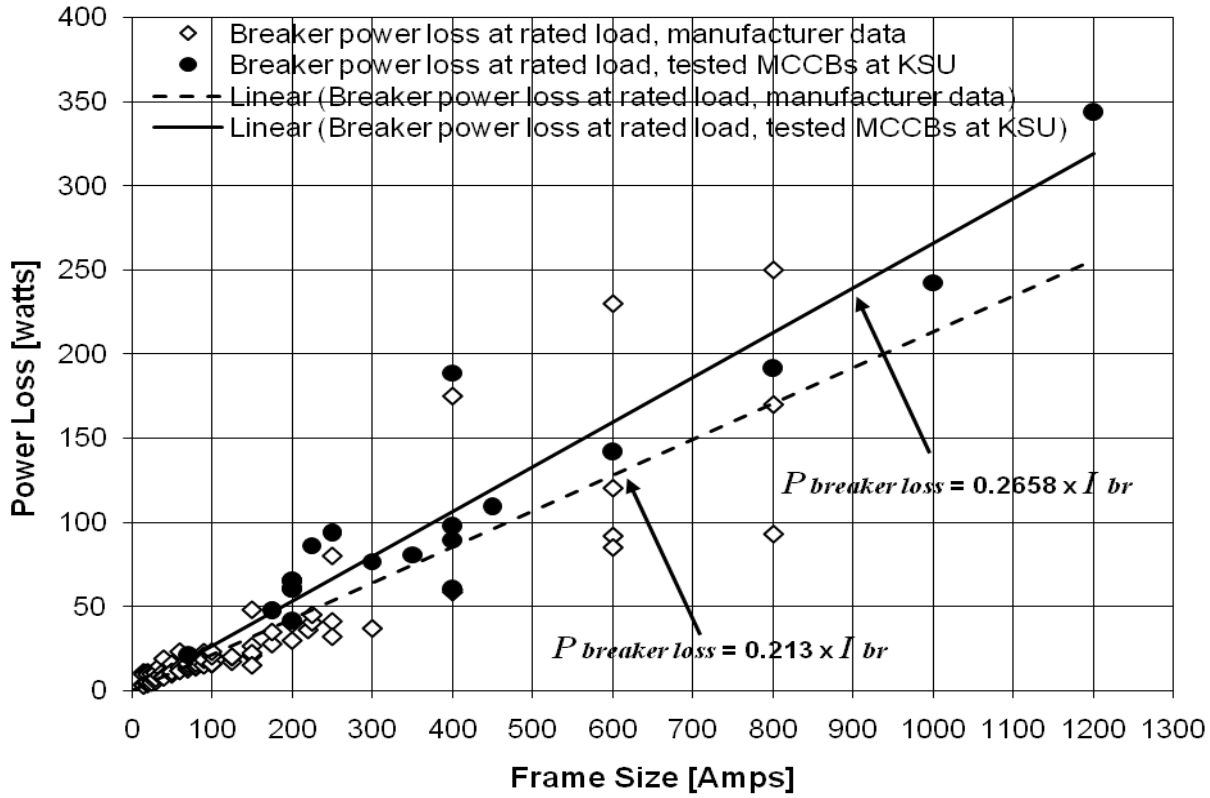

Figure 2.3: Comparison of Breaker Power Loss Model with Manufacturer Values

Balanced Three Phase Power Loss Model

The model of breaker power loss at any load can be determined by the scaling load factor , $K_{b\ load}$, times the power loss at rated load, P_{br}. The power loss of a breaker at any load can be determined by

$$\begin{aligned} P_{breaker\_loss} &= K_{b\_load} \times P_{br} \\ &= \left((Df \times I)/I_{br}\right)^2 \times P_{br} \\ &= \left(Df \times I\right)^2 \times \left(0.2658/I_{br}\right) \end{aligned} \tag{2.4}$$

where $P_{breaker\ loss}$ is breaker power loss in watts, I is the breaker phase current in amperes, and Df is the diversity factor.

The diversity factor is given by the following calculation. The load will usually vary in a cyclic manner during a period of time. The current flowing through the breaker is averaged so that over the same time span the average current adds the same amount of heat to the environment. If it is expected that the breaker would have a low current, I_L, in amps flowing during a length of time, T_1, and a high current, I_H, in amps flowing during a length of time, T_2, then the average current, I_{AVE}, in amps can be determined by

$$I_{AVE} = \sqrt{\frac{T_1 \times I^2_L + T_2 \times I^2_H}{T_1 + T_2}} \tag{2.5}$$

which can be thought of as the average RMS current.

The load diversity factor is defined by

$$Df = \frac{I_{AVE}}{I_H} = \frac{\sqrt{\dfrac{T_1 \times I^2_L + T_2 \times I^2_H}{T_1 + T_2}}}{I_H}. \tag{2.6}$$

The load diversity factor is equal to 1 (100%) for full load applications, 0.8 (80%) for commercial applications, and 0.5 (50%) for critical applications. These numbers were reported in White et al. (2004b).

To illustrate the use of equation (2.4), it was applied to three 60, 100 and 225 amps breaker frame sizes. Figure 2.4 shows the breaker power losses in watts at different load currents for a diversity factor equal to 0.8. The breaker power loss curves show a parabolic variation as a function of the current.

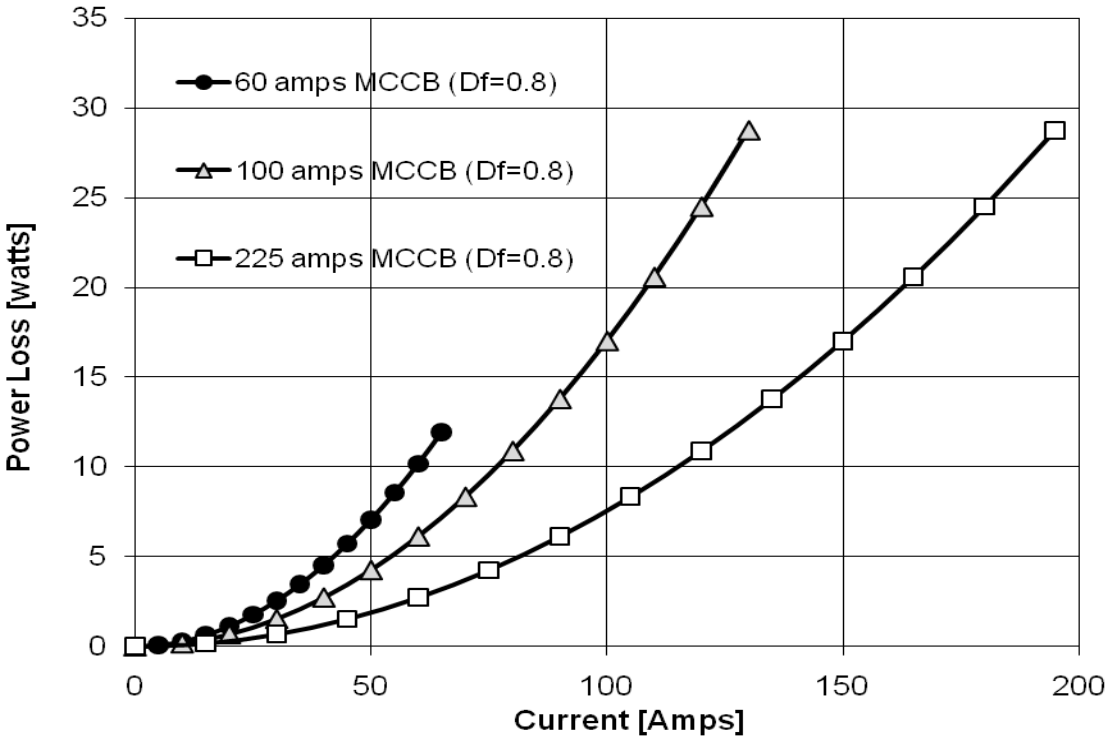

Figure 2.4: Molded Case Circuit Breakers. Power Losses by Equation (2.4)

Chapter Summary

The model of breaker power loss at any load provided by equation (2.4) was based on test data. The calculated breaker power losses at rated loads from equation (2.3) were compared with power losses at rated loads reported by McDonald & Hickok (1985) and Rubin (1979) in Figures 2.1 and 2.2. In Figure 2.2, the calculated breaker power losses agreed with the data published for breaker frame sizes below 600 amps. A second comparison was made using updated data obtained from manufacturer literature in Figure 2.3. As an example, equation (2.4) was applied to 60, 100, and 225 amps breaker frame sizes for a diversity factor of 0.8. The breaker power loss curves showed a parabolic variation of the breaker power loss with respect to the current as shown in Figure 2.4.

CHAPTER 3 – Fusible Switches

The objective of this chapter is to find models to estimate the power losses in low voltage general and motor application fusible switches used in power panelboards. The steps used to create the model for the fusible switch power losses are (1) collecting manufacturer fuse and switch power loss data for rated loads, (2) fitting the data, (3) comparing the fitted power loss with independent data for verification, and (4) creating power loss models for any load. Finally, power loss models at any load are used to estimate the power losses of three general and three motor application fusible switches.

Electrical Equipment Description

The low voltage fusible switches used in power panelboards are formed by a three-pole disconnect switch and three low voltage fuses. The low voltage fusible switch is inside of a metallic box. In the fusible switch, the switch works as a disconnecting device and the fuses work as a protection device. The low voltage switches in power panelboards are three-pole devices that are rated up to 1000 VAC and up to 600 amps. The low voltage switches are always used with fuses that protect the main elements of the circuit such as cables, heaters, motors, and lighting from overloads. The low voltage fuses in power panelboards are single pole devices that are rated up to 1000 VAC and up to 600 amps. The low voltage fuse is a protective device that is connected in series with the circuit being protected. The main component of a typical low-voltage fuse is the fuse-element or wire. The interruption time of the fuse depends on the sum of the melting and arcing time. The interruption time of the fuse is inversely proportional to the current. The low voltage fuses are designed, manufactured, and tested according to Underwriters Laboratories (UL) or International Electrotechnical Commission (IEC) standards. They are classified based on their fuse voltage rating, ampere rating (nominal and interrupting current), shape, and applications which are motor, conductor, or lighting. The low voltage fuse classification according to the IEC and UL standards is shown in Table 3.1.

Table 3.1: Low Voltage Fuse Classification according to the IEC and UL Standards

Low Voltage Fuse Classification according to the IEC Standards		
Fuse Type	**Standard**	**Typical Application**
gG	IEC 60269-2-2006	General purpose fuses essentially for conductor protection
Gm		Motor protection applications
aM		Motor circuits protection against short circuit only (these fuses cannot be used as overload protection by motor starting operating)
gN		Conductor protection
gD		General purpose time-delay fuses for motor circuit protection and conductor protection
aR		Semiconductor protection
gTr		Transformer protection
gR, gS		Semiconductor protection and conductor protection
Low Voltage Fuse Classification according to the UL Standards		
Fuse Class	**Standard**	**Typical Application**
L	UL 248-10-2000	Transformers, main feeders
K	UL 248-9-2000	Motors, main feeders, and load centers
RK1	UL 248-12-2000	Branch, feeder circuits, motors, and transformers
RK5		
J	UL 248-8-2000	
CC	UL 248-4-2000	Street lighting, lighting ballasts, heating, motor control circuits, small motors or transformer circuits, and general purpose
G	UL 248-5-2000	Small motors and transformers and general purpose
T	UL 248-15-2000	Heating and lighting circuits (residential use)
K5	UL 248-9-2000	Motor, branch circuits
H	UL 248-6-2000 UL 248-7-2000 UL 248-9-2000	Residential use

Power Loss - Collected Data and Results

During this study, fuse and switch power losses corresponding to rated loads were collected from manufacturer documents to provide data for the curve fit power loss models for

fusible switches. Using these curve fit models, the fusible switch power loss at any load is determined.

Fuse power losses corresponding to rated loads for general (gG) and motor (aM) application up to 630 ampere and 690 VAC ratings were collected from more than 50 publications from Ferraz Shawmut and Cooper Bussmann as shown in Table 3.2. The low voltage fuse power losses were compiled and the fuse power loss data were segregated according to general (gG) and motor (aM) applications. Manufacturer data is shown in Table 3.2. Table 3.3 shows the maximum power loss for low voltage fuses according to the standard IEC 60269-2-2006. Figure 3.1 shows the general application loss results from manufacturers and the IEC standard. Figure 3.2 shows the same information for motor application.

Table 3.2: Low Voltage Fuse Power Losses and Resistances from Manufacturers

Ampere Ratings	gG-660VAC-Bolted Fuse		gG-550VAC-Bolted Fuse		gG-240VAC-Bolted Fuse		aM-690VAC-Cylindrical Fuse		aM-690VAC-NH Size Fuse		aM-550VAC-Bolted Fuse		aM-415VAC-Bolted Fuse	
	watts	uΩ	watts	uΩ	watts	uΩ	watts	uΩ	watts	uΩ	watts	uΩ	watts	uΩ
1							0.1	100000						
2	1.5	375000	1.2	300000	0.5	125000	0.3	75000						
4	2.7	168750	1.4	87500	1	62500	0.5	31250						
6	3.3	91667	1.8	50000	1.6	44444	0.6	16667						
8							0.8	12500						
10	2.8	28000	2.4	24000	1.2	12000	1	10000						
12							1.2	8333						
16	2.8	10938	2.9	11328	1.5	5859	1.5	5859	1.1	4297				
20	2.7	6750	3.1	7750	1.7	4250	1.8	4500	1.4	3500				
25	3.1	4960	3.2	5120	1.8	2880	2	3200	1.7	2720	1.6	2560		
32	3.3	3223	3.5	3418	2.4	2344	2.6	2539	2.2	2148	1.1	1074		
35	0								2.4	1959			1.9	1551
40	4	2500	4.7	2938			3.2	2000	2.8	1750	3	1875	1.4	875
50	4.8	1920	4.9	1960			3.9	1560	3.6	1440	2	800	1	400
63	5.7	1436	5.6	1411			4.7	1184	4.6	1159	4.4	1109		
80	7.2	1125	7.2	1125			5.9	922	6	938	4.4	688	3.4	531
100	8.2	820	8.5	850			6.5	650	7.5	750	3.4	340	6.5	650
125	11	704					9.5	608	9.5	608			6.5	416
160	13	508							12.7	496			5	195
200	15.5	388							18	450			3.5	88
224									21.5	428				
250	19	304							29	464			11	176
315	25	252							29	292			9	91
355	19	151							32	254				
400	25	156							34	213			15	94
425									38.5	213				
450	32	158												
500	38	152							45	180	27	108	24	96
560	43	137												
630	50	126							60	151				

Table 3.3: Maximum Power Losses at Rated Currents in Fuses (IEC-60269-2-2006)

Ampere Ratings [Amps]	Fuse Shape	Type of Fuse	Maximum Power Loss [watts]
25	cylindrical	gG-400 to 690	3
40	cylindrical	gG-400 to 690	5
100	cylindrical	gG-400 to 690	9.5
16	cylindrical	aM -400 to 690	1.2
50	cylindrical	aM -400 to 690	3
100	cylindrical	aM -400 to 690	7
100	cube (NH)	gG –aM-660	12
160	cube (NH)	gG –aM-660	25
250	cube (NH)	gG –aM-660	32
400	cube (NH)	gG –aM-660	45
630	cube (NH)	gG –aM-660	60
100	cube (NH)	gG –aM-500	7.5
160	cube (NH)	gG –aM-500	16
250	cube (NH)	gG –aM-500	23
400	cube (NH)	gG –aM-500	34
630	cube (NH)	gG –aM-500	48

NH: Blade style fuses according to the IEC-60269-2-2006 Std.

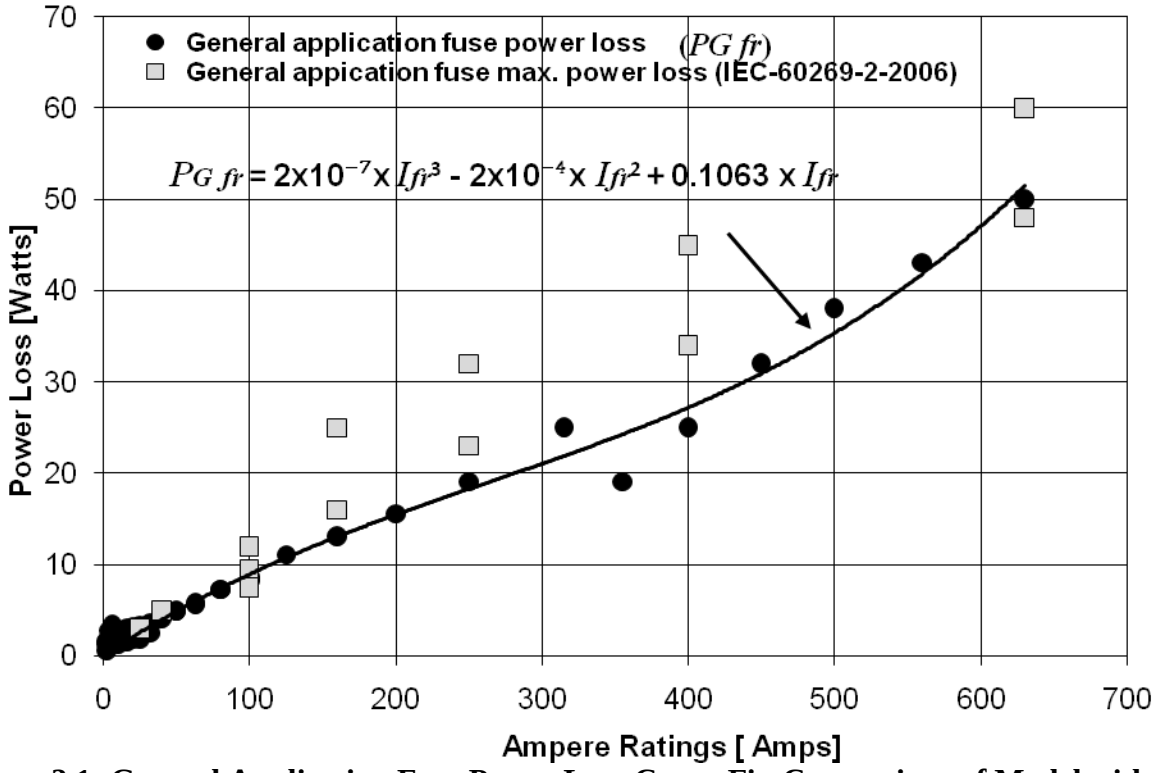

Figure 3.1: General Application Fuse Power Loss Curve Fit. Comparison of Model with the IEC 60269-2-2006 Std.

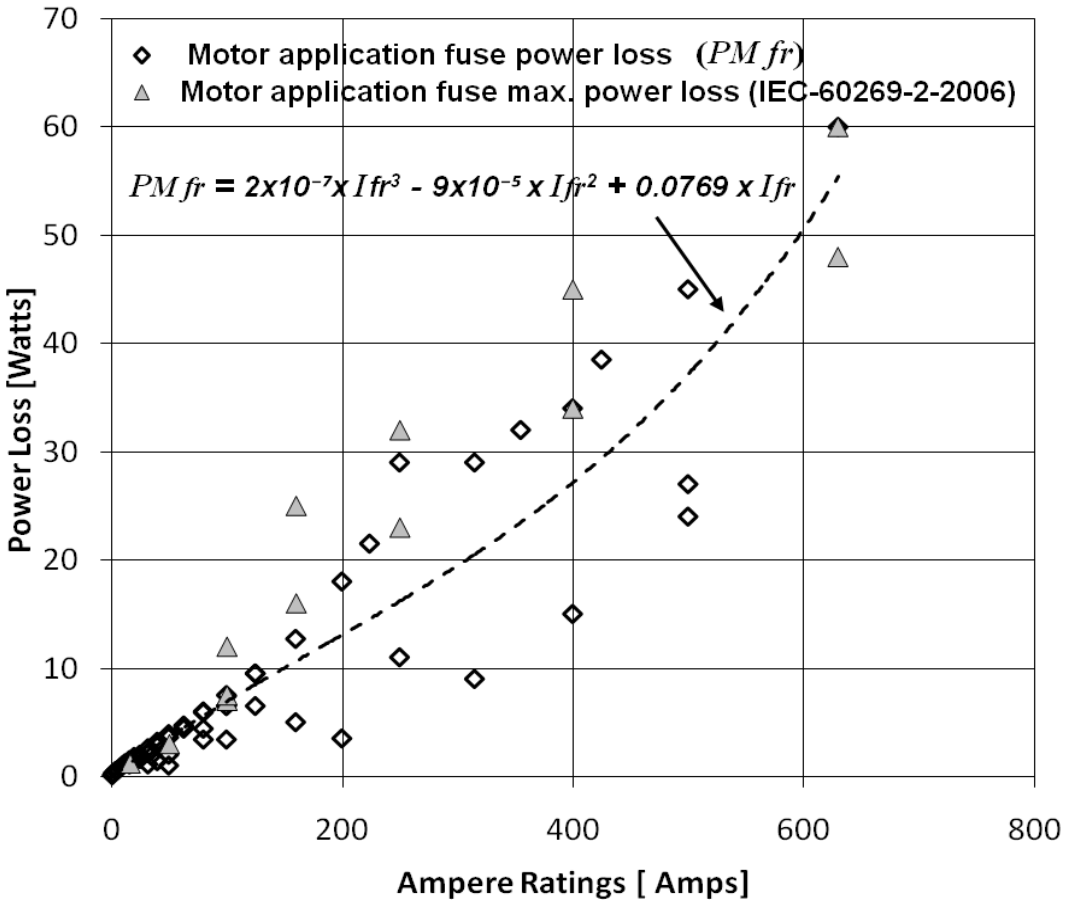

Figure 3.2: Motor Application Fusible Switch Model with the IEC 60269-2-2006 Std.

The fuse power loss curve fit models for general and motor applications are

$$P_{G\,fr} = 2\times10^{-7}\times I_{fr}^{\ 3} - 2\times10^{-4}\times I_{fr}^{\ 2} + 0.1063\times I_{fr} \tag{3.1}$$

and

$$P_{M\,fr} = 2\times10^{-7}\times I_{fr}^{\ 3} - 9\times10^{-5}\times I_{fr}^{\ 2} + 0.0769\times I_{fr}, \tag{3.2}$$

respectively, where $P_{G\,fr}$ is the power loss in watts for general application fuses, I_{fr} is the fuse ampere rating in amperes, and $P_{M\,fr}$ is the power loss in watts for motor application fuses.

To estimate the general and motor application fuse power losses at any loads, equations (3.1) and (3.2) were multiplied by the scaling load factor for the fuses, $K_{f\,load}$. Performing this step yields

$$P_{G\,fuse\,loss} = K_{f\,load}\times P_{G\,fr} = \left(\left(Df\times I\right)/I_{fr}\right)^2\times P_{G\,fr} = \left(Df\times I\right)^2\times\left(2\times10^{-7}\times I_{fr} - 2\times10^{-4} + 0.1063\times I_{fr}^{\ -1}\right) \tag{3.3}$$

and

$$P_{M\,fuse\,loss} = K_{f\,load}\times P_{M\,fr} = \left(\left(Df\times I\right)/I_{fr}\right)^2\times P_{M\,fr} = \left(Df\times I\right)^2\times\left(2\times10^{-7}\times I_{fr} - 9\times10^{-5} + 0.0769\times I_{fr}^{\ -1}\right) \tag{3.4}$$

where $P_{G\ fuse\ loss}$ is the general application fuse power loss at any load in watts, $P_{M\ fuse\ loss}$ is the motor application fuse power loss at any load in watts, I is the load current flowing through the fuse in amperes, and Df is the diversity factor applied to the load.

In the second step of this study, three phase low voltage switch power losses at rated loads from manufacturer publications were collected. The three phase low voltage switch rated power losses were collected from Asea Brown Boveri, Ferraz Shawmut and Cooper Bussmann. The collected data are shown in Table 3.4, and they correspond to balanced currents and 60 Hz.

Table 3.4: Low Voltage Three Phase Switch Power Losses at Rated Loads from Manufacturers

Manufacturer	Ampere Rating [Amps]	Power Loss (3 poles) [watts]
Ferraz Shawmut	30	6
	60	12
	100	27
	200	24
	400	90
	600	165
Asea Brown Boveri	63	12
	160	27
	250	33
	400	90
	630	165
	63	12
Cooper Bussmann	16	0.9
	25	1.8
	32	3
	45	4.2
	63	8.4
	30	3
	60	4.8
	100	12
	160	19.5
	200	19.5
	400	30
	600	120
	30[1]	6
	60[1]	12
	100[1]	27
	200[1]	24

[1] Other low voltage switch model of Cooper Bussmann

The data in Table 3.4 are plotted in Figure 3.3 together with the curve fit of the data. These manufacturer losses were not compared to measured values because test data were not found in any publications and the maximum power losses were not reported in the standard IEC 60947-3-2008. The curve fit of the manufacturer data is given by

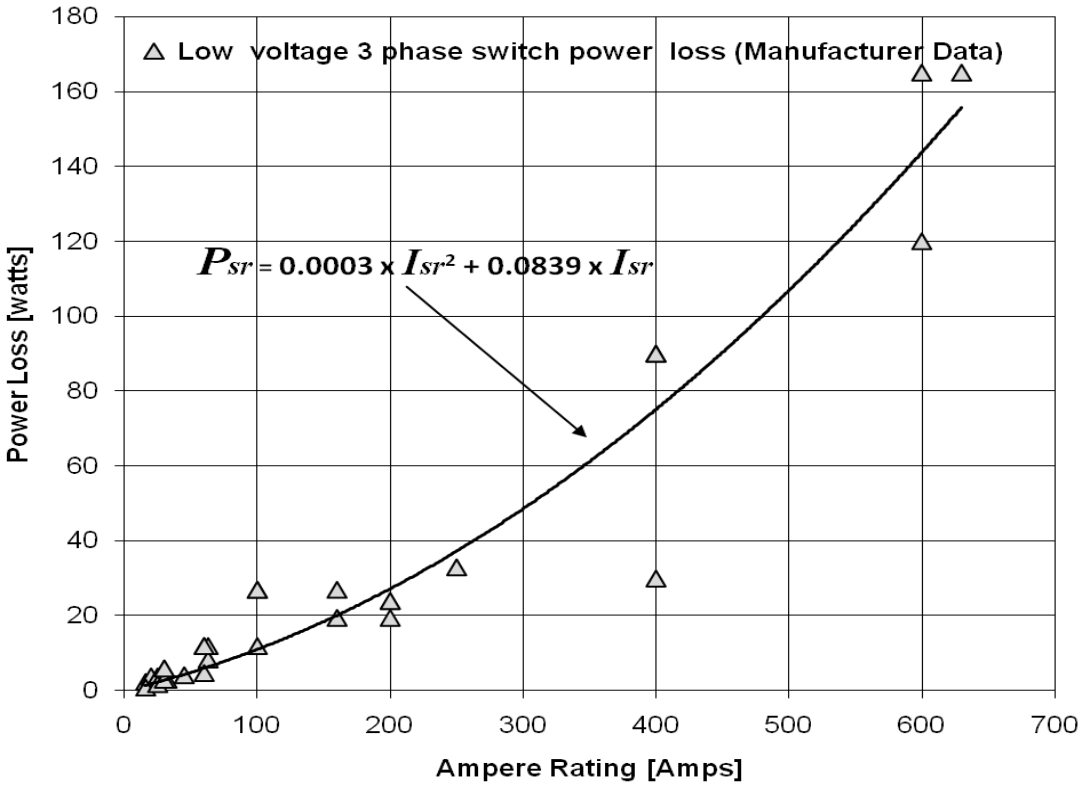

Figure 3.3: Switch Power Loss Curve Fit

$$P_{sr} = 0.0003 \times I_{sr}^{\ 2} + 0.0839 \times I_{sr} \tag{3.5}$$

where P_{sr} is the three phase switch power loss at rated load in watts and I_{sr} is the rated current in amperes.

As the fusible switch used in power panelboards has a three phase switch with three fuses, the power loss at rated load for general and motor applications can be represented as

$$P_{\ fusible\ switch\ power\ loss} = P_{\ sr} + 3 \times P_{\ fuse\ power\ loss} \tag{3.6}$$

where $P_{\ fuse\ power\ loss}$ is either P_{Gfr} or P_{Mfr}.

From equation (3.6) the power loss of a fusible switch for general and motor application is given by

$$P_{\ Gfsr} = \left\{ [0.0003 \times I_{sr}^{\ 2} + 0.0839 \times I_{sr}] + 3 \times [2 \times 10^{-7} \times I_{fr}^{\ 3} - 2 \times 10^{-4} \times I_{fr}^{\ 2} + 0.1063 \times I_{fr}] \right\} \tag{3.7}$$

and

$$P_{\ Mfsr} = \left\{ [0.0003 \times I_{sr}^{\ 2} + 0.0839 \times I_{sr}] + 3 \times [2 \times 10^{-7} \times I_{fr}^{\ 3} - 9 \times 10^{-5} \times I_{fr}^{\ 2} + 0.0769 \times I_{fr}] \right\}, \tag{3.8}$$

respectively. Note that equations (3.7) and (3.8) correspond to power losses at rated loads.

McDonald & Hickok (1985) and Rubin (1979) reported fusible switch power losses but they did not specify the type of fuse application, i.e. motor or general purpose. However, the general and motor application fusible switch power losses using equations (3.7) and (3.8), respectively were compared with McDonald & Hickok (1985) and Rubin (1979) fusible switch power data and this comparison is shown in Figure 3.4.

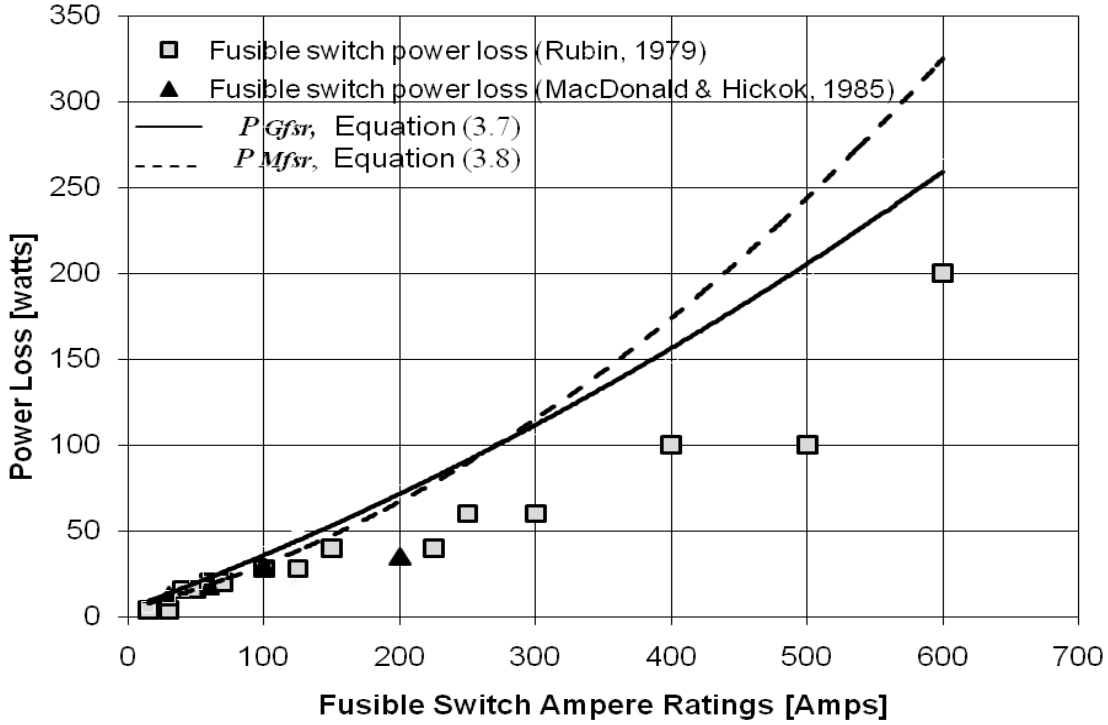

Figure 3.4: Fusible Switch Models with McDonald & Hickok (1985) and Rubin (1979)

These power losses were matched for certain ampere ratings. The published and calculated losses showed similar results up to current ratings of 150 amps. Information on power losses for fusible switch ampere ratings greater than 200 amps was not available from MacDonald and Hickok (1985). In Rubin's paper, the fusible switch power losses were considered the same as molded case circuit breakers of similar ampere ratings. This assumption in Rubin' s paper is not correct because the power losses in fusible switches are greater than in breakers of similar ampere ratings due to the extra power losses created by the fuses. That is the reason why the calculated power losses are higher than those reported by MacDonald and Hickok (1985) and Rubin (1979). These papers are not good sources to estimate the power losses of fusible switches.

A comparison of equations (3.7) and (3.8) with measured data is possible. The general and motor application fusible switch power losses using equations (3.7) and (3.8), respectively are compared with test data. These loss data were collected from a loss calculator found at the

website, http://pps2.com/b1/ndb/. These loss data is shown in Table 3.5. This calculator was made by Eaton based on their own laboratory test data of Cooper Bussmann fusible switches. This comparison is shown in Figure 3.5, and the general and motor application fusible switch power losses using equations (3.7) and (3.8) matched with the test data.

Table 3.5: Loss Calculated Data – Power Losses at Rated Loads for Fusible Switches (http://pps2.com/b1/ndb/)

Power Losses at Rated Loads for Fusible Switches		
Type of Fuse	**Class J**	**Class RK5**
Ampere Ratings	**Power Loss – 3 Poles [watts]**	**Power Loss -3 Poles [watts]**
20	13.4	17.2
30	13.4	17.2
40	16.4	20.6
50	19.4	24
60	22.3	24.5
70	22.9	31
80	23.4	34.7
90	23.9	38.5
100	24.4	37.2
125	40.6	48
175	72.9	77.8
200	89.1	95.7
225	104.7	137
250	120.2	145.8
300	151.2	165.4
350	182.1	187.4
400	212.9	204.6
500	274.3	267.8
600	335.1	313.8

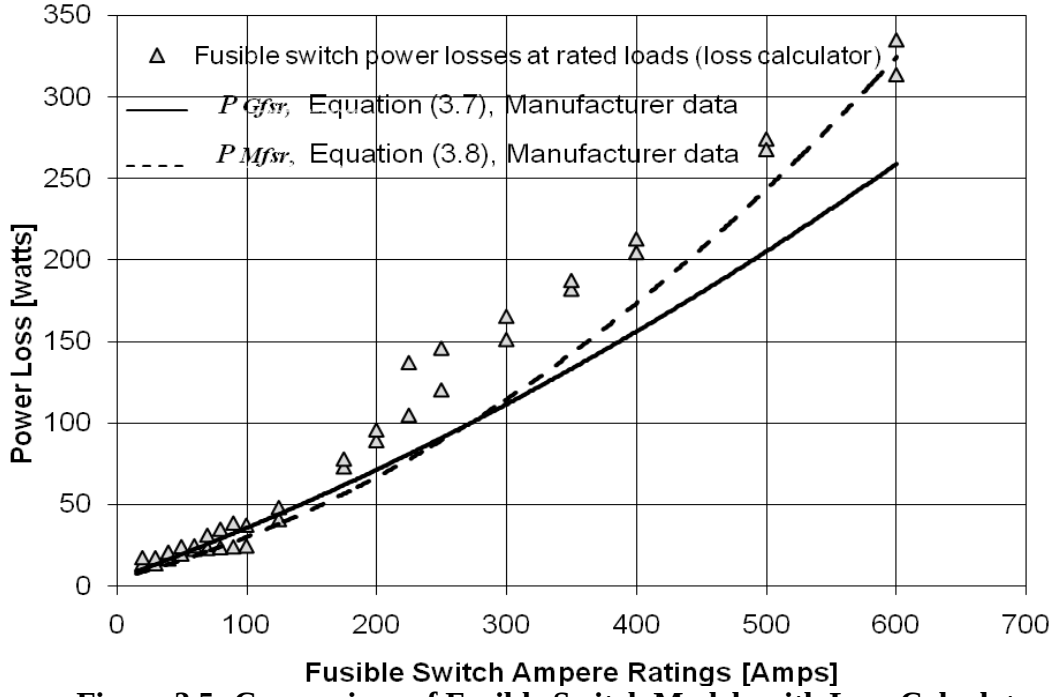

Figure 3.5: Comparison of Fusible Switch Models with Loss Calculator.

Power Loss Curve Fit Models - Balanced Three Phase Currents

In the fusible switches used in power panelboards, the ampere ratings of fuses and three phase switches are not always the same. The power loss models created must allow selection of the ampere ratings for each device independently. As the fuses used in three phase low voltage switches can be either general or motor application type, the power loss model to estimate the fusible switch power losses at any loads for general application is

$$P_{G\ fusible\ switch\ loss} = K_{s\ load} \times P_{sr} + K_{f\ load} \times 3 \times P_{Gfr}$$

$$= \left(Df \times I / I_{sr} \right)^2 \times P_{sr} + \left(Df \times I / I_{fr} \right)^2 \times 3 \times P_{Gfr}$$

$$= \left[Df \times I \right]^2 \times \left\{ [0.0839 \times I_{sr}^{-1}] + [6 \times 10^{-7} \times I_{fr} - 3 \times 10^{-4} + 0.3189 \times I_{fr}^{-1}] \right\} \quad (3.9)$$

and the power loss model to estimate the fusible switch power losses at any loads for motor application is

$$P_{M\ fusible\ switch\ loss} = K_{s\ load} \times P_{sr} + K_{f\ load} \times 3 \times P_{Mfr}$$

$$= \left(Df \times I / I_{sr} \right)^2 \times P_{sr} + \left(Df \times I / I_{fr} \right)^2 \times 3 \times P_{Mfr}$$

$$= \left[Df \times I \right]^2 \times \left\{ [0.0839 \times I_{sr}^{-1}] + [6 \times 10^{-7} \times I_{fr} + 3 \times 10^{-5} + 0.2307 \times I_{fr}^{-1}] \right\} \quad (3.10)$$

where $K_{s\ load}$ is the switch scaling load factor, $K_{f\ load}$ is the scaling load factor for the fuses, I is the phase current in amperes, and Df is the diversity factor applied to the load feed by the fusible switch.

To illustrate the use of equations (3.9) and (3.10), they were applied to three different fuse/switch ampere ratings (32/32, 63/63, and 160/160 amps), respectively. Figure 3.6 and 3.7 show the fusible switch power losses in watts at different load currents for a diversity factor equal to 0.8. The fusible switch power loss curves show a parabolic variation as a function of the current.

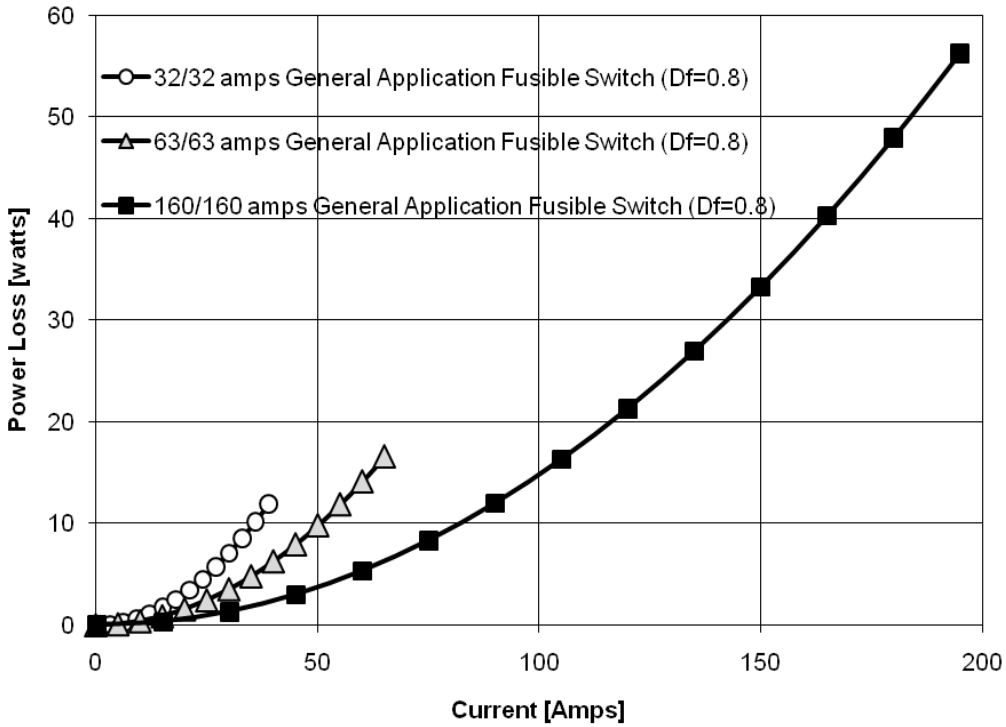

Figure 3.6: Fusible Switches for General Application. Power Losses by Equation (3.9)

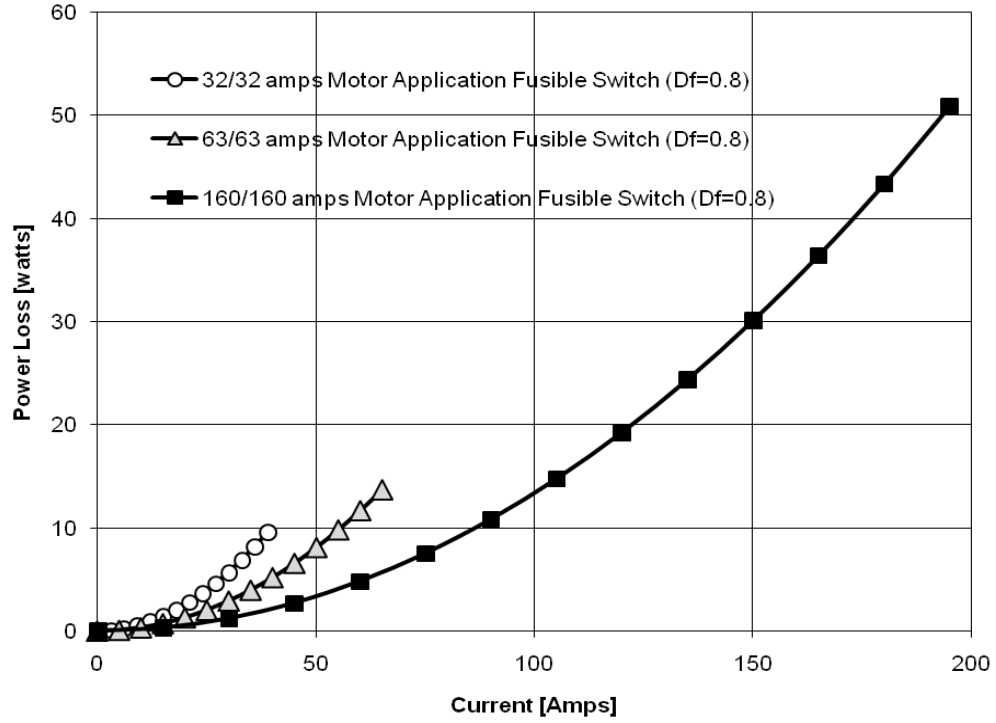

Figure 3.7: Fusible Switches for Motor Application. Power Losses by Equation (3.10)

Chapter Summary

Having collected general and motor application fuse and switch power loss data from manufacturer publications, power loss models at rated load were created. These models were created from least squares regression.

The models of fuse power losses at rated loads are given by equations (3.1) and (3.2). These calculated power losses at rated loads were compared with the maximum loss values provided by the standard IEC-60269-2-2006. The models of fusible switch power losses at rated loads are given by equations (3.7) and (3.8). These calculated power losses at rated loads were compared with published power losses reported by McDonald & Hickok (1985) and Rubin (1979) as shown in Figure 3.4. The calculated losses from the models did not match with the data of these papers. A new comparison was made using data from the loss calculator of http://pps2.com/b1/ndb/, and the models did match the test data.

Finally, the curve fit models of fusible switches for general and motor applications were created and are given by equations (3.9) and (3.10), respectively. As an example, these loss models were applied to three different fuse/switch ampere ratings for a diversity factor of 0.8. The fusible switch power loss curves showed a parabolic variation of the power loss respect with respect to the current in Figures 3.6 and 3.7.

CHAPTER 4 - Motor Starters

The objective of this chapter is to find models to estimate the power losses in full voltage non reversing (FVNR) motor starters used in power panelboards. The steps used to create the models for motor starter losses are developed in the following sequence: collecting and fitting test FVNR motor starter power loss data, comparing the power loss data with independent data for verification, and creating the power loss models through least square regression. Finally, the loss models are used to estimate the power losses of four NEMA motor starters.

Electrical Equipment Description

The NEMA motor starter has the functions of motor control together with overload and short circuit protections. The overload is given by a non-normal operation of the motor that can produce a high current flowing through the motor starter circuit. The short circuit is given by an electrical circuit that allows a high current to travel along a different path from the original motor starter circuit. These protection functions are given by a relay for the overloads, and a circuit breaker or fusible switch for the short circuits. The motor starter's circuit has a contactor with auxiliary contacts, which can control the motor remotely using on and off push buttons. The motor starters can be configured to perform full voltage non-reversing and full voltage reversing (FVR) tasks. This study focuses on FVNR motor starters because they are used in power panelboards. The FVNR motor starters apply the full voltage to the motor and permit only one direction of shaft rotation. Figure 4.1 shows the circuit and elements of a FVNR motor starter.

The motor starters can be classified as NEMA sizes 00, 0, 1, 2, 3, 4, 5, 6, 7, 8 and 9. Table 4.1 shows the maximum horsepower for different NEMA size starters for three phase motors using full voltage reported in the NEMA ICS 2-2000 standard. The starters listed in Table 4.1 are used in both motor control centers and power panelboards. FVNR motor starters up to 15 hp correspond to a NEMA 2 (230 volts) that are used in power panelboards as reported by the General Electric Company. FVNR motor starters up to NEMA 3 and 4 sizes are used in power panelboards as reported by the Siemens and Square D, respectively. This study focuses on FVNR motor starters up to NEMA 3 that was the highest tested NEMA size reported in the

Heat Gain from Electrical and Control Equipment in Industrial Plants, ASHRAE Research Project-1104.

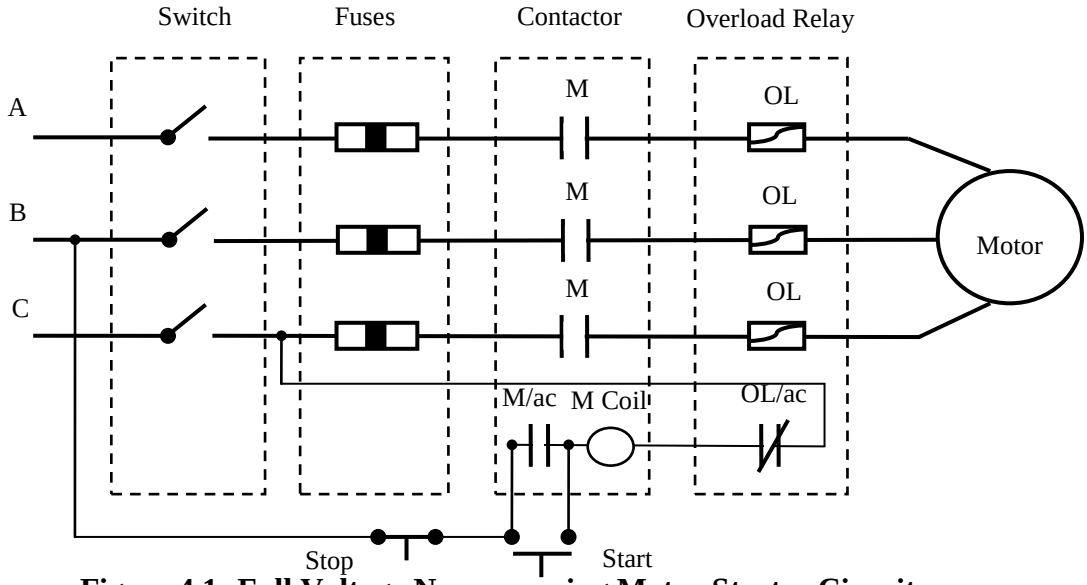

Figure 4.1: Full Voltage Non-reversing Motor Starter Circuit

Table 4.1: Maximum Horsepower for Different NEMA Motor Starters

NEMA Size	NEMA Continuous Ampere Rating	Horsepower	
		230V	460V
00	9	1	2
0	18	3	**5**
1	27	7	10
2	45	15	25
3	90	30	50
4	135	50	100
5	270	100	200
6	540	200	400
7	810	300	600
8	1215	450	900
9	2250	800	1600

Power Loss - Collected Data and Results

In this thesis, test data from the Heat Gain from Electrical and Control Equipment in Industrial Plants, ASHRAE Research Project-1104 was used. In that research, motor starters from General Electric Company (NEMA 0), Eaton (NEMA 1 and 3) and Allen-Bradley (NEMA 2) were tested. All measurements were conducted by running a single phase current up and down adjacent phases, connecting the three phases of the motor starter in series, and using the temperature controlled chamber as is shown in Figure 4.2. The temperature controlled chamber

was used to control the environmental temperature of the tested device using a light bulb and cooling fan. The NEMA 0, 1 and 3 FVNR motor starters were tested at temperature of 25 ˚C, 30˚C, 40˚C and 50˚C; the measured power losses samples at different temperatures showed a variation smaller than 1 watt. For this reason, the NEMA 2 FVNR motor starter was tested without controlling temperature. The coil power loss was measured with a wattmeter separately from the power loss of the reminder of the motor starter. The NEMA 1, 2 and 3 motor starter relays were energized by a 120V/60 Hz supply, and the NEMA 0 motor starter relay was energized by a 480V/60 Hz supply.

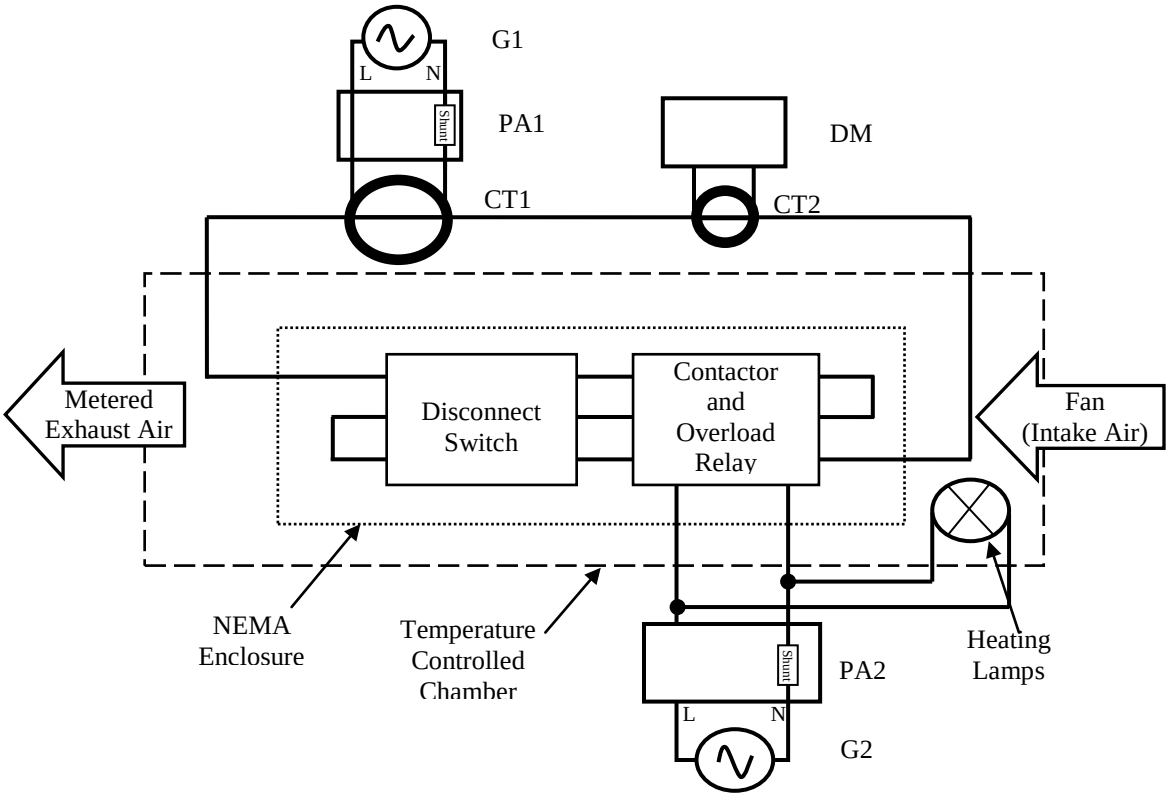

G1: Variac Autotransformer(General Radio Co., 25 Amp-W50HG3BBM); G2: Power Supply (120 Volt, 60 Hz); PA1: Power Analyzer (Extech, True RMS-Model 380801); PA2: Power Analyzer (Valhalla 2101); CT1: Current Transformer (ABB, Type CLE, S#7524A63G06, 5:1000/2000 Amps); CT2: Current Transformer (Fluke 80I-600); DM: Digital Multimeter (Fluke 8010A)

Figure 4.2: Temperature Controlled Chamber and Circuit for Measuring NEMA 0, 1, 2 and 3 FVNR Fusible Switch Motor Starter Losses

The tests were made by determining the power losses of the circuit without the starter connected to the test circuit. The starter was removed from the circuit and the jumper wires were connected together to complete the circuit. This loss measurement without the starter in place was called baseline or wire loss measurement, W_{loss}. The starter was then connected in place and the measurement, WS_{loss}, process was repeated. The difference between the loss measurement with the starter in place and the wire loss measurement was the starter loss, $WS_{loss} - W_{loss}$, and the

sum of the starter loss and the coil loss, R_{loss}, was the total loss of the starter, $WS_{loss} - W_{loss} + R_{loss}$. During these tests, the experimental error of the measurements was estimated as ±5% of full scale. From the NEMA 0, 1, 2 and 3 fusible switch motor starter losses that were collected in these experiments and are shown in Tables 4.2 to 4.5. The regression for each device was developed. The models of Figures 4.3 to 4.6 were obtained by fitting the data with a function that consisted of a constant plus factor times the square of the current.

Table 4.2: NEMA 0 FVNR Fusible Switch Motor Starter Test and Curve Fit Loss Values

N° Sample	Chamber Temp. [°C]	Current [Amps]	Wire Loss [watts]	Wire+Starter Loss [watts]	Coil Loss [watts]	NEMA FVNR Motor Starter Loss [watts]	NEMA FVNR Motor Starter Curve Fit Loss [watts]
	T	I	W_{loss}	WS_{loss}	R_{loss}	$WS_{loss} - W_{loss} + R_{loss}$	$6+0.055xI^2$
1	25	0	0	0	6	6	6.0
2	25	2	0.1	0.5	6	6.4	6.2
3	25	4	0.4	1.7	6	7.3	6.9
4	25	6	0.9	3.4	6	8.5	8.0
5	25	8	1.6	5.4	6	9.8	9.5
6	25	10	3	9	6	12	11.5
7	25	12	4	12	6	14	13.9
8	25	14	5	16	6	17	16.8
9	25	16	7	20	6	19	20.1
10	25	18	9	25	6	22	23.8
11	25	20	11	31	6	26	28.0
12	30	0	0	0	6	6	6.0
13	30	2	0.1	0.6	6	6.5	6.2
14	30	4	0.4	1.8	6	7.4	6.9
15	30	6	0.9	3.4	6	8.5	8.0
16	30	8	1.7	5.7	6	10	9.5
17	30	10	3	9	6	12	11.5
18	30	12	4	13	6	15	13.9
19	30	14	5	17	6	18	16.8
20	30	16	7	21	6	20	20.1
21	30	18	9	26	6	23	23.8
22	30	20	11	32	6	27	28.0
23	40	0	0	0	6	6	6.0
24	40	2	0.1	0.7	6	6.6	6.2
25	40	4	0.4	1.9	6	7.5	6.9
26	40	6	1	3.6	6	8.6	8.0
27	40	8	1.7	5.9	6	10.2	9.5
28	40	10	3	10	6	13	11.5
29	40	12	4	13	6	15	13.9
30	40	14	5	17	6	18	16.8
31	40	16	7	21	6	20	20.1
32	40	18	9	26	6	23	23.8
33	40	20	11	32	6	27	28.0
34	50	0	0	0	6	6	6.0
35	50	2	0.1	0.7	6	6.6	6.2
36	50	4	0.4	1.9	6	7.5	6.9
37	50	6	1	3.6	6	8.6	8.0
38	50	8	1.7	6	6	10.3	9.5
39	50	10	3	10	6	13	11.5
40	50	12	4	13	6	15	13.9
41	50	14	5	17	6	18	16.8
42	50	16	7	21	6	20	20.1
43	50	18	9	26	6	23	23.8
44	50	20	11	32	6	27	28.0

Table 4.3: NEMA 1 FVNR Fusible Switch Motor Starter Test and Curve Fit Loss Values

N° Sample	Chamber Temp. [°C]	Current [Amps]	Wire Loss [watts]	Wire+Starter Loss [watts]	Coil Loss [watts]	NEMA FVNR Motor Starter Loss [watts]	NEMA FVNR Motor Starter Curve Fit Loss [watts]
	T	I	W_{loss}	WS_{loss}	R_{loss}	$WS_{loss} - W_{loss} + R_{loss}$	$7+0.033xI^2$
1	25	0	0	0	7	7	7.0
2	25	3	0	0.3	7	7.3	7.3
3	25	6	0.5	1.9	7	8.4	8.2
4	25	9	1.5	4.2	7	9.7	9.7
5	25	12	2.8	7.5	7	11.7	11.8
6	25	15	4.4	11.8	7	14.4	14.4
7	25	18	6.5	17.1	7	17.6	17.7
8	25	21	8.8	23.3	7	21.5	21.6
9	25	24	11.6	30.4	7	25.8	26.0
10	25	27	14.8	39.1	7	31.3	31.1
11	25	30	18.3	48.8	7	37.5	36.7
12	25	31	19.6	52.4	7	39.8	38.7
13	30	0	0	0	7	7	7.0
14	30	3	0	0.3	7	7.3	7.3
15	30	6	0.6	1.8	7	8.2	8.2
16	30	9	1.5	4.2	7	9.7	9.7
17	30	12	2.9	7.5	7	11.6	11.8
18	30	15	4.6	11.9	7	14.3	14.4
19	30	18	6.7	17.2	7	17.5	17.7
20	30	21	9	23.3	7	21.3	21.6
21	30	24	11.8	30.5	7	25.7	26.0
22	30	27	15	39.1	7	31.1	31.1
23	30	30	18.6	48.8	7	37.2	36.7
24	30	31	19.9	52.4	7	39.5	38.7
25	40	0	0	0	7	7	7.0
26	40	3	0	0.3	7	7.3	7.3
27	40	6	0.6	1.8	7	8.2	8.2
28	40	9	1.5	4.2	7	9.7	9.7
29	40	12	2.9	7.5	7	11.6	11.8
30	40	15	4.6	11.8	7	14.2	14.4
31	40	18	6.7	17.1	7	17.4	17.7
32	40	21	9.1	23.2	7	21.1	21.6
33	40	24	11.9	30.5	7	25.6	26.0
34	40	27	15.1	39.1	7	31	31.1
35	40	30	18.5	48.9	7	37.4	36.7
36	40	31	20.1	52.4	7	39.3	38.7
37	50	0	0	0	7	7	7.0
38	50	3	0	0.3	7	7.3	7.3
39	50	6	0.6	1.8	7	8.2	8.2
40	50	9	1.6	4.2	7	9.6	9.7
41	50	12	2.9	7.5	7	11.6	11.8
42	50	15	4.7	11.9	7	14.2	14.4
43	50	18	6.8	17.3	7	17.5	17.7
44	50	21	9.2	23.3	7	21.1	21.6
45	50	24	12.1	30.7	7	25.6	26.0
46	50	27	15.4	39.4	7	31	31.1
47	50	30	19.1	49.4	7	37.3	36.7
48	50	31	20.6	53.3	7	39.7	38.7

Table 4.4: NEMA 2 FVNR Fusible Switch Motor Starter Test and Curve Fit Loss Values

N˚ Sample	Current [Amps]	Wire Loss [watts]	Wire+Starter Loss [watts]	Coil Loss [watts]	NEMA FVNR Motor Starter Loss [watts]	NEMA FVNR Motor Starter Curve Fit Loss [watts]
	I	W_{loss}	WS_{loss}	R_{loss}	$WS_{loss} - W_{loss} + R_{loss}$	$8.7+0.018xI^2$
1	0	0	0	6	6	8.7
2	10	0.6	5.2	6	10.6	10.5
3	20	3.4	15.2	6	17.8	15.9
4	30	7.9	27.3	6	25.4	24.9
5	40	14.4	45.6	6	37.2	37.5
6	50	22.9	68.4	6	51.5	53.7

Table 4.5: NEMA 3 FVNR Fusible Switch Motor Starter Test and Curve Fit Loss Values

N˚ Sample	Chamber Temp. [˚C]	Current [Amps]	Wire Loss [watts]	Wire+Starter Loss [watts]	Coil Loss [watts]	NEMA FVNR Motor Starter Loss [watts]	NEMA FVNR Motor Starter Curve Fit Loss [watts]
	T	I	W_{loss}	WS_{loss}	R_{loss}	$WS_{loss} - W_{loss} + R_{loss}$	$15.5+0.004xI^2$
1	25	0	0.0	0.0	15.5	15.5	15.5
2	25	10	1.1	1.5	15.5	15.9	15.9
3	25	20	5.2	6.8	15.5	17.1	17.1
4	25	30	12	15.6	15.5	19.1	19.1
5	25	40	21.5	28	15.5	22	21.9
6	25	50	33.9	44.4	15.5	26	25.5
7	25	60	49	64.5	15.5	31	29.9
8	25	70	67	87.8	15.5	36.3	35.1
9	25	80	87.6	115	15.5	42.9	41.1
10	25	90	110.8	144.4	15.5	49.1	47.9
11	25	100	136.8	178.7	15.5	57.4	55.5
12	25	110	165.4	218	15.5	68.1	63.9
13	25	120	197.1	257	15.5	75.4	73.1
14	25	130	228	300	15.5	87.5	83.1
15	25	140	263	343	15.5	95.5	93.9
16	30	0	0.0	0.0	15.5	15.5	15.5
17	30	10	1.2	1.6	15.5	15.9	15.9
18	30	20	5.2	7.1	15.5	17.4	17.1
19	30	30	12.1	16.4	15.5	19.8	19.1
20	30	40	21.7	30	15.5	23.8	21.9
21	30	50	34.1	46.8	15.5	28.2	25.5
22	30	60	49.3	67	15.5	33.2	29.9
23	30	70	77.2	89.6	15.5	27.9	35.1
24	30	80	88	117	15.5	44.5	41.1
25	30	90	111.4	147.2	15.5	51.3	47.9
26	30	100	137.6	181	15.5	58.9	55.5
27	30	110	165.6	218	15.5	67.9	63.9
28	30	120	197.2	259	15.5	77.3	73.1
29	30	130	228	302	15.5	89.5	83.1
30	30	140	263	344	15.5	96.5	93.9

Table 4.5 (cont.)

N° Sample	Chamber Temp. [°C]	Current [Amps]	Wire Loss [watts]	Wire+Starter Loss [watts]	Coil Loss [watts]	NEMA FVNR Motor Starter Loss [watts]	NEMA FVNR Motor Starter Curve Fit Loss [watts]
	T	I	W_{loss}	WS_{loss}	R_{loss}	$WS_{loss} - W_{loss} + R_{loss}$	$15.5+0.004xI^2$
31	40	0	0.0	0.0	15.5	15.5	15.5
32	40	10	1.1	1.5	15.5	15.9	15.9
33	40	20	5.2	6.9	15.5	17.2	17.1
34	40	30	12.1	15.7	15.5	19.1	19.1
35	40	40	21.8	28.4	15.5	22.1	21.9
36	40	50	34.1	44.8	15.5	26.2	25.5
37	40	60	49.4	65	15.5	31.1	29.9
38	40	70	67.3	88.3	15.5	36.5	35.1
39	40	80	88.4	115	15.5	42.1	41.1
40	40	90	111.8	146.6	15.5	50.3	47.9
41	40	100	138.1	180.5	15.5	57.9	55.5
42	40	110	165.5	217	15.5	67	63.9
43	40	120	197.2	256	15.5	74.3	73.1
44	40	130	229	300	15.5	86.5	83.1
45	40	140	264	343	15.5	94.5	93.9
46	50	0	0.0	0.0	15.5	15.5	15.5
47	50	10	1.1	1.5	15.5	15.9	15.9
48	50	20	5.2	6.9	15.5	17.2	17.1
49	50	30	12.1	15.8	15.5	19.2	19.1
50	50	40	21.8	28.2	15.5	21.9	21.9
51	50	50	34.2	44.6	15.5	25.9	25.5
52	50	60	49.7	65	15.5	30.8	29.9
53	50	70	67.8	88.6	15.5	36.3	35.1
54	50	80	88.7	115.9	15.5	42.7	41.1
55	50	90	112.2	146.7	15.5	50	47.9
56	50	100	139.3	180.6	15.5	56.8	55.5
57	50	110	165.6	217	15.5	66.9	63.9
58	50	120	197.2	256	15.5	74.3	73.1
59	50	130	230	299	15.5	84.5	83.1
60	50	140	265	344	15.5	94.5	93.9

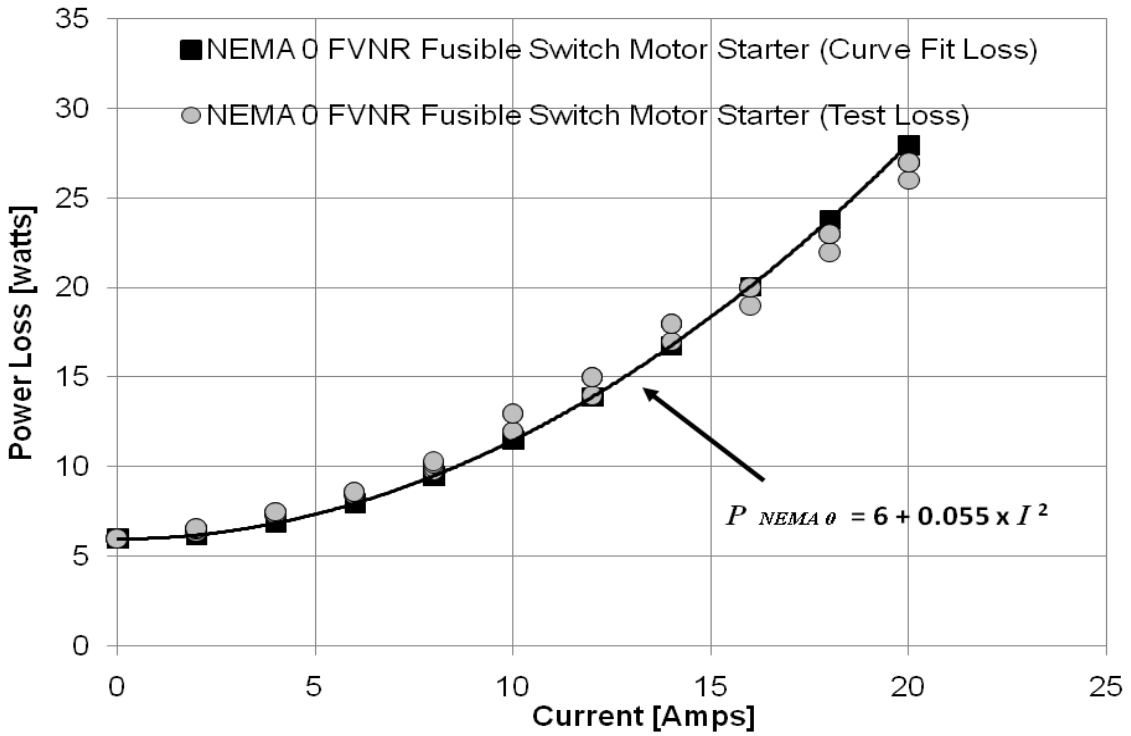

Figure 4.3: NEMA 0 FVNR Fusible Switch Motor Starter. Power Loss Model from Table 4.2

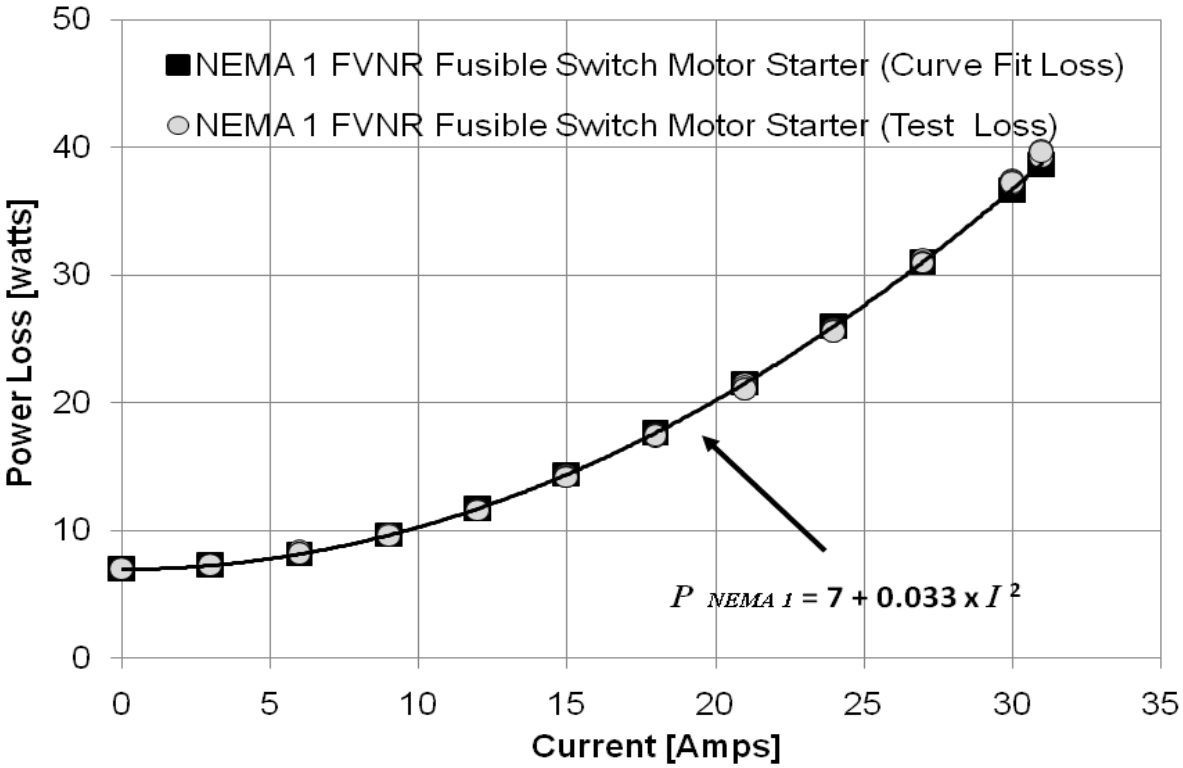

Figure 4.4: NEMA 1 FVNR Fusible Switch Motor Starter. Power Loss Model from Table 4.3

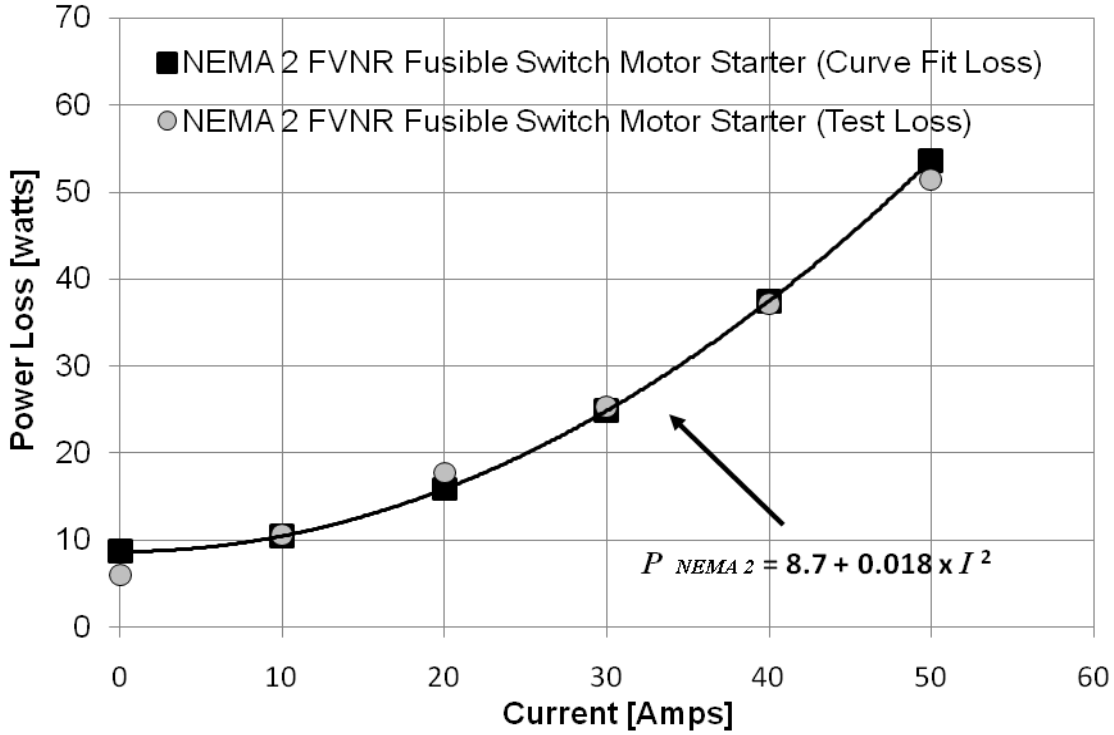

Figure 4.5: NEMA 2 FVNR Fusible Switch Motor Starter. Power Loss Model from Table 4.4

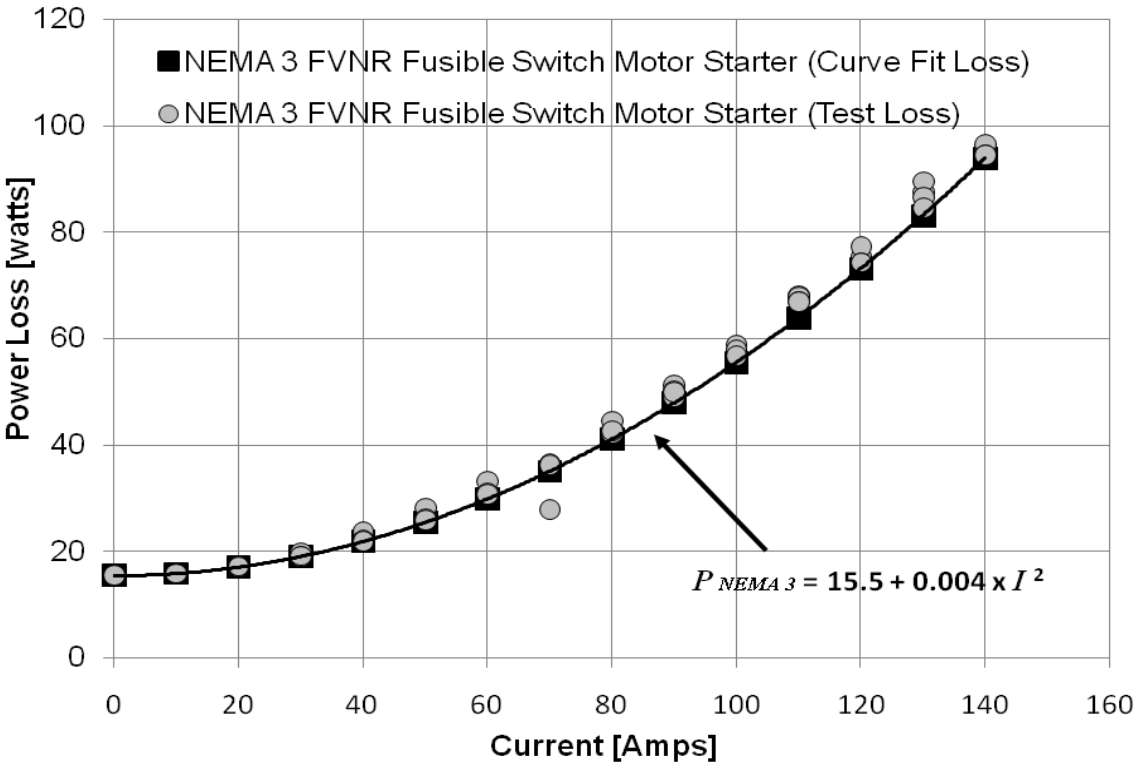

Figure 4.6: NEMA 3 FVNR Fusible Switch Motor Starter. Power Loss Model from Table 4.5

The test data fitted in Figures 4.3 to 4.6 are the loss models for the NEMA 0, 1, 2 and 3 FVNR motor starters. In these models given by equations (4.1) to (4.4), the first term is the constant coil loss of the motor starter in watts, and the first factor of the second term is the resistance in ohms of the NEMA motor starter. The models are given by

$$P_{NEMA0} = 6 + 0.055 \times I^2 \quad (4.1)$$

$$P_{NEMA1} = 7 + 0.033 \times I^2 \quad (4.2)$$

$$P_{NEMA2} = 8.7 + 0.018 \times I^2 \quad (4.3)$$

$$P_{NEMA3} = 15.5 + 0.004 \times I^2 \quad (4.4)$$

where $P_{NEMA\,0}$, $P_{NEMA\,1}$, $P_{NEMA\,2}$ and $P_{NEMA\,3}$ are the NEMA 0, 1, 2 and 3 FVNR motor starter power losses in watts and I is the current flowing through the motor starter in amperes.

Data from NEMA 0, 1, 2 and 3 motor starters listed in Tables 4.2 to 4.5 were acquired without fuses. Users select fuses according to the motor-loads according to the application. The tested NEMA 0, 1, 2 and 3 motor starters were FVNR and fusible switch type, but instead of fuses, the starters had metallic bars where the fuses should be as shown in Figure 4.7. To compare the test motor starter power loss models of equations (4.1) to (4.4) with independent data, the fuse power losses had to be added. Equation (3.4) was used to account for the fuse losses using the current rating values of Table 4.1.

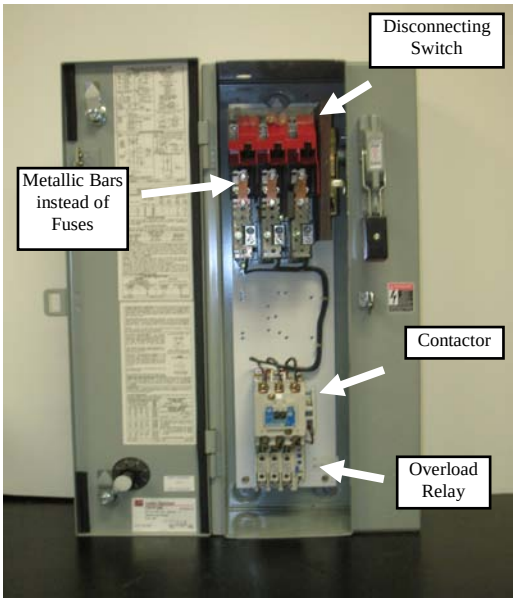

Figure 4.7: NEMA FVNR Fusible Switch Motor Starter

The motor starter power losses were compared with the losses reported by McDonald & Hickok (1985) and Rubin (1979). McDonald & Hickok (1985) and Rubin (1979) only reported the motor starter losses for NEMA sizes 1 to 6. This comparison is made in Table 4.6 and shown in Figure

4.8. The NEMA 0 motor starter is not compared because no data is reported in these papers. MacDonald & Hickok (1985) matched better than Rubin (1979) showing a variation less than ± 37 % with respect to test losses. However, caution must be exercised when comparing these results since these authors did not specify if the combination starter losses corresponded to FVNR or FVR, and fusible switch or breaker types.

Table 4.6: Comparison of Test Losses with McDonald & Hickok (1985) and Rubin (1979)

Power Loss Curve Fit Equations (Figures 4.3 to 4.6)			Fuse Power Loss	Power Losses at Rated Loads			
				Test Power Losses		McDonald & Hickok (1985)	Rubin (1979)
NEMA Size	NEMA Continuous Ampere Ratings "I" [Amps]	Test FVNR NEMA Non-fused Motor Starter Equations [watts]	Fuse Power Loss Eq. (3.4), (x3 units) [watts]	NEMA FVNR Motor Starter Power Loss at Rated Load without Fuses [watts]	NEMA FVNR Motor Starter Power Loss at Rated Load with Fuses [watts]	NEMA Motor Starter Power Loss at Rated Load [watts]	NEMA Motor Starter Power Loss at Rated Load [watts]
0	18	$6^{1} + 0.055 \times I^{2}$	4.1	23.8	27.9	NA	NA
1	27	$7^{1} + 0.033 \times I^{2}$	6.0	31.1	37.1	27	60
2	45	$8.7^{1} + 0.018 \times I^{2}$	9.9	45.2	55.1	57	90
3	90	$15.5^{1} + 0.004 \times I^{2}$	19.0	47.9	66.9	99	140

[1]= constant coil power loss in watts; NA = not available

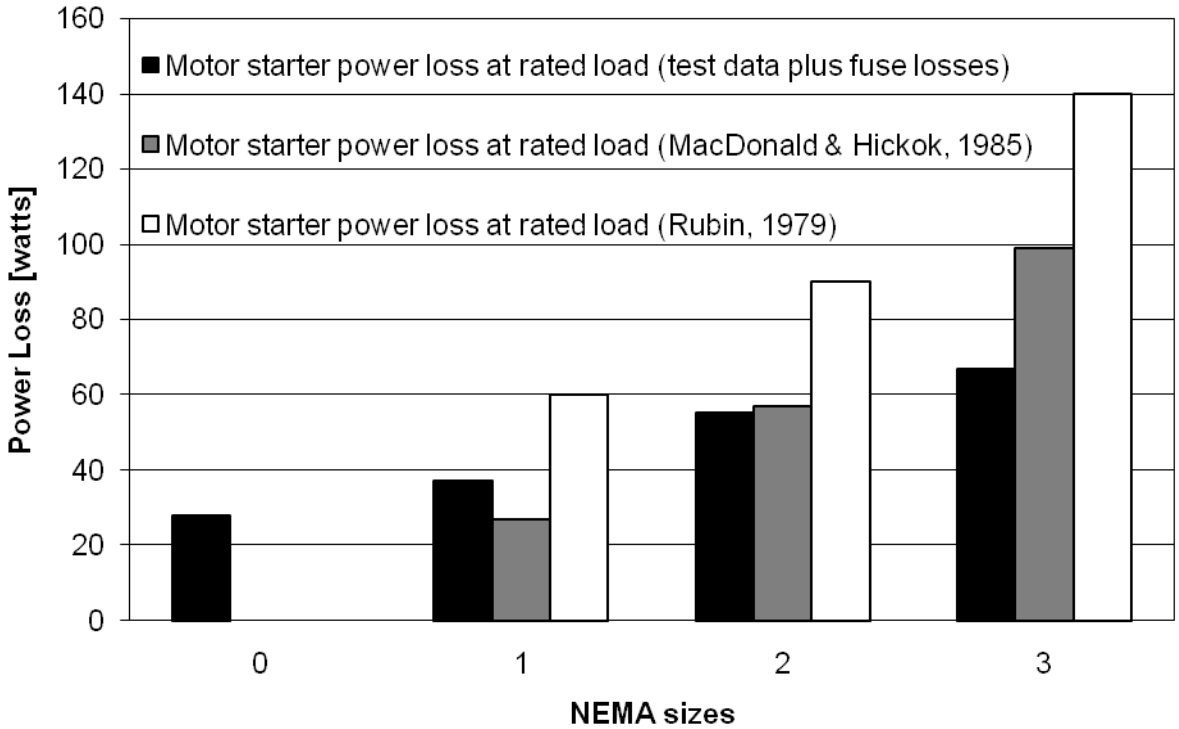

Figure 4.8: Comparison of Test Losses with McDonald & Hickok (1985) and Rubin (1979)

A second comparison is made using manufacturer data. The motor starter test data are compared with manufacturer losses reported by Eaton. This comparison is made and shown in Table 4.7 and Figure 4.9. No manufacturer losses were found for the NEMA 0 motor starter. The test and manufacturer losses of NEMA 1, 2 and 3 motor starters match with a variation of less than ± 25 %.

Table 4.7: Comparison of Test Losses with Manufacturer Data (Eaton)

Power Loss Curve Fit Equations (Figures 4.3 to 4.6)			Fuse Power Loss	Power Losses at Rated Loads		
				Test Power Losses		Manufacturer Power Losses (Eaton)
NEMA Size	NEMA Continuous Ampere Ratings "*I*" [Amps]	Test FVNR NEMA Non-fused Motor Starter Equations [watts]	Fuse Power Loss Eq. (3.4), (x3 units) [watts]	NEMA FVNR Motor Starter Power Loss at Rated Load without Fuses [watts]	NEMA FVNR Motor Starter Power Loss at Rated Load with Fuses [watts]	NEMA FVNR Motor Starter Rated Power Loss [watts]
0	18	$6^{1} + 0.055 \times I^{2}$	4.1	23.8	27.9	NA
1	27	$7^{1} + 0.033 \times I^{2}$	6.0	31.1	37.1	30
2	45	$8.7^{1} + 0.018 \times I^{2}$	9.9	45.2	55.1	50
3	90	$15.5^{1} + 0.004 \times I^{2}$	19.0	47.9	66.9	90

[1]= constant coil power loss in watts; NA = not available

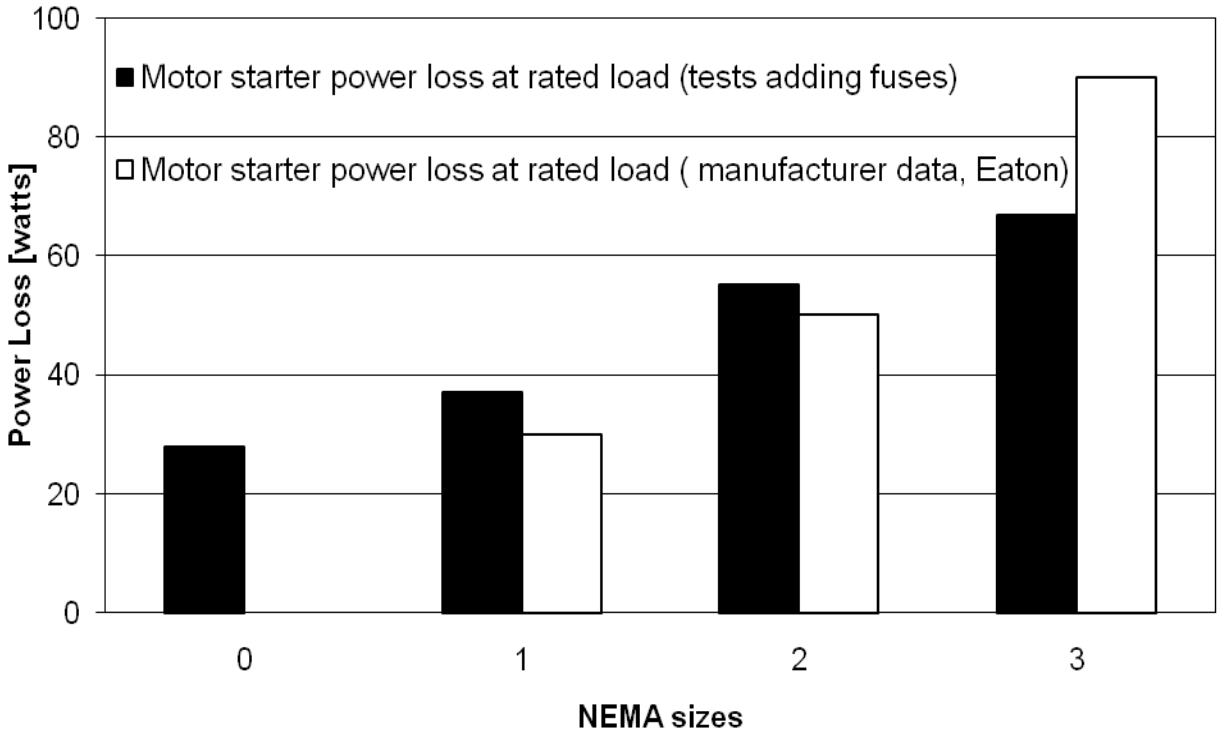

Figure 4.9: Comparison of Test Losses with Manufacturer Data (Eaton)

Power Loss Curve Fit Models - Balanced Three Phase Currents

To create the power loss models at any load for the NEMA 0, 1, 2 and 3 FVNR motor starters, the second terms of equations (4.1) to (4.4) are multiplied by the square load diversity factor. The fuse loss of equation (3.4) is added to equations (4.1) to (4.4), but as fusible switches in motor starters have three poles, the fuse loss is also multiplied by 3. The power loss models at any load for the NEMA 0, 1, 2 and 3 FVNR fusible switch motor starters are

NEMA 0 FVNR fusible switch motor starter for ratings of less than 5 hp

$$P_0 = 6 + 0.055 \times (Df \times I)^2 + 3 \times P_{M\ fuse\ loss}$$

$$= 6 + [(Df \times I)^2 \times (6 \times 10^{-7} \times I_{fr} + 0.05473 + 0.2307 \times I_{fr}^{-1})] \quad (4.5)$$

NEMA 1 FVNR fusible switch motor starter for ratings of 5 to 10 hp

$$P_1 = 7 + 0.033 \times (Df \times I)^2 + 3 \times P_{M\ fuse\ loss}$$

$$= 7 + [(Df \times I)^2 \times (6 \times 10^{-7} \times I_{fr} + 0.03273 + 0.2307 \times I_{fr}^{-1})] \quad (4.6)$$

NEMA 2 FVNR fusible switch motor starter for ratings of 10 to 25 hp

$$P_2 = 8.7 + 0.018 \times (Df \times I)^2 + 3 \times P_{M\ fuse\ loss}$$

$$= 8.7 + [(Df \times I)^2 \times (6 \times 10^{-7} \times I_{fr} + 0.01773 + 0.2307 \times I_{fr}^{-1})] \quad (4.7)$$

NEMA 3 FVNR fusible switch motor starter for ratings of 25 to 50 hp

$$P_3 = 15.5 + 0.004 \times (Df \times I)^2 + 3 \times P_{M\ fuse\ loss}$$

$$= 15.5 + [(Df \times I)^2 \times (6 \times 10^{-7} \times I_{fr} + 0.00373 + 0.2307 \times I_{fr}^{-1})] \quad (4.8)$$

where P_0, P_1 , P_2 and P_3 are the NEMA 0, 1, 2 and 3 fusible switch, motor starter power losses in watts at any load, I is the load current flowing through the fuse-switch in amperes, I_{fr} is the fuse ampere rating in amperes, and Df is the diversity factor applied to the motor-load.

To illustrate the use of equations (4.5) to (4.8), they were applied to four different NEMA size/fuse ampere ratings of 0/16, 1/25, 2/40 and 3/80 amps, respectively. Figures 4.10 and 4.11 show the motor starter power losses in watts at different load currents for a diversity factor equal to 0.8. The motor starter power loss curves show a parabolic variation as a function of the current.

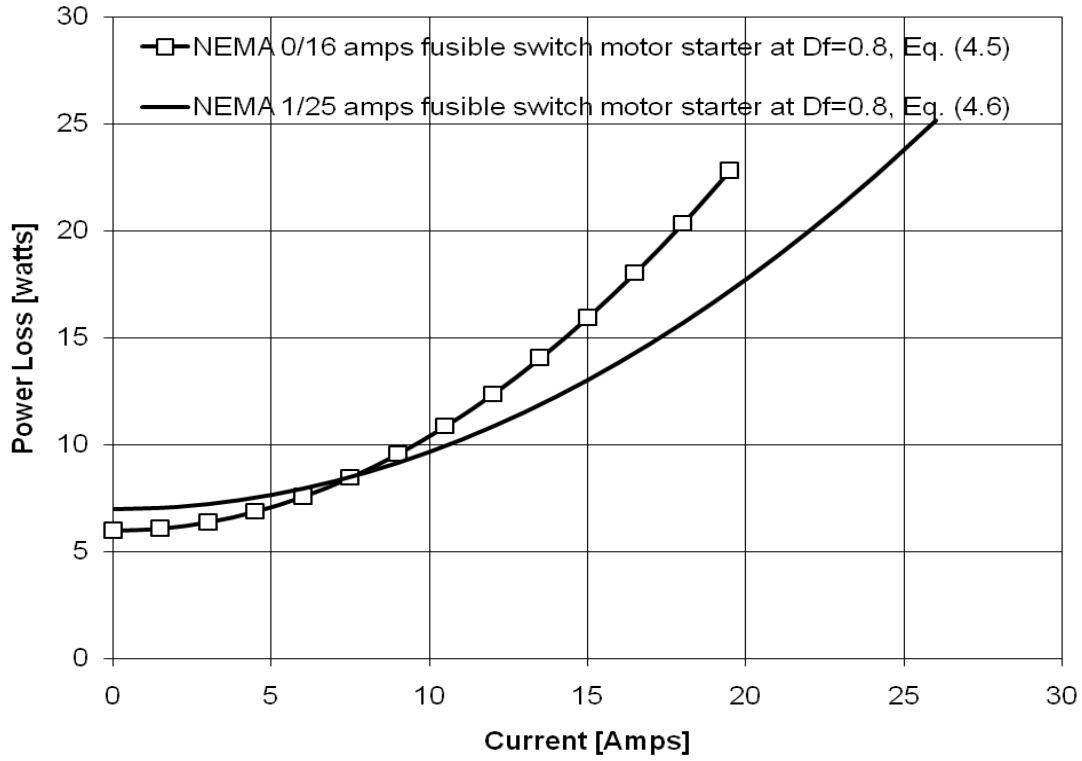

Figure 4.10: FVNR Fusible Switch Motor Starters. Power Losses by Equations (4.5) and (4.6)

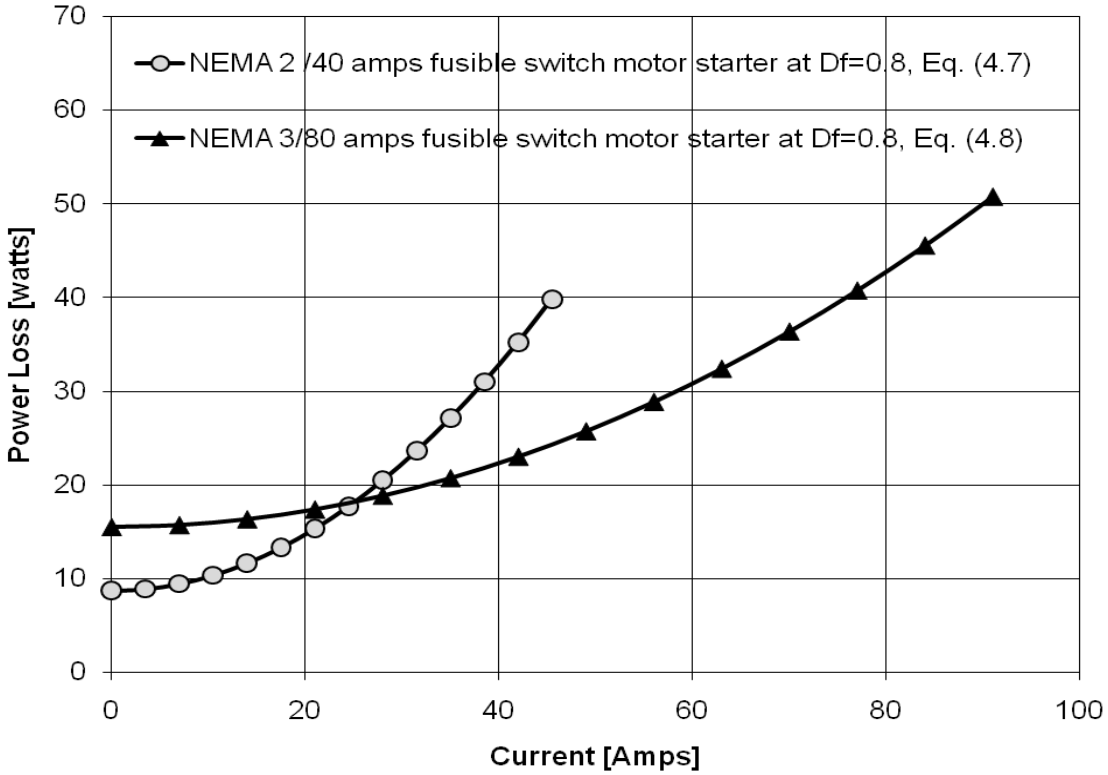

Figure 4.11: FVNR Fusible Switch Motor Starters. Power Losses by Equations (4.7) and (4.8)

Chapter Summary

The curve fit power loss models for the NEMA 0, 1, 2 and 3 FVNR motor starters were based on test data from ASHRAE Research Project-1104. Those test losses were curve fitted for each motor starter and the loss models for these tests were created. The calculated motor starter losses for rated load given by equations (4.1) to (4.4) were compared with power losses reported by McDonald & Hickok (1985) and Rubin (1979) in Figure 4.8. A second comparison was made using manufacturer data published by Eaton in Figure 4.9.

The curves fitted from the measured data were used to create the NEMA 0, 1, 2 and 3 FVNR motor starters power loss models represented by equations (4.5) to (4.8). As an example, those equations were applied to four different NEMA size/fuse ampere ratings for a diversity factor equal to 0.8. The motor starter loss curves showed parabolic variations as a function of the currents. The results were shown in Figures 4.10 and 4.11.

CHAPTER 5 - Enclosure and Three Phase Bus bars

The objective of this chapter is to create a curve fit model to estimate the power losses in the enclosure-bus bar components used in power panelboards. The steps used to create the enclosure-bus bar power loss model are the collection of enclosure and bus bar dimensions, material information, bus bar ampere ratings, and operating temperatures from industrial standards, analytical models and finally the creation of a power loss model for the enclosure-bus bar at any load. The model will be used to estimate the power losses for three different panelboard examples.

Electrical Equipment Description

Enclosure-bus bar equipment in power panelboards are built according to the UL 67-1993 standard. The enclosure is formed by a metallic box made of a galvanized sheet steel and the bus bar is made of either copper or aluminum. The bus bars form a three phase circuit which is installed in the center of the enclosure as shown in Figure 5.1.

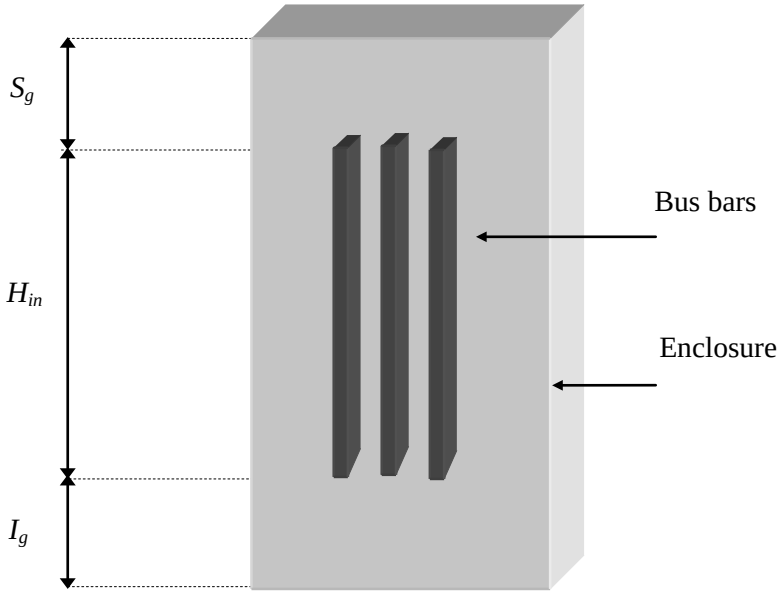

Figure 5.1: Enclosure-Bus Bar Configuration by General Electric Company (S_g=Superior gutter height, H_{in}=Interior height, I_g=Interior gutter height)

The bus bars are the main conductors of the power panelboard and they distribute loads to all circuits that are connected along the bus bars. Each circuit consists of a circuit breaker, fusible

switch, or motor starter connected to a load. Three types of enclosure-bus bars were found in the manufacturer literature. In Figure 5.2, examples of these three types of enclosure-bus bar constructions manufactured by General Electric Company, Square D, and Siemens are shown. These enclosure-bus bars can have non-flat or flat three phase configurations. In non-flat configurations, the bus bars are parallel to each other and arranged either vertically or horizontally. In the flat configuration they are not parallel but serial. The study of this chapter was based only in the non-flat vertical enclosure-bus bar configuration used by the General Electric Company, which offered more enclosure dimension data than the other manufacturers. This data is shown in Table B.1 of Appendix B.

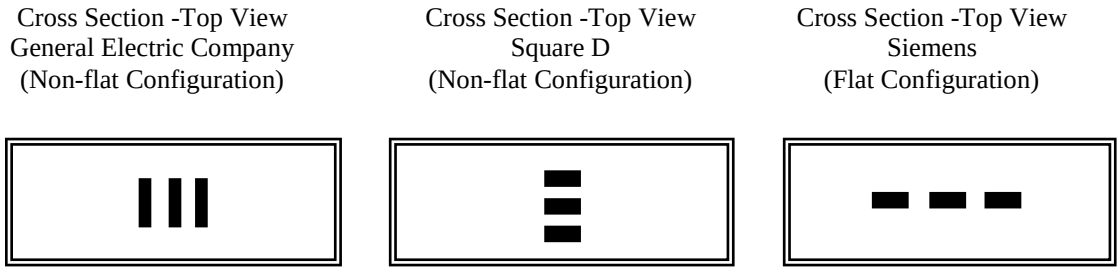

Figure 5.2: General Electric Company, Square D, and Siemens Enclosure-Bus Bar Configurations for Power Panelboards

The dimensions of enclosures and bus bars depend on the power panelboard ampere ratings and the number of disconnecting devices installed (feeder capacity) in the power panelboards. Bus bar dimensions for 250, 400, 600, 800 and 1200 amp ratings were selected from the UL 67-1993 standard and are shown in Table B.2 of Appendix B. In Appendix B, the ambient and bus bar maximum operating temperatures from the UL 891-1992 standard are listed and bus bar copper standard material information from the IEC 60028-1925 is included.

The enclosure-bus bar power losses in panelboards are produced by electrical and electromagnetic power loss effects which usually increase the electrical resistance of the conductor. The enclosure power loss is produced by the stray loss effect. The bus bar power loss is produced by the ohmic, skin loss, and proximity loss effects.

The stray effect power loss occurs when current carrying conductors set up magnetic fields in the vicinity of conducting materials. In power panelboards, this effect occurs because of the three-phase bus bars parallel to the enclosure sheet at the front, back, and lateral sides of the panelboard.

The ohmic power in the bus bars is determined by the square of the conductor current times the resistance of the conductor. The ohmic power usually produces the greatest losses in conductors.

The skin effect power loss occurs when alternating current flows. The changing magnetic field created by the alternating current induces voltages in the conducting material that cause other currents to also flow in the conductor. The net result is that the current crowds to the edges of the conductor while little current flows in the center of the conductor. Because the current flows through an effectively smaller area, the resistance is greater. This larger resistance accounts for proportionally larger power losses.

The proximity effect occurs when current carrying conductors set up magnetic fields in the vicinity of other conductor/s. When this current is an alternating current, the created magnetic field is able to induce voltages in surrounding conductors and cause currents to flow. The induced voltage causes a current to flow and there is ohmic heating associated with the induced current. If the nearby conductor is carrying its own current, then the induced current can alter the current distribution over the cross-section. This rearrangement of current can both increase and decrease the total ohmic losses. Whether the change is a greater, smaller, or unvarying amount depends on the shape, current, and relative placement of the conductors.

In this chapter, the stray effect power losses are estimated for panels, and the power losses stem from ohmic heating, skin effect and proximity effect are estimated for three phase bus bars.

Enclosure Power Loss - Collected Data and Results

The power losses in the panels were estimated by the model presented by Del Vecchio (2003). To estimate the enclosure or stray power losses at rated panelboard loads of 250, 400, 600, 800 and 1200 amps, the enclosure and bus bar dimensions described in Table B.2 of Appendix B were used. Twenty one enclosure-bus bar dimension cases from Table B.2 are shown in Table 5.1 and Figure 5.3. The enclosure or stray power losses at rated loads were estimated for galvanized steel panels, balanced three phase loads, and 60 Hz.

In this study, a spreadsheet linked to a visual basic program and shown in Appendix C which is based on the model reported by Del Vecchio (2003) was created. The enclosure power losses at rated loads for the twenty one enclosure-bus bar cases were calculated. For a given bus

bar current rating, the stray losses in the adjacent panels were determined for each possible size. The total power loss was determined by summing the power loss contributions for all four adjacent panels. The total power losses for all the different sizes corresponding to this current rating were averaged. The average enclosure power loss is shown in the last column of Table 5.1.

Table 5.1: Enclosure-Bus Bar Dimensions & Calculated Enclosure Power Losses at Rated Loads

Power Panelboard Ampere Ratings I_{bus} [Amps]	Conductor & Plate Dimensions (Bus Bar & Enclosure) [mm]							Calculated Enclosure Power Losses at Rated Loads [watts/meter]					
	B	*A*	*D*	*C*	*P*	*S*	*W*	Front Side Power Loss [*F*]	Back Side Power Loss [*B*]	Left Side Power Loss [*L*]	Right Side Power Loss [*R*]	Total Power Loss [*F*+*B*+*L*+*R*]	Enclosure Power Loss [P_{enc}]
250	25.4	6.4	1.75	133.4	287.15	44.4	685.8	0.05	0.05	0.02	0.02	0.14	0.13
	25.4	6.4	1.75	133.4	337.95	44.4	787.4	0.05	0.05	0.02	0.02	0.14	
	25.4	6.4	1.75	133.4	401.45	44.4	914.4	0.05	0.05	0.01	0.01	0.12	
400	50.8	6.4	1.75	120.7	236.35	95.2	685.8	0.54	0.54	0.20	0.20	1.48	1.45
	50.8	6.4	1.75	120.7	287.15	95.2	787.4	0.54	0.54	0.16	0.16	1.40	
	50.8	6.4	1.75	120.7	350.65	95.2	914.4	0.54	0.54	0.13	0.13	1.34	
	50.8	6.4	1.75	120.7	401.45	95.2	1016	0.54	0.54	0.11	0.11	1.30	
	50.8	6.4	2.74	120.7	451.25	95.2	1117.6	0.75	0.75	0.12	0.12	1.74	
600	63.5	6.4	1.75	114.3	210.95	120.6	685.8	1.84	1.84	0.72	0.72	5.12	5.01
	63.5	6.4	1.75	114.3	261.75	120.6	787.4	1.84	1.84	0.59	0.59	4.86	
	63.5	6.4	1.75	114.3	325.25	120.6	914.4	1.84	1.84	0.47	0.47	4.62	
	63.5	6.4	1.75	114.3	376.05	120.6	1016	1.84	1.84	0.40	0.40	4.48	
	63.5	6.4	2.74	114.3	425.85	120.6	1117.6	2.57	2.57	0.41	0.41	5.96	
800	88.9	6.4	1.75	101.6	210.95	171.4	787.4	6.04	6.04	2.11	2.11	16.30	16.58
	88.9	6.4	1.75	101.6	274.45	171.4	914.4	6.04	6.04	1.67	1.67	15.42	
	88.9	6.4	1.75	101.6	325.25	171.4	1016	6.04	6.04	1.42	1.42	14.92	
	88.9	6.4	2.74	101.6	375.05	171.4	1117.6	8.38	8.38	1.45	1.45	19.66	
1200	63.5	12.7	1.75	114.3	258.6	114.3	787.4	8.98	8.98	2.41	2.41	22.78	23.63
	63.5	12.7	1.75	114.3	322.1	114.3	914.4	8.98	8.98	1.91	1.91	21.78	
	63.5	12.7	1.75	114.3	372.9	114.3	1016	8.98	8.98	1.63	1.63	21.22	
	63.5	12.7	2.74	114.3	422.71	114.3	1117.6	12.70	12.70	1.67	1.67	28.74	

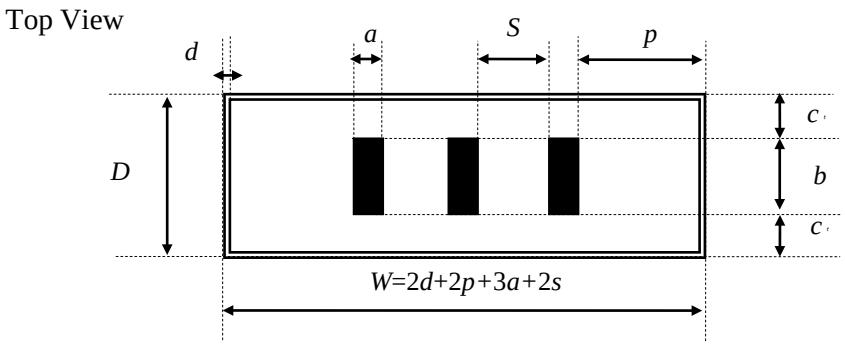

Figure 5.3: Enclosure and Bus Bars - Top View from Figure 5.1

Three Phase Bus Bar Power Loss - Collected Data and Results

The power losses in the conductors were determined by the numerical method of White and Piesciorovsky (2009). The panelboard three phase bus bar power losses corresponding to the rated loads of 250, 400, 600, 800 and 1200 amps were determined for the bar sizes shown in Table B.2 of Appendix B. The conductivity of copper for bus bars is 100% IACS according to the IEC 60028-1925 standard. However, lower conductivities are used in copper bus bars for panelboards, increasing losses. In this study, a copper conductivity of 98.9% and resistivity of copper at 20˚C, $\rho_{20^\circ C}$, of 0.01743μΩ-m will be used for the three phase bus bar model. The resistivity of the copper corresponding to a 90˚C rise above an ambient temperature of 20˚C is

$$\rho = \rho_{20^\circ C} \times \left[1 + \alpha_{20^\circ C}(T - 20°C)\right]$$
$$= 0.01743\,\mu\Omega - m \times \left[1 + 0.003922°C^{-1}(90°C - 20°C)\right] = 0.022215\,\mu\Omega - m \quad (5.1)$$

where $\alpha_{20^\circ C}$ is the copper temperature coefficient in ˚C⁻¹ and T is the conductor temperature in ˚C corresponding to a 25˚C room temperature and a 65˚C bus bar rise temperature. The DC resistance per unit length in μΩ/m is

$$R_{DC} = \frac{\rho \times l}{a \times b} = \frac{0.022215\mu\Omega - m}{a \times b} \quad (5.2)$$

where a is the width of conductor in meters, b is the height of conductor in meters, and l is 1 m, the unit length of the bar.

Table 5.2: Bus Bar Dimensions & Calculated Single Phase DC Resistances

Power Panelboard Ampere Rating I_{bus} [Amps]	Bus Bar Dimensions [m]			Calculated Single Phase DC Resistances [μΩ/m]
	b	a	S	R_{DC}
250	0.0254	0.0064	0.0444	136.66
400	0.0508	0.0064	0.0952	68.33
600	0.0635	0.0064	0.1206	54.66
800	0.0889	0.0064	0.1714	39.05
1200	0.0635	0.0127	0.1143	27.55

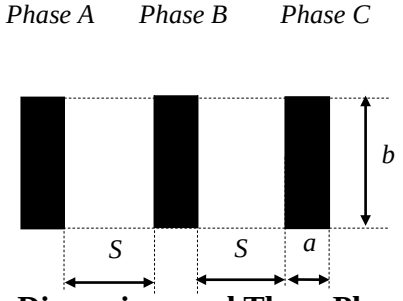

Figure 5.4: Bus Bar Dimensions and Three Phase Configuration

The power loss ratio for the three phase bus bars is defined as

$$K = \frac{Three\ phase\ AC\ power\ loss}{Single\ phase\ DC\ power\ loss} = \frac{I^2 \times R_{AC}}{I^2 \times R_{DC}} = \frac{R_{AC}}{R_{DC}} \tag{5.3}$$

where I is bus bar current in amps, R_{AC} is the three phase AC resistance per unit length in micro-ohms/m, and R_{DC} is the single phase DC resistance per unit length in micro-ohms/m. The calculated power loss ratios, K, were estimated using the m-file shown in Appendix D. This m-file is based on the integral equation solution method that was reported in White and Piesciorovsky (2009). The method subdivides the three phase conductors into square elements or cells. For each cell, an equation for the current density is written. This current density equation depends upon the current densities of all of the other cells. These linear equations are solved simultaneously for the current density values. This calculation includes both the skin and proximity effects.

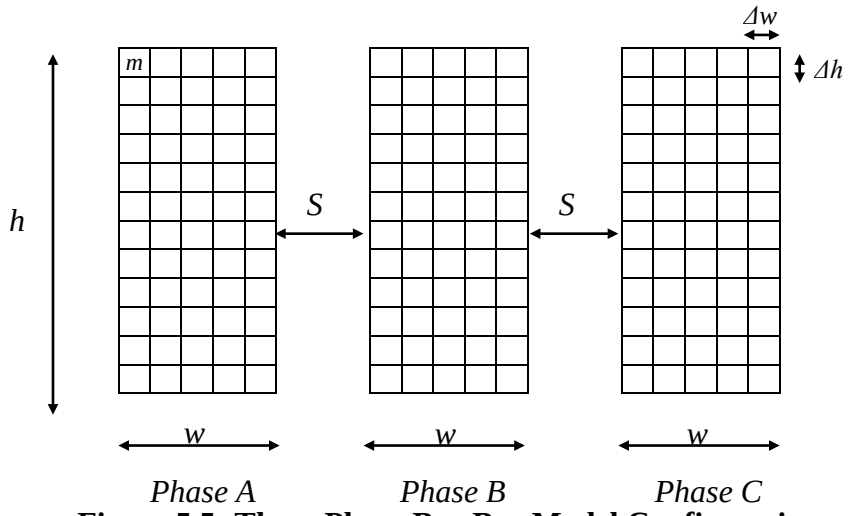

Figure 5.5: Three Phase Bus Bar Model Configuration

The integral equation solution method reported by White and Piesciorovsky (2009) was used to estimate the power loss ratios, K, under the following conditions:

1-The three phase conductors have the same conductivity and dimensions.

2-The conductor was divided in to N cells formed by equal squares ($\Delta w = \Delta h$= constant)

3- The conductor lengths are assumed to be infinite.

4- The current density within each cell is a constant.

5- The sum of all cell currents is equal to the conductor current.

6- The three phase currents are balanced

Once all the DC resistances, R_{DC}, of a single bar and the power loss ratio, K, were determined, the three phase bus bar power losses at rated loads, P_{bus}, in watts per meter are calculated. These power losses are calculated for the five copper bus bar ampere ratings and configurations of Table 5.3. The conductor temperature is 90˚C, the bus bar conductivity is 98.9% IACS, and the frequency is 60 Hz. The three phase bus bar power loss is given by

$$P_{bus} = 10^{-6} \times R_{AC} \times I_{bus}{}^{2} = 10^{-6} \times \frac{R_{AC}}{R_{DC}} \times R_{DC} \times I_{bus}{}^{2} = 10^{-6} \times K \times R_{DC} \times I_{bus}{}^{2} \qquad (5.4)$$

where I_{bus} is the bus bar ampere rating. The three phase bus bar power losses for rated loads, P_{bus}, are shown in the last column of Table 5.3.

Table 5.3: Bus Bar Dimensions & Calculated Three Phase Bus Bar Power Losses

Power Panelboard Ampere Rating I_{bus} [Amps]	Bus bar Dimensions [m]			Calculated DC Resistance per Phase [μΩ/m]	Calculated Ratio of Three Phase AC to Single Phase DC Resistances	Calculated Three Phase Bus Bar Power Loss [watts/m]
	b	a	S	R_{DC}	$K = R_{AC} / R_{DC}$	P_{bus}
250	0.0254	0.0064	0.0444	136.66	3.0253	25.84
400	0.0508	0.0064	0.0952	68.33	3.0982	33.87
600	0.0635	0.0064	0.1206	54.66	3.1453	61.89
800	0.0889	0.0064	0.1714	39.05	3.1494	78.71
1200	0.0635	0.0127	0.1143	27.55	3.4440	136.63

The three phase bus bar power losses were estimated for the three phase panelboard geometry from the General Electric Company data because this manufacturer offered more enclosure and bus bar size data than either Siemens or Square D. In the case that it is desired to estimate the power losses of enclosure-bus bar configurations for panelboards from other manufacturers, the General Electric Company power losses can be used as a reference for manufacturer designs that have similar geometries. As the materials and sizes of bus bars and enclosures are similar for panelboards having similar ratings, the main power loss variable between paneboard designs is the three phase bus bar configuration. These configurations are shown in Figure 5.2 and can be called non-flat, such as the General Electric Company or Square D and flat, such as Siemens. In White and Piesciorovsky (2009), flat and non-flat three phase bus bar configurations were analyzed. The power loss ratio for a given bus bar separation in flat configurations is greater than in non-flat configurations, indicating that the non-flat configurations are more energy efficient. General Electric Company and Square D have less power losses than Siemens for the same current and conductor size.

Enclosure and Three Phase Bus Bar Power Losses - Collected Data and Results

The enclosure-bus bar power losses at rated loads are defined as the sum of the watts dissipated by the AC resistance and the stray loss in the enclosure. The enclosure-bus bar power loss, $P_{enc\ bus}$, at rated loads in watts per meter is given by

$$P_{enc\ bus} = P_{enc} + P_{bus} \tag{5.5}$$

where P_{enc} and P_{bus} are the enclosure and three phase bus bar power losses at rated loads in watts per meter. By using equation (5.5), data were compiled for the enclosure-bus bar model. The compiled data are shown in Table (5.4)

Table 5.4: Calculated Enclosure-Bus Bar Power Losses

Power Panelboard Ampere Ratings I_{bus} [Amps]	Bus bar Dimensions [m]			Calculated Enclosure –Bus Bar Power Losses [$P_{enc\ bus} = P_{enc} + P_{bus}$]		
	b	*a*	*S*	Calculated Enclosure Power Loss P_{enc} [watts/m]	Calculated Three Phase Bus Bar Power Loss P_{bus} [watts/m]	Calculated Enclosure-Bus Bar Power Loss $P_{enc\ bus}$ [watts/m]
250	0.0254	0.0064	0.0444	0.13	25.84	25.97
400	0.0508	0.0064	0.0952	1.45	33.87	35.32
600	0.0635	0.0064	0.1206	5.01	61.89	66.90
800	0.0889	0.0064	0.1714	16.58	78.71	95.29
1200	0.0635	0.0127	0.1143	23.63	136.63	160.26

The enclosure-bus bar power losses at rated loads shown in last column of Table 5.4 were fitted with the polynomial

$$P_{enc\ bus} = 0.00004 \times I_{bus}{}^{2} + 0.0839 \times I_{bus} \tag{5.6}$$

where the variables and units are defined in Table 5.4. The data and the curve fit are shown in Figure 5.6.

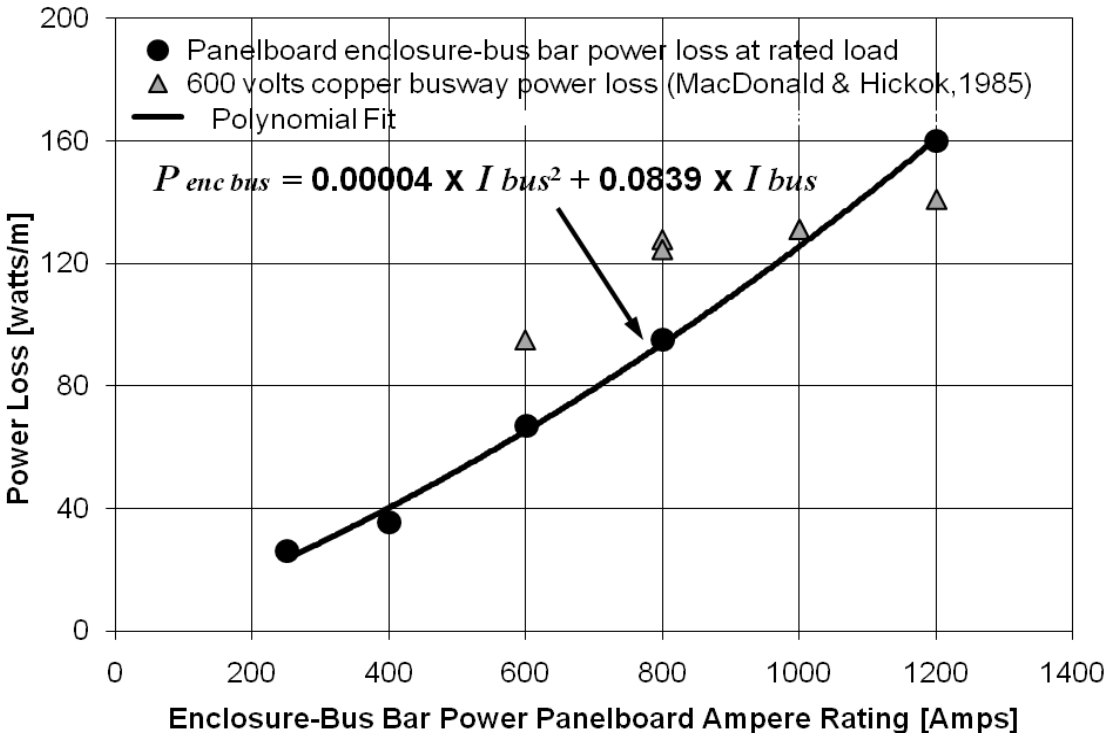

Figure 5.6: Panelboard Enclosure-Bus Bar Power Losses at Rated Load

During this study, no enclosure-bus bar power losses in power panelboards were tested or found in publications. However, as the panelboard enclosure-bus bar power loss model shown in Figure 5.3 consists of three phase bus bars inside of a rectangular metallic enclosure, this model could be considered similar to a 600 volt copper bus-way and enclosure. As a check on the reasonableness of the presented results, the 600 volts copper bus-way power losses reported by McDonald & Hickok (1985) were compared with the panelboard enclosure-bus bar power losses at rated loads. This information is also shown in Figure 5.6. This comparison shows a variation of ±30 %. However, caution must be exercised when comparing these results since the 600 volt copper bus-way and panelboard enclosure-bus bar have some design differences, such as panelboard enclosures having greater dimensions than the bus-way enclosures.

Power Losses for Non-rated Currents

The enclosure-bus bar power loss at any load is given by

$$P_{any\ \ load} = \left((Df \times I) / I_{bus}\right)^2 \times H_{in} \times P_{\ enc\ \ bus}$$

$$= \left(Df \times I\right)^2 \times H_{in} \times \left(0.00004 + 0.0839 \times I_{bus}^{\ -1}\right) \qquad (5.7)$$

where $P_{any\ load}$ is the panelboard enclosure-bus bar power loss at any load in watts, I is the load current flowing through a single bus bar in amperes, H_{in} is the interior height in meters as shown in Figure 5.1, and Df is the load diversity factor applied to the main disconnecting device.

To illustrate the use of equation (5.7), it was applied to three different enclosure-bus bar power panelboard ampere ratings of 400, 800 and 1200 amps for a load diversity factor of 0.8 and an interior height of 1.15 meters which was obtained from Table B.1 of Appendix B. The enclosure- bus bar power loss curves for these three power panelboards show a parabolic variation as a function of the current. The results are shown in Figure 5.7.

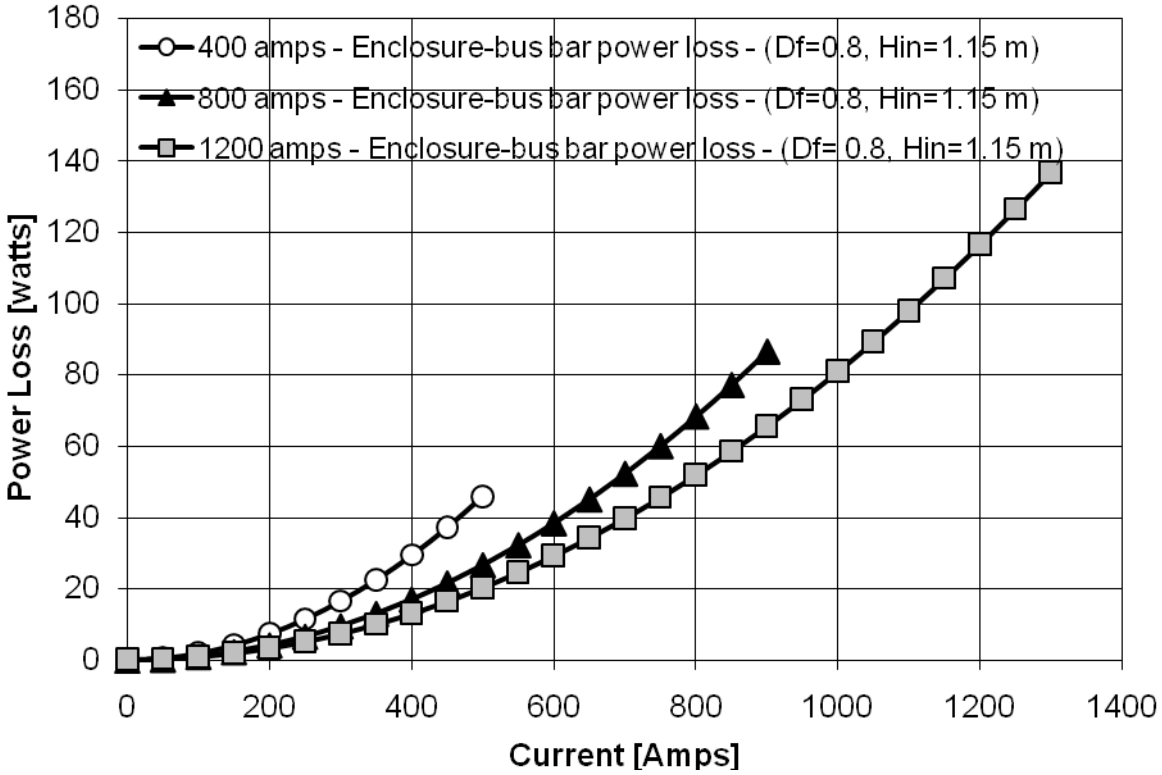

Figure 5.7: Illustrates of Results from Equation (5.7)

Chapter Summary

The model of enclosure-bus bar power loss at any load represented by equation (5.7) is based on the enclosure-bus bar power losses at rated loads determined by the sum of the enclosure and three phase bus bars power losses at rated loads. In this study, the power panelboard enclosure dimensions were collected from the General Electric Company data. Bus bar dimensions for 250, 400, 600, 800 and 1200 amps ratings were selected from the UL 67-1993 standard and the ambient and bus bar operating temperatures were chosen from the UL 891-1992 standard. The enclosure and three phase bus bar power losses at rated loads were

estimated from analytical models reported by Del Vecchio (2003) and White and Piesciorovsky (2009), respectively.

The panelboard enclosure-bus bar model studied in this chapter has certain similarities with a bus-way geometry. The published 600 volts copper bus-way power losses at rated loads reported by McDonald & Hickok (1985) were compared with the calculated panelboard enclosure-bus bar power losses at rated loads and this comparison showed similarities with a variation of ±30 % as shown in Figure 5.6.

CHAPTER 6 – Power Panelboard

The objective of this chapter is to create the panelboard power loss models that could estimate the power losses in the main breaker and main fusible switch power panelboards. The loss model is based on the sum of the breaker, fusible switch, motor starter, and enclosure-bus bar dissipated power estimations described in previous chapters. An example using the main breaker and fusible switch panelboard power loss models and Rubin's (1979) method will be presented.

Panelboard Power Loss Model

The panelboard power loss model can be represented by a one line diagram as shown in Figure 6.1. The panelboard power loss model has a main branch that feeds all secondary branches. The main branch has a main disconnecting device (breaker or fusible switch) and an enclosure-bus bar, while the secondary branches have breakers, fusible switches, and motor starters.

Two panelboard power loss models were created in this study being the main breaker and main switch fusible panelboard power loss models. The panelboard power loss model was created based on the electrical devices found in power panelboards.

The dissipated power is determined by summing the main branch enclosure-bus bar loss given by equation (5.7), the main and/or secondary branch breaker losses given by equation (2.4), the main and/or secondary branch general application fusible switch loss given by equation (3.9), the secondary branch motor application fusible switch loss given by equation (3.10), the secondary branch FVNR motor starter loss for ratings of less than 5 hp and given by equation (4.5), the secondary branch FVNR motor starter loss for ratings of 5 hp to 10 hp and given by equation (4.6), the secondary branch FVNR motor starter loss for ratings of 10 hp to 15 hp and given by equation (4.7), and the secondary branch FVNR motor starter loss for ratings of 15 hp to 50 hp and given by equation (4.8).

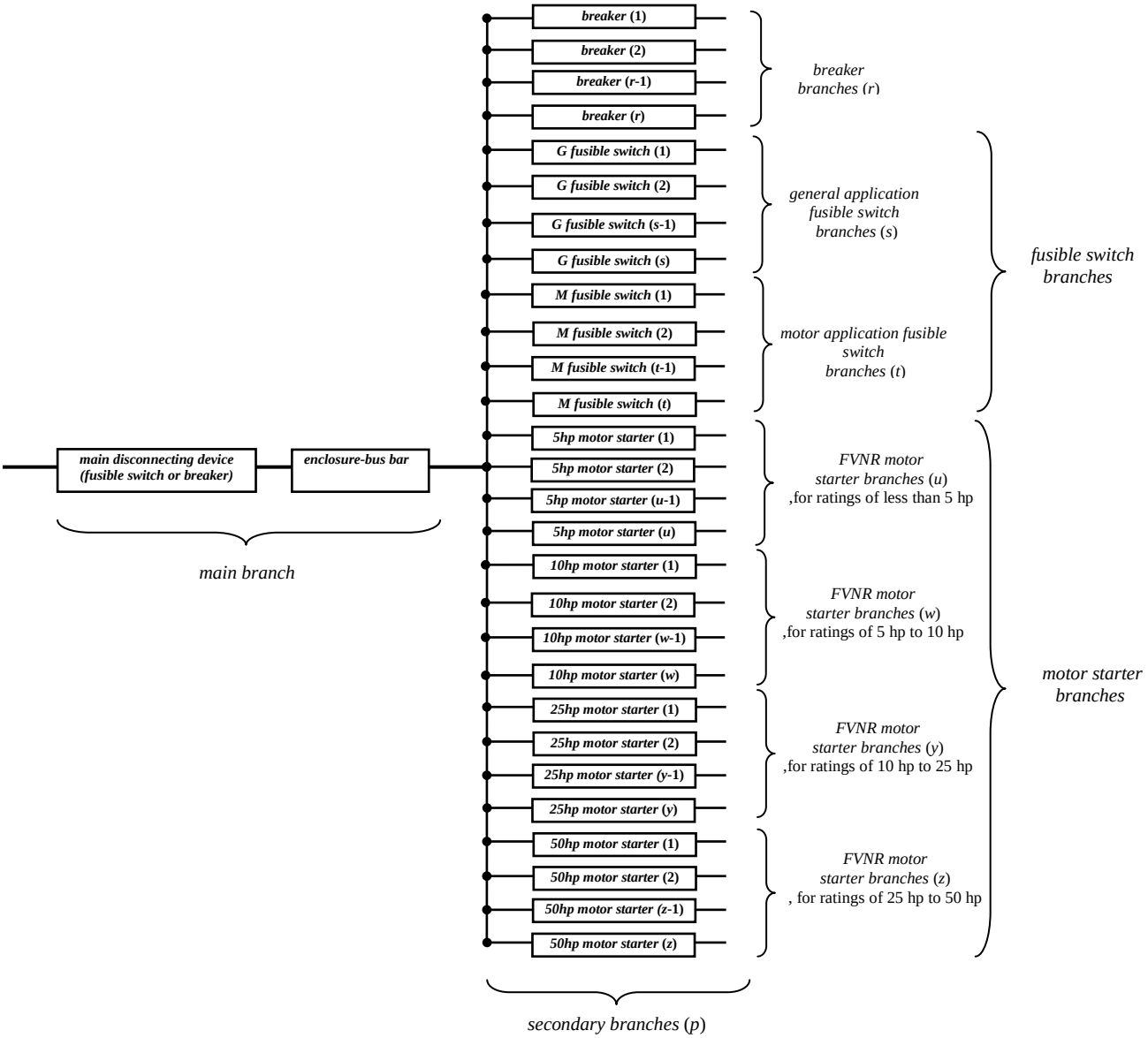

p=number of secondary branches($p=r+s+t+u+w+y+z$) where *r*=number of breakers, *s*=number of general application fusible switches, *t*=number of motor application fusible switches, *u*=number of FVNR motor starters for ratings of less than 5 hp, *w*=number of FVNR motor starters for ratings of 5 to 10 hp, and *y*=number of FVNR motor starters for ratings of 10 to 25 hp, and *z*=number of FVNR motor starters for ratings of 25 to 50 hp.

Figure 6.1: One Line Diagram Panelboard Power Loss Model

By inspection of Figure 6.1, the main disconnecting device and enclosure-bus bar load, *I*, in amps is provided by

$$I = \sum_{c=1}^{p} I_c \tag{6.1}$$

where I_c is the secondary branch device load in amps. The main disconnecting device and enclosure-bus bar diversity load factor, *Df*, depends on the diversity load factors given by the secondary branches. Multiplying the currents of equation (6.1) by their corresponding diversity load factors, the main disconnecting device and enclosure-bus bar diversity load factor can be represented by

$$Df = \sum_{c=1}^{p} Df_c \times \frac{I_c}{I} \tag{6.2}$$

where Df_c is the secondary branch device diversity load factor. Equations (6.1) and (6.2) are also used in the main breaker and main fusible switch panelboard loss model. The main breaker panelboard power loss model is given by

$$\begin{aligned}
&Panelboard_{\text{main breaker loss}} = \\
&Main\ Breaker_{loss} \\
&+ Enclosure\ bus\ bar_{loss} \\
&+ Breaker_{loss} \\
&+ General\ application\ fusible\ switch_{loss} \\
&+ Motor\ application\ fusible\ switch_{loss} \\
&+ FVNR\ motor\ starter\ \ for\ ratings\ of\ \ less\ than\ 5\ hp_{loss} \\
&+ FVNR\ motor\ starter\ \ for\ ratings\ of\ \ 5\ hp\ to\ 10\ hp_{loss} \\
&+ FVNR\ motor\ starter\ \ for\ ratings\ of\ \ 10\ hp\ to\ 25\ hp_{loss} \\
&+ FVNR\ motor\ starter\ \ for\ ratings\ of\ \ 25\ hp\ to\ 50\ hp_{loss}.
\end{aligned}$$

By substituting for the various quantities produces

$$\begin{aligned}
&Panelboard_{\text{main breaker loss}} = \\
&\left(\left\{ \left[\sum_{c=1}^{p} Df_c \times \frac{I_c}{I} \right] \times \left[\sum_{c=1}^{p} I_c \right] \right\}^2 \times \left[\frac{0.2658}{I_{br}} \right] \right) \\
&+ \left(\left\{ \left[\sum_{c=1}^{p} Df_c \times \frac{I_c}{I} \right] \times \left[\sum_{c=1}^{p} I_c \right] \right\}^2 \times H_{in} \times \left[0.00004 + 0.0839 \times I_{bus}^{-1} \right] \right) \\
&+ \left(\sum_{e=1}^{r} \left[Df_e \times I_e \right]^2 \times \left[\frac{0.2658}{I_{br_e}} \right] \right) \\
&+ \left(\sum_{g=1}^{s} \left[Df_g \times I_g \right]^2 \times \left\{ [0.0839 \times I_{sr\,g}^{-1}] + [6 \times 10^{-7} \times I_{fr\,g} - 3 \times 10^{-4} + 0.3189 \times I_{fr\,g}^{-1}] \right\} \right) \\
&+ \left(\sum_{h=1}^{t} \left[Df_h \times I_h \right]^2 \times \left\{ [0.0839 \times I_{sr_h}^{-1}] + [6 \times 10^{-7} \times I_{fr_h} + 3 \times 10^{-5} + 0.2307 \times I_{fr_h}^{-1}] \right\} \right) \\
&+ \left(\sum_{j=1}^{u} 6 + \left\{ \left[Df_j \times I_j \right]^2 \times \left[6 \times 10^{-7} \times I_{fr\,j} + 0.05473 + 0.2307 \times I_{fr\,j}^{-1} \right] \right\} \right) \\
&+ \left(\sum_{k=1}^{w} 7 + \left\{ \left[Df_k \times I_k \right]^2 \times \left[6 \times 10^{-7} \times I_{fr_k} + 0.03273 + 0.2307 \times I_{fr_k}^{-1} \right] \right\} \right) \\
&+ \left(\sum_{m=1}^{y} 8.7 + \left\{ \left[Df_m \times I_m \right]^2 \times \left[6 \times 10^{-7} \times I_{fr_m} + 0.01773 + 0.2307 \times I_{fr_m}^{-1} \right] \right\} \right) \\
&+ \left(\sum_{n=1}^{z} 15.5 + \left\{ \left[Df_n \times I_n \right]^2 \times \left[6 \times 10^{-7} \times I_{fr_n} + 0.00373 + 0.2307 \times I_{fr_n}^{-1} \right] \right\} \right)
\end{aligned} \tag{6.3}$$

where the various quantities are defined in Table 6.1.

Table 6.1: Symbols, Definitions and Units of Power Loss Models for Panelboards

Symbols	Definitions	Units
$Panelboard_{\ main\ breaker\ loss}$	Panelboard power loss	watts
Df_c	Load diversity factor of secondary branch device	0 to 1
I_c	Main breaker ampere rating	Amps
I	Total load of secondary branches	Amps
Ibr	Main breaker ampere rating	Amps
Hin	Interior height	meters
$Ibus$	Bus bar ampere rating	Amps
Df_e	Load diversity factor of secondary branch breaker	0 to 1
I_e	Breaker load of secondary branch	Amps
Ibr_e	Breaker ampere rating of secondary branch	Amps
Df_g	Load diversity factor of general application fusible switch in secondary branch	0 to 1
I_g	Load of general application fusible switch in secondary branch	Amps
Isr_g	Ampere rating of general application switch in secondary branch	Amps
Ifr_g	Ampere rating of general application fuse in secondary branch	Amps
Df_h	Load diversity factor of motor application fusible switch in secondary branch	0 to 1
I_h	Load of motor application fusible switch in secondary branch	Amps
Isr_h	Ampere rating of motor application switch in secondary branch	Amps
Ifr_h	Ampere rating of motor application fuse in secondary branch	Amps
Df_j	Load diversity factor of FVNR motor starter for ratings of less than 5 hp	0 to 1
I_j	Load of FVNR motor starter for ratings of less than 5 hp	Amps
Ifr_j	Fuse ampere rating of FVNR motor starter for ratings of less than 5 hp	Amps
Df_k	Load diversity factor of FVNR motor starter for ratings of 5 to 10 hp	0 to 1
I_k	Load of FVNR motor starter for ratings of 5 to 10 hp	Amps
Ifr_k	Fuse ampere rating of FVNR motor starter for ratings of 5 to 10 hp	Amps
Df_m	Load diversity factor of FVNR motor starter for ratings of 10 to 25 hp	0 to 1
I_m	Load of FVNR motor starter for ratings of 10 to 25 hp	Amps
Ifr_m	Fuse ampere rating of FVNR motor starter for ratings of 10 to 25 hp	Amps
Df_n	Load diversity factor of FVNR motor starter for ratings of 25 to 50 hp	0 to 1
I_n	Load of FVNR motor starter for ratings of 25 to 50 hp	Amps
Ifr_n	Fuse ampere rating of FVNR motor starter for ratings of 25 to 50 hp	Amps

The main fusible switch panelboard power loss model is given by

$$
\begin{aligned}
&Panelboard_{\,main\ fusible\ switch\ loss} = \\
&Main\ fusible\ switch_{loss} \\
&+ Enclosure\ bus\ bar_{loss} \\
&+ Breaker_{loss} \\
&+ General\ application\ fusible\ switch_{loss} \\
&+ Motor\ application\ fusible\ switch_{loss} \\
&+ FVNR\ motor\ starter\ \ for\ ratings\ of\ less\ than\ 5\ hp_{loss} \\
&+ FVNR\ motor\ starter\ \ for\ ratings\ of\ 5\ hp\ to\ 10\ hp_{loss} \\
&+ FVNR\ motor\ starter\ \ for\ ratings\ of\ 10\ hp\ to\ 25\ hp_{loss} \\
&+ FVNR\ motor\ starter\ \ for\ ratings\ of\ 25\ hp\ to\ 50\ hp_{loss}.
\end{aligned}
$$

By substituting for the various quantities produces

$$
\begin{aligned}
&Panelboard_{main\ \ fusible\ \ switch\ \ loss} = \\
&\left(\left\{\left[\sum_{c=1}^{p} Df_c \times \frac{I_c}{I}\right] \times \left[\sum_{c=1}^{p} I_c\right]\right\}^2 \times \left\{[0.0839 \times I_{sr}{}^{-1}] + [6 \times 10^{-7} \times I_{fr} - 3 \times 10^{-4} + 0.3189 \times I_{fr}{}^{-1}]\right\}\right) \\
&+ \left(\left\{\left[\sum_{c=1}^{p} Df_c \times \frac{I_c}{I}\right] \times \left[\sum_{c=1}^{p} I_c\right]\right\}^2 \times H_{in} \times \left[0.00004 + 0.0839 \times I_{bus}{}^{-1}\right]\right) \\
&+ \left(\sum_{e=1}^{r} [Df_e \times I_e]^2 \times \left[\frac{0.2658}{I_{br_e}}\right]\right) \\
&+ \left(\sum_{g=1}^{s} [Df_g \times I_g]^2 \times \left\{[0.0839 \times I_{sr\,g}{}^{-1}] + [6 \times 10^{-7} \times I_{fr\,g} - 3 \times 10^{-4} + 0.3189 \times I_{fr\,g}{}^{-1}]\right\}\right) \\
&+ \left(\sum_{h=1}^{t} [Df_h \times I_h]^2 \times \left\{[0.0839 \times I_{sr_h}{}^{-1}] + [6 \times 10^{-7} \times I_{fr_h} + 3 \times 10^{-5} + 0.2307 \times I_{fr_h}{}^{-1}]\right\}\right) \\
&+ \left(\sum_{j=1}^{u} 6 + \left\{[Df_j \times I_j]^2 \times \left[6 \times 10^{-7} \times I_{fr\,j} + 0.05473 + 0.2307 \times I_{fr\,j}{}^{-1}\right]\right\}\right) \\
&+ \left(\sum_{k=1}^{w} 7 + \left\{[Df_k \times I_k]^2 \times \left[6 \times 10^{-7} \times I_{fr_k} + 0.03273 + 0.2307 \times I_{fr_k}{}^{-1}\right]\right\}\right) \\
&+ \left(\sum_{m=1}^{y} 8.7 + \left\{[Df_m \times I_m]^2 \times \left[6 \times 10^{-7} \times I_{fr_m} + 0.01773 + 0.2307 \times I_{fr_m}{}^{-1}\right]\right\}\right) \\
&+ \left(\sum_{n=1}^{z} 15.5 + \left\{[Df_n \times I_n]^2 \times \left[6 \times 10^{-7} \times I_{fr_n} + 0.00373 + 0.2307 \times I_{fr_n}{}^{-1}\right]\right\}\right)
\end{aligned}
\qquad (6.4)
$$

where $Panelboard_{\,main\ fusible\ loss}$ is the panelboard power loss in watts, I_{sr} is the main switch current rating in amps, and I_{fr} is the main fuse current rating in amps.

The power loss in panelboards can be estimated by collecting and summing switch, fuse, breaker, FVNR motor starter, and bus bar power losses from manufacturer literature. This method is too complicated because too much information has to be considered from different sources. Equations (6.3) and (6.4) summarize the power loss information that was collected

from tests and publications and these main breaker and fusible switch panelboard power loss models are valid under the following conditions:

Indoor panelboard of 0.6/1 kV
Normal frequency of 60 Hz
Three phase balanced currents (no fault situations or unbalanced loads)
Copper bus bar conductivity of 98.9 % IACS
Galvanized steel sheet enclosure
Room temperature of 25^{0}C
Bus bar temperature rise of 65^{0}C

Example based on Power Loss Models

An 800 ampere main breaker panelboard and a 600 ampere main fusible switch power paneboard will be installed in a room and the dissipated power loss from the panelboards has to be estimated to size the HVAC equipment. Both panelboards are 480 volts.

In Figure 6.2, the front view of the power panelboards are shown. The electrical equipment and load characteristics of the main and secondary branch feeders are shown in each cubicle. In this example, the panelboard enclosure interior height dimension was obtained from Table B.1 of Appendix B.

The 800 ampere power panelboard has a main breaker that feeds the secondary branch devices which consist of 3 fusible switches, 4 breakers, and 3 FVNR motor starters. The 600 ampere power panelboard has a main fusible switch that feeds the secondary branch devices which consist of 4 fusible switches and 6 breakers.

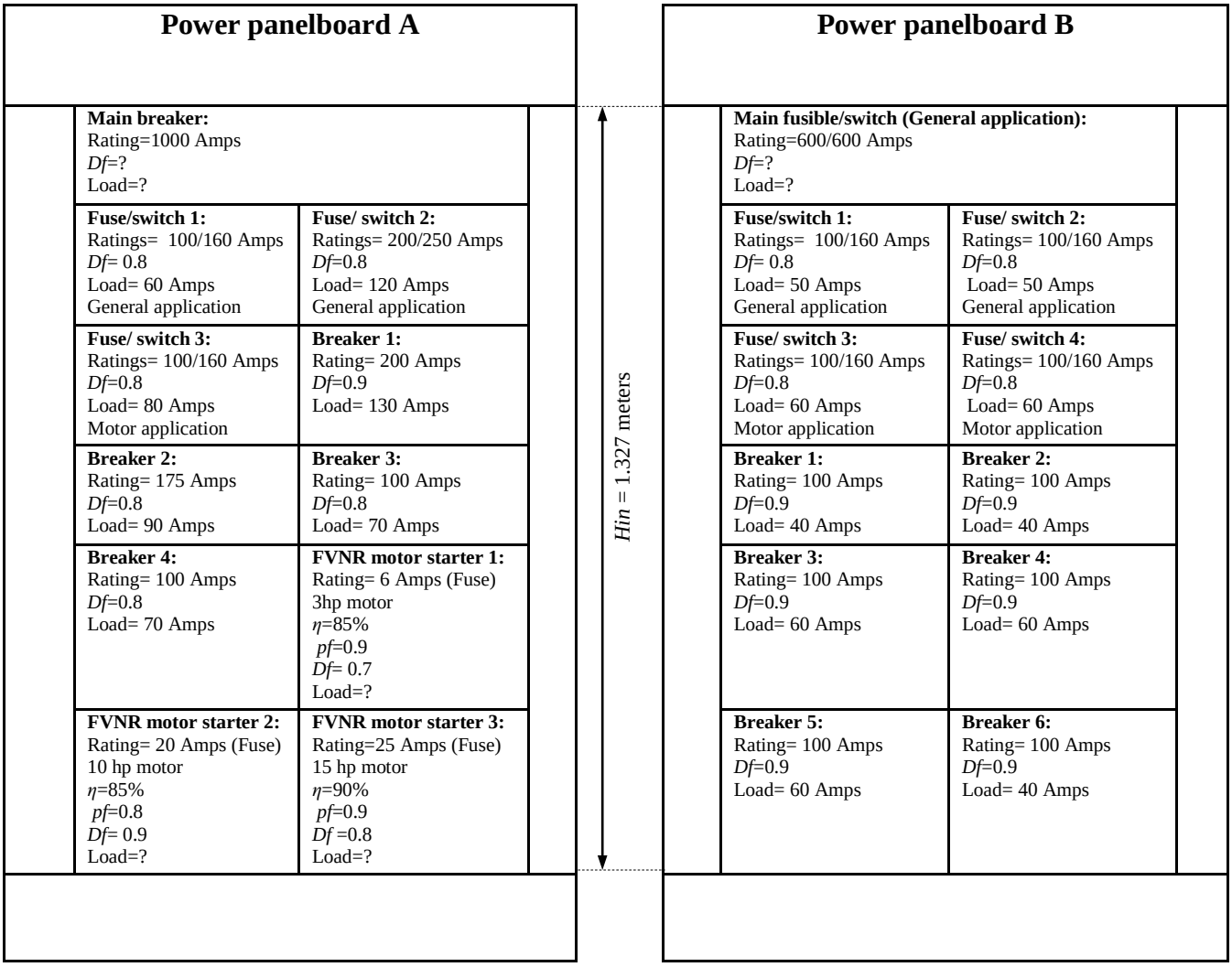

Df= diversity factor, *pf*= motor power factor, η= motor efficiency, and *Hin*=interior height

Figure 6.2: Main Breaker (left) and Fusible Switch (right) Power Panelboards - Front View

The approach taken for estimating the heat loss rate is to (1) calculate the FVNR motor starter, bus bar, and main disconnecting device load currents, (2) determine the main breaker and fusible switch diversity factors, and (3) compute the main breaker and fusible switch power losses and total power loss.

1) Load Currents

The FVNR motor starter load currents are found from

$$I = \frac{\left[\dfrac{P_{hp} \times 0.746}{\eta / 100}\right] \times 1000}{V_{line} \times \sqrt{3} \times pf} \tag{6.5}$$

where I is the motor starter load in amps, P_{hp} is the motor power in horse-power, η is the motor efficiency in percent, V_{line} is the motor line to line voltage in volts, and pf is the motor power factor. Equation (6.5) was developed in White et al. (2004b). The FVNR motor starter load currents designated as I_j, I_k, and I_m are determined in Table 6.2.

Table 6.2: **Determination of FVNR starter load currents**

Power panelboard A
FVNR motor starter 1, for ratings of less than 5 hp**:** $$I_j = \frac{\left[\frac{3hp \times 0.746}{85\%/100}\right] \times 1000}{480volts \times \sqrt{3} \times 0.9} = \frac{2.6329 \times 1000}{748.24} = 3.5amps$$
FVNR motor starter 2, for ratings of 5 hp to 10 hp: $$I_k = \frac{\left[\frac{10hp \times 0.746}{85\%/100}\right] \times 1000}{480volts \times \sqrt{3} \times 0.8} = \frac{8.77647 \times 1000}{665.11} = 13.2amps$$
FVNR motor starter 3, for ratings of 10 hp to 25 hp**:** $$I_m = \frac{\left[\frac{15hp \times 0.746}{90\%/100}\right] \times 1000}{480volts \times \sqrt{3} \times 0.9} = \frac{12.4333 \times 1000}{748.24} = 16.6amps$$
Power panelboard B
The power panelboard B does not have FVNR motor starters.

The bus bar, and main device load current, I, in amps is found using equation (6.1). For panelboard A the main breaker and bus bar load current is

$$I = \sum_{c=1}^{p} I_c = 60 + 120 + 80 + 130 + 90 + 70 + 70 + 3.5 + 13.2 + 16.6 = 653.3amps \qquad (6.6)$$

while the main fusible switch and bus bar load current for panelboard B is

$$I = \sum_{c=1}^{p} I_c = 50 + 50 + 60 + 60 + 40 + 40 + 60 + 60 + 60 + 40 = 520amps \quad . \qquad (6.7)$$

2) Diversity Factors

The main breaker (or fusible switch) and bus bar diversity factor, Df , is determined by equation (6.2) and data shown in Figure 6.2. For panelboard A, the diversity factor is

$$Df = \sum_{c=1}^{p} Df_c \times \frac{I_c}{I} = 0.8 \times \frac{60}{653.3} + 0.8 \times \frac{120}{653.3} + 0.8 \times \frac{80}{653.3} + 0.9 \times \frac{130}{653.3} + 0.8 \times \frac{90}{653.3} + 0.8 \times \frac{70}{653.3}$$
$$+ 0.8 \times \frac{70}{653.3} + 0.7 \times \frac{3.5}{653.3} + 0.9 \times \frac{13.2}{653.3} + 0.8 \times \frac{16.6}{653.3} = 0.073 + 0.147 + 0.098 + 0.179 + 0.110 + 0.086 \quad (6.8)$$
$$+ 0.086 + 0.004 + 0.018 + 0.020 = 0.82$$

while for panelboard B, the diversity factor is

$$Df = \sum_{c=1}^{p} Df_c \times \frac{I_c}{I} = 0.8 \times \frac{50}{520} + 0.8 \times \frac{50}{520} + 0.8 \times \frac{60}{520} + 0.8 \times \frac{60}{520} + 0.9 \times \frac{40}{520} + 0.9 \times \frac{40}{520}$$
$$+ 0.9 \times \frac{60}{520} + 0.9 \times \frac{60}{520} + 0.9 \times \frac{60}{520} + 0.9 \times \frac{40}{520} = 0.077 + 0.077 + 0.092 + 0.092 + 0.069 + 0.069 \quad (6.9)$$
$$+ 0.104 + 0.104 + 0.104 + 0.069 = 0.86$$

3) Component and Total Losses

The partial power losses are obtained from the main breaker panelboard power loss model given by equation (6.3) and the main fusible switch panelboard power loss model given by equation (6.4).
For panelboard A

$$Panelboard_{\,main\ breaker\ loss} =$$
$$\left(\{0.82 \times 653.3\}^2 \times \left[\frac{0.2658}{1000} \right] \right) \quad (6.10)$$
$$+ \left(\{0.82 \times 653.3\}^2 \times 1.327 \times \left[0.00004 + 0.0839 \times 800^{-1} \right] \right)$$
$$+ \left(\left[0.9 \times 130 \right]^2 \times \left[\frac{0.2658}{200} \right] \right) + \left(\left[0.8 \times 90 \right]^2 \times \left[\frac{0.2658}{175} \right] \right)$$
$$+ \left(\left[0.8 \times 70 \right]^2 \times \left[\frac{0.2658}{100} \right] \right) + \left(\left[0.8 \times 70 \right]^2 \times \left[\frac{0.2658}{100} \right] \right)$$
$$+ \left(\left[0.8 \times 60 \right]^2 \times \left\{ \left[0.0839 \times 160^{-1} \right] + \left[6 \times 10^{-7} \times 100 - 3 \times 10^{-4} + 0.3189 \times 100^{-1} \right] \right\} \right)$$
$$+ \left(\left[0.8 \times 120 \right]^2 \times \left\{ \left[0.0839 \times 250^{-1} \right] + \left[6 \times 10^{-7} \times 200 - 3 \times 10^{-4} + 0.3189 \times 200^{-1} \right] \right\} \right)$$
$$+ \left(\left[0.8 \times 80 \right]^2 \times \left\{ \left[0.0839 \times 160^{-1} \right] + \left[6 \times 10^{-7} \times 100 + 3 \times 10^{-5} + 0.2307 \times 100^{-1} \right] \right\} \right)$$
$$+ \left(6 + \left\{ \left[0.7 \times 3.5 \right]^2 \times \left[6 \times 10^{-7} \times 6 + 0.05473 + 0.2307 \times 6^{-1} \right] \right\} \right)$$
$$+ \left(7 + \left\{ \left[0.9 \times 13.2 \right]^2 \times \left[6 \times 10^{-7} \times 20 + 0.03273 + 0.2307 \times 20^{-1} \right] \right\} \right)$$
$$+ \left(8.7 + \left\{ \left[0.8 \times 16.6 \right]^2 \times \left[6 \times 10^{-7} \times 25 + 0.01773 + 0.2307 \times 25^{-1} \right] \right\} \right)$$

$$= 76.28 watts + 55.10 watts + 18.19 watts + 7.87 watts + 8.33 watts + 8.33 watts + 8.00 watts$$
$$+ 16.13 watts + 11.97 watts + 6.60 watts + 13.25 watts + 13.46 watts = 244 watts.$$

For panelboard B

$$
\begin{aligned}
&Panelboard_{\ main\ fusible\ switch\ loss} = \\
&\left(\left[0.86\times 520\right]^2 \times \left\{\left[0.0839\times 600^{-1}\right]+\left[6\times 10^{-7}\times 600-3\times 10^{-4}+0.3189\times 600^{-1}\right]\right\}\right) \\
&+\left(\left\{0.86\times 520\right\}^2 \times 1.327\times\left[0.00004+0.0839\times 800^{-1}\right]\right) \\
&+\left(\left[0.9\times 40\right]^2\times\left[\frac{0.2658}{100}\right]\right)+\left(\left[0.9\times 40\right]^2\times\left[\frac{0.2658}{100}\right]\right) \\
&+\left(\left[0.9\times 60\right]^2\times\left[\frac{0.2658}{100}\right]\right)+\left(\left[0.9\times 60\right]^2\times\left[\frac{0.2658}{100}\right]\right) \\
&+\left(\left[0.9\times 60\right]^2\times\left[\frac{0.2658}{100}\right]\right)+\left(\left[0.9\times 40\right]^2\times\left[\frac{0.2658}{100}\right]\right) \\
&+\left(\left[0.8\times 50\right]^2 \times \left\{\left[0.0839\times 160^{-1}\right]+\left[6\times 10^{-7}\times 100-3\times 10^{-4}+0.3189\times 100^{-1}\right]\right\}\right) \\
&+\left(\left[0.8\times 50\right]^2 \times \left\{\left[0.0839\times 160^{-1}\right]+\left[6\times 10^{-7}\times 100-3\times 10^{-4}+0.3189\times 100^{-1}\right]\right\}\right) \\
&+\left(\left[0.8\times 60\right]^2 \times \left\{\left[0.0839\times 160^{-1}\right]+\left[6\times 10^{-7}\times 100+3\times 10^{-5}+0.2307\times 100^{-1}\right]\right\}\right) \\
&+\left(\left[0.8\times 60\right]^2 \times \left\{\left[0.0839\times 160^{-1}\right]+\left[6\times 10^{-7}\times 100+3\times 10^{-5}+0.2307\times 100^{-1}\right]\right\}\right)
\end{aligned}
\qquad (6.11)
$$

$$
\begin{aligned}
&= 146.25watts + 38.41watts + 3.45watts + 3.45watts + 7.75watts + 7.75watts + 7.75watts \\
&+ 3.45watts + 5.56watts + 5.56watts + 6.73watts + 6.73watts = 243watts.
\end{aligned}
$$

Finally, the total power loss of panelboard A and B is

$$244watts + 243watts = 487watts.$$

Example based on Rubin's (1979) Method

Rubin (1979) reported power panelboard losses based on the number of single pole circuit breakers used by the power panelboard (Table 1.1). The panelboard losses are determined from Table 1.1 and the total number of single pole circuit breakers given by all single poles of all breakers, fusible switches and motor starters in the panelboard A and B of Figure 6.2.

In this case, each panelboard has eleven three pole devices. The number of single pole devices is 33 (11 x 3) for each panelboard. To estimate the power loss of a 33 single pole panelboard, a linear interpolation between the 24 (300 watts) and 36 (450 watts) single pole devices is made by

$$Power\ Loss_x = Power\ Loss_0 + \frac{\left(N^\circ\ poles_x - N^\circ\ poles_0\right)\times\left(Power\ Loss_1 - Power\ Loss_0\right)}{\left(N^\circ\ poles_1 - N^\circ\ poles_0\right)} \qquad (6.12)$$

$$= 300watts + \frac{(24-33)\times(450watts - 300watts)}{(36-24)} = 412.5watts$$

where $Power\ Loss_x$ is the unknown power loss in watts, $Power\ Loss_0$ and $Power\ Loss_1$ are the known adjacent power loss values in watts, $N^\circ poles_x$ is the number of single poles corresponding to $Power\ Loss_x$, and $N^\circ poles_0$ and $N^\circ poles_1$ are the number of single poles corresponding to $Power\ Loss_0$ and $Power\ Loss_1$, respectively. The total power losses of the panelboards A and B will be 825 watts. The power loss estimated by Rubin (1979) overestimated the power losses by approximately 70% with respect to the results obtained with the power loss models.

Chapter Summary

The main breaker and main fusible switch panelboard power loss models were created based on the electrical devices that make up these equipment. Equations (6.3) and (6.4) represent the main breaker and main fusible switch panelboard power loss models for estimating the rate of dissipated heat. In this chapter, the main breaker and main fusible switch panelboard power losses were determined from the component losses from the breaker, fusible switch, FVNR motor starter, and enclosure bus bar models which have been verified in the previous chapters.

Application of these models and Rubin's method was shown in an example. Then, the results obtained from Rubin's method and the power loss models were compared. Rubin (1979) overestimated the power losses by approximately 70% with respect to the results obtained with these power loss models.

CHAPTER 7 – Conclusions

The creation of power loss models that replace and simplify the estimation of electrical equipment power losses based on tabulated data is the main goal of this thesis. Breaker, fusible switch, FVNR motor starter, and enclosure- bus bar published and test power loss data were collected and power loss models were created through regression for each electrical device used in power panelboards. The main breaker and main fusible switch panelboard power loss models were created based on the sum of the power losses from each of the component devices making up the power panelboards. Equations (6.3) and (6.4) provide the loss models for estimating the losses for a given load. Using these loss models and Rubin's method in the same loss example, it was shown that panelboard power losses can be significantly overestimated when calculated with one of the methods currently used. This can result in erroneous sizing of HVAC equipment.

Contribution for Estimating Panelboard Power Losses to Size HVAC Equipment

To size the required HVAC equipment in industrial and commercial buildings, design engineers must estimate the power losses from heat sources, such as power panelboards and other electrical equipment. Today, papers from McDonald & Hickok (1985) and Rubin (1979) are used by HVAC designers to estimate the heat rejected by indoor electrical power distribution equipment. However, no accurate power panelboard loss model has been reported.

In this thesis, breaker, fusible switch, FVNR motor starter, and enclosure- bus bar updated power losses collected from published sources and tests were converted into a curve fit power loss model for each panelboard component device. The main breaker and main fusible switch loss models for power panelboards, equations (6.3) and (6.4), respectively, were created based on the sum of breaker, fusible switch, FVNR motor starter, and enclosure- bus bar models.

Electrical Equipment Power Loss Update

The papers of Hickok (1978) and Rubin (1979) were published in the late 70's which contained tables of electrical equipment power loss data. Equipment design modifications have

altered some of the estimate. Old and new power loss estimates were compared in this study. The breaker, fusible switch, FVNR motor starter, and enclosure-bus bar calculated (updated) power losses were compared with McDonald & Hickok (1985) and Rubin (1979) published (dated) power losses.

In Chapter 2, the breaker power loss model was based on test data and was provided by equation (2.2). A comparison of calculated breaker power losses with breaker power losses published by McDonald & Hickok (1985) and Rubin (1979) was performed and is shown in Figures 2.1 and 2.2. In Figure 2.2, the calculated breaker power losses agreed with the published data for breaker frame sizes below 600 amps.

In Chapter 3, the general and motor application fusible switch power loss models were created based on data collected from updated manufacturer literature and are given by equations (3.7) and (3.8). A comparison of calculated losses with losses published by McDonald & Hickok (1985) and Rubin (1979) was shown in Figure 3.4. The calculated fusible switch power losses agreed with the published data for ampere ratings below 150 amps. A second comparison was made in Figure 3.5, where the general and motor application fusible switch power losses using equations (3.7) and (3.8), respectively were compared with the loss data collected from a loss calculator found at the website, http://pps2.com/b1/ndb/. There was some agreement.

In Chapter 4, the NEMA 0, 1, 2 and 3 FVNR fusible switch motor starter power loss models were shown as equations (4.5), (4.6), (4.7), and (4.8), respectively. A comparison of calculated losses with losses provided by McDonald & Hickok (1985) and Rubin (1979) was made in Table 4.6 and shown in Figure 4.7. None of the authors reported the NEMA 0 size motor starter losses or specified the motor starter type (breaker or fusible switch) and configuration (FVNR or FVR). A second comparison of calculated losses with updated losses provided by manufacturer literature from Eaton was made in Table 4.7 and shown in Figure 4.8. There was some agreement. This manufacturer literature did not report the NEMA 0 size motor starter loss and motor starter type (breaker or fusible switch).

In Chapter 5, the panelboard enclosure-bus bar power loss model was based on analytical methods reported by Del Vecchio (2003) and White and Piesciorovsky (2009). In this case, no enclosure-bus bar losses in panelboards were found in publications for comparison.

Breaker and Fusible Switch Power Losses

Sometimes, engineers have to decide between breakers or fusible switches. In this study, an interesting conclusion was obtained comparing the breaker and fusible switch loss models given by equations (2.3), (3.7) and (3.8). For the same frame size-amps or ampere ratings, the fusible switches dissipated more losses than breakers. This means breakers are more energy efficient than fusible switches.

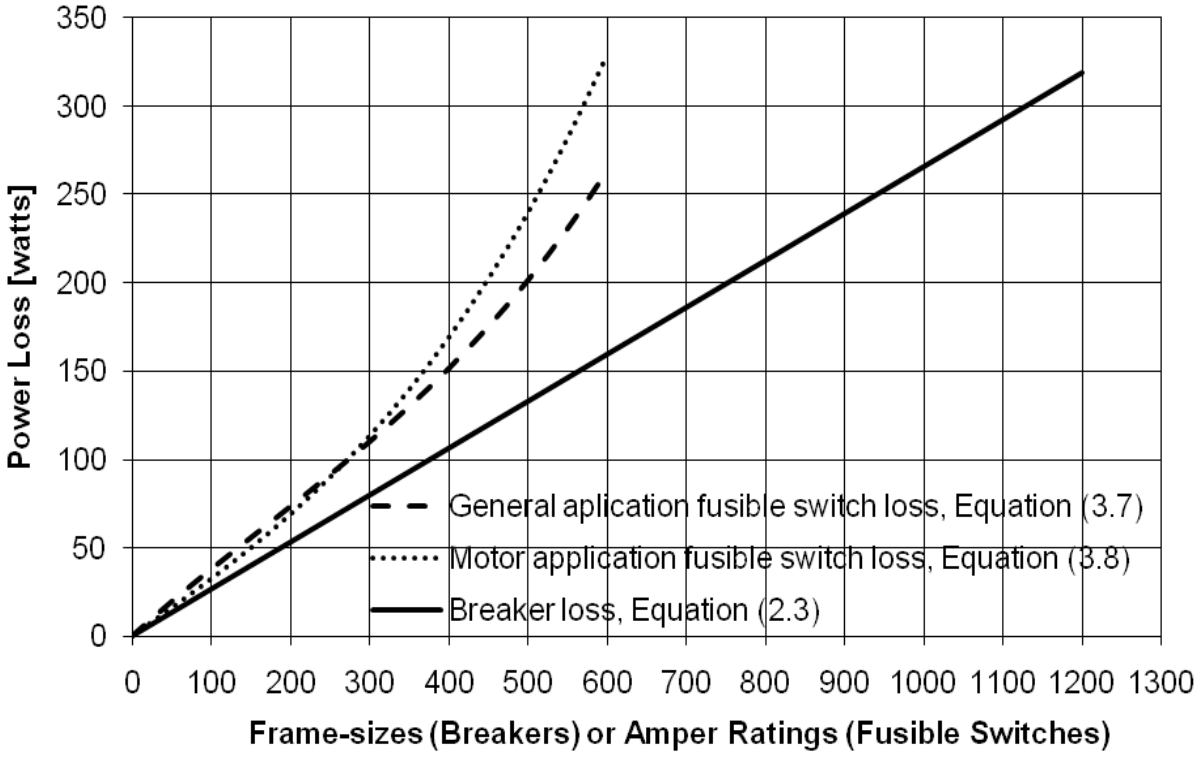

Figure 7.1: Breaker and Fusible Switch Losses. Power Loss Models

Application of Power Panelboard Power Loss Models and Rubin (1979) Method on a Practical Example

The application of the main breaker and main fusible switch panelboard power loss models, equations (6.3) and (6.4), was demonstrated with an example in Chapter 6. These models and Rubin's method were applied to the same example. The results obtained from Rubin's method and the power loss models were compared. Rubin (1979) overestimated the losses by approximately 70% with respect to the results obtained with the power loss models. This can result in erroneous sizing of HVAC equipment.

Future Work

The papers of McDonald & Hickok (1985) and Rubin (1979), and manufacturer literature are used for estimating the rate of heat rejected by switchboards, motor control centers, and switchgears. In those publications, the switchboard, motor control center, and switchgear power losses are based on the power loss sum of electrical components such as enclosures, bus bars, and control and protection devices are presented in tabular form. Using tables to determine the power loss is not as easy as the evaluation of a relatively simple formula. Regression could be used to create switchboard, motor control center, and switchgear power loss models.

Significance of the Work

During this work, a power loss model was created to estimate the heat gain dissipated from power panelboards to size HVAC equipment in industrial plants and buildings. This model represents a more realistic estimation of power losses than Rubin's (1979) method, the model will be very useful for HVAC designers that have to estimate the heat gain created by power panelboards. The calculation has greater accuracy which avoids the oversizing of HVAC equipment and the associated additional equipment cost.

References

Cockcroft, John D. (1929). Skin Effect in Rectangular Conductors at High Frequencies. *Proceedings of the Royal Society A*, vol. 122, pp. 533-542.

Del Vecchio, Robert M. (2003). Eddy-Current Losses in a Conducting Plate Due to a Collection of Bus Bars Carrying Currents of Different Magnitudes and Phases. *IEEE Transactions on Magnetics*, vol. 39 (1), pp. 549-552.

Dwight, Herbert B. (1918). Skin Effect in Tubular and Flat Conductors. *Trans. AIEE*, vol. 37 (II), pp. 1379-1403.

Dwight, Herbert B. (1947). Effective Resistance of Isolated Nonmagnetic Rectangular Conductors. *Trans. AIEE*, vol. 66, pp. 549-552.

Hickok, Herbert. N. (1978). Energy losses in electrical power systems. *IEEE Transactions on Industry Applications*, vol. IA-14 (5), pp 373-387.

IEC 60028-1925. International Standard of Resistance for Copper (Edition 2). *International Electrotechnical Commission*.

IEC 60269-2-2006. Low Voltage Fuses (Edition 3), Part 2: Supplementary requirements for fuses for use by authorized persons (fuses mainly for industrial application) Examples of standardized systems of fuses A to I. *International Electrotechnical Commission*.

IEC 60287-2-1-1994. Electric cables, Calculation of the current rating, Part 2: Thermal resistance, Section 1: Calculation of thermal resistance. *International Electrotechnical Commission*.

IEC 60947-3-2008. Low-voltage switchgear and controlgear (Edition 3), Part 3: Switches, disconnectors, switch disconnectors and fuse-combination units. *International Electrotechnical Commission*.

IEEE C37.13-2008. IEEE Standard for Low-Voltage AC Power Circuit Breakers Used in Enclosures. *The Institute of Electrical and Electronics Engineers*, New York.

IEEE 1458-2005. IEEE Standard Recommended Practice for the Selection, Field Testing, and Life Expectancy of Molded Case Circuit Breakers for Industrial Applications. *The Institute of Electrical and Electronics Engineers*, New York.

IEEE C37.20.1-2002. IEEE Standard for Metal-Enclosed Low-Voltage Power Circuit Breaker Switchgear. *The Institute of Electrical and Electronics Engineers*, New York.

IEEE C37.20.2-1999. IEEE Standard for Metal-Clad Switchgear. *The Institute of Electrical and Electronics Engineers*, New York.

IEEE C37.23-2003. IEEE Standard for Metal-Enclosed Bus. *The Institute of Electrical and Electronics Engineers*, New York.

McDonald, William J., and Herbert N. Hickok (1985). Energy Losses in Electrical Power Systems. *IEEE Transactions on Industry Applications*, vol. IA-21(4), pp 803-819.

NEMA ICS 2-2000. Industrial Control and Systems Controllers, Contactors and Overload Relays Rated 600 Volts. *National Electrical Manufacturers Association*, Virginia.

Rubin, Ira M. (1979). Heat Losses from Electrical Equipment in Generating Stations. *IEEE Transactions on Power Apparatus and Systems*, vol. PAS-98 (4), pp. 1149-1152.

UL 67-1993. Standard for Panelboards. *Underwriters Laboratories*, Eleventh Edition.

UL 248-4-2000. Low-Voltage Fuses - Part 4: Class CC Fuses. *Underwriters Laboratories*, Second Edition.

UL 248-5-2000. Low-Voltage Fuses - Part 5: Class G. *Underwriters Laboratories*, Second Edition.

UL 248-6-2000. Low-Voltage Fuses - Part 6: Class H Non-Renewable Fuses. *Underwriters Laboratories*, Second Edition.

UL 248-7-2000. Low-Voltage Fuses - Part 7: Class H Renewable Fuses. *Underwriters Laboratories*, Second Edition.

UL 248-8-2000. Low-Voltage Fuses - Part 8: Class J Fuses. *Underwriters Laboratories*, Second Edition.

UL 248-9-2000. Low-Voltage Fuses - Part 9: Class K Fuses. *Underwriters Laboratories*, Second Edition.

UL 248-10-2000. Low-Voltage Fuses - Part 10: Class L Fuses. *Underwriters Laboratories*, Second Edition.

UL 248-12-2000. Low-Voltage Fuses - Part 12: Class R Fuses. *Underwriters Laboratories*, Second Edition.

UL 248-15-2000. Low-Voltage Fuses - Part 15: Class T Fuses. *Underwriters Laboratories*, Second Edition.

UL 489-1996. Molded-Case Circuit Breakers, Molded-Case Switches, and Circuit Breaker Enclosures. *Underwriters Laboratories*, Ninth Edition.

UL 891-1992. Dead-Front Switchboards. *Underwriters Laboratories*, Eleventh Edition.

UL 1066-1997. Low-Voltage AC and DC Power Circuit Breakers Used in Enclosures. *Underwriters Laboratories*, Third Edition.

White, Warren N., Anil Pahwa, and Chris Cruz (2004a). Heat Loss from Electrical and Control Equipment in Industrial Plants: Part I – Methods and Scope. *ASHRAE Transactions*, vol. 110 (2), pp. 842-851.

White, Warren N., Anil Pahwa, and Chris Cruz (2004b). Heat Loss from Electrical and Control Equipment in Industrial Plants: Part II – Results and Comparisons. *ASHRAE Transactions*, vol. 110 (2), pp. 852-870.

White, Warren N., and Emilio C. Piesciorovsky (2009). Building Heat Load Contributions from Medium and Low Voltage Switchgear: Part I – Solid Rectangular Bus Bar Heat Losses. *ASHRAE Transactions*, vol. 115 (2), pp. 370-381.

Appendix A: Measurement Cart & Molded Case Circuit Breakers

Measurement Cart Description and Circuit

The measurement cart is a portable measurement station that was used to collect test data for breakers. The measurement cart had three 1:60 (turns ratio) potential transformers (PTs), a three phase power analyzer, three flexible high current transformers (CTs), one laptop PC, a toolbox, voltage probe leads, a serial connection between PC and analyzer, and various power cables. The portable measurement station is shown in Figure A.1.

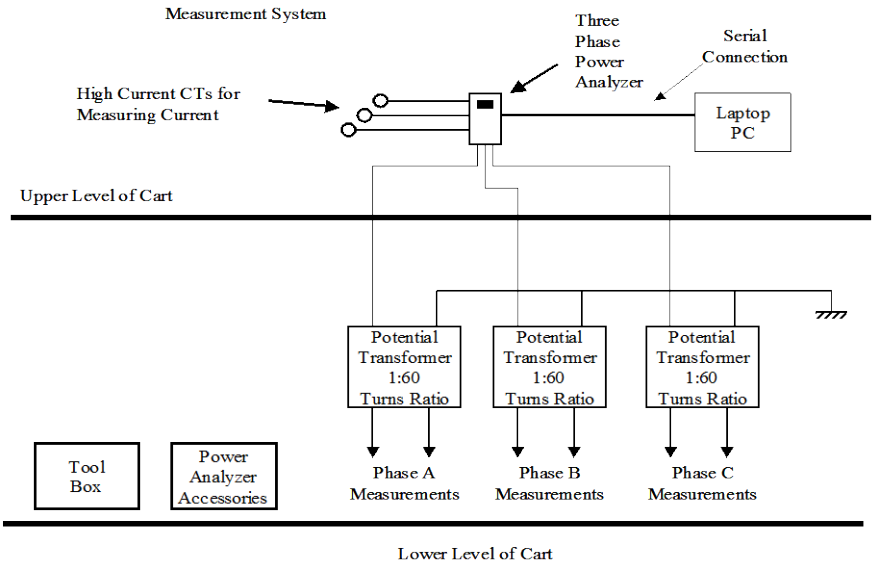

Figure A.1: Measurement Cart System

The measurement cart was used in power panelboards to measure power losses in molded case circuit breakers up to 1200 amps. Power measurements were sampled regularly over a period of several minutes. At each sample point, the resistance of each device phase was calculated and averaged. The resistance at each point in time was determeined as

$$R = (Ratio \times P)/(I)^2 \tag{A.1}$$

where R is the resistance per phase, $Ratio$ is the potential transformer turns ratio (1/60), P is the power loss per phase in watts, and I is the phase current in amperes.

Using the test average resistances per phase of each device (Ra_{Avg}, Rb_{Avg}, Rc_{Avg}), the total resistance (R_T) and power losses for rated current were determined. The device resistances included the enclosure and lug resistances because the breaker was connected to the bus at the time the tests were performed.

Figure A.2 shows the measurement cart during an *in situ* test. The cart with the transformers weighed about 400 lbs. The cart had 6-inch polyurethane wheels that provided smooth and quiet rolling to go from one site to another to take the measurements.

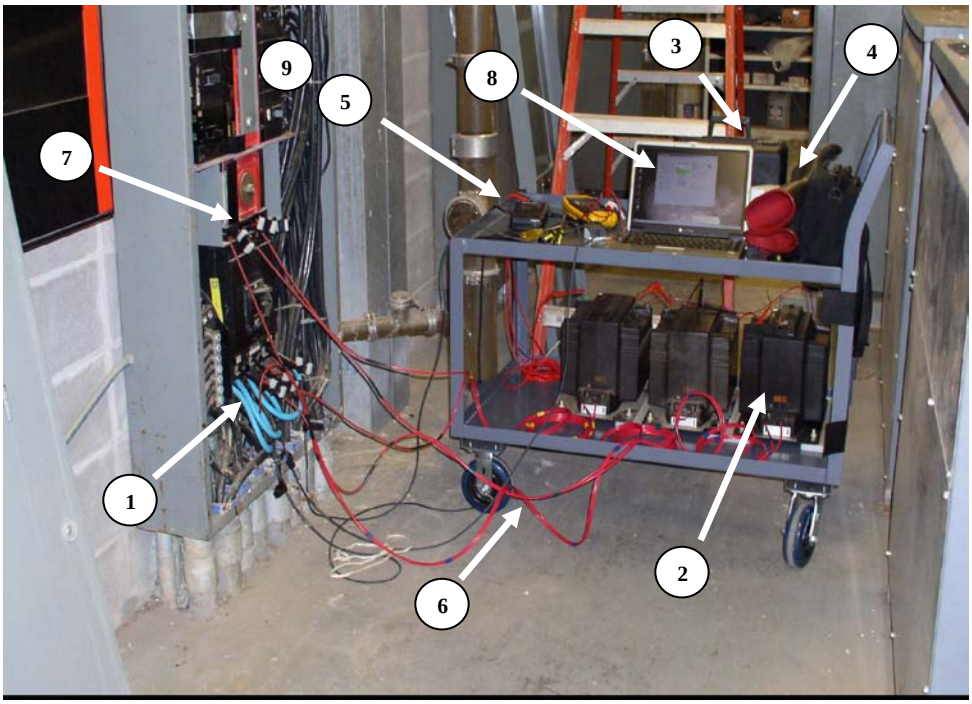

Figure A.2: Portable Measurement Cart

Portable Measurement Cart Accessories

The portable measurement cart (Figure A.2) had the following accessories or parts:

1- Current Transformers: Three flexible high current transformers (CTs) rated from 1 to 3000 amp. This kit also included three 10 to 1000 amp clamp type CTs, and one 400 amp DC CT.

2- Power Transformer: Three single phase potential transformers rated at 15/ 0.25 kV (1:60 turns ratio)

3- Toolbox: It contained several tools such as electric, flat head, and Phillips head screwdrivers, hammer, box of screws, wrench, and others.

4- Electrical Gloves: one pair of gloves (15 kV insulation level)

5- Battery Powered Digital Multimeter: It provided checks on the measurements as necessary (it was included in item 9).

6-Voltage Leads: They provided the necessary conduction from the voltage proves to the power transformer inputs, the potential transformer leads were rated at 40 kV.

7- Voltage Probes: They were designed according to different applications. They were called insulated tip, bus bar and long bus bar probes.

8- Laptop

9- Three Phase Power Analyzer: The data logger from Summit Technologies (Walnut Creek, CA) was used to measure power, current and voltages.

Live Line Testing

For the *in situ* tests performed during this work, each measurement required dismantling of front panels on the equipment, conducting the tests, and re-attaching the panels. The test cart was used to test 70, 175, 200, 225, 250, 300, 350, 400, 450, 600, 800, 1000, 1200 amps molded case circuit breakers in panelboards (Table 3.2). Figure A.3 shows a 1200 amps molded case circuit breaker power loss measurement.

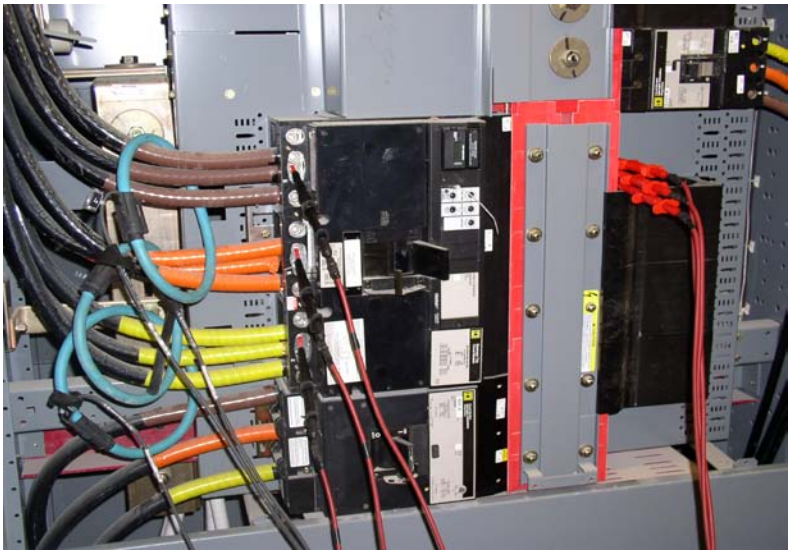

Figure A.3: 1200 Amps Molded Case Circuit Breaker Power Loss Measurement

Appendix B: Enclosure and Bus Bar for Power Panelboards

Enclosure and Bus Bar Cases

The power panelboard enclosure dimensions shown in Table B.1 were collected from General Electric Company literature. The power panelboard enclosures are made of galvanized steel sheet and two types of box thicknesses are used, 1.75 mm for enclosure boxes up to 1016 mm and 2.74 mm for enclosure boxes greater than 1016 mm in width.

Table B.1: Enclosure Power Panelboard Dimensions (115 Cases)

Enclosure Power Panelboard Dimensions in Millimeters							
Power Panelboard Ampere Rating (I_{bus}) [Amps]	Interior Height (H_{in})	Superior Gutter (S_g)	Inferior Gutter (I_g)	Total Height ($H=H_{in}+S_g+I_g$)	Width (W)	Depth (D)	Power Panelboard Enclosure Box Cases
250	628.65	506.47	506.47	1641.59	685.8 / 787.4 / 914.4	292.1	15
	803.4	506.47	333.5	1643.37			
	977.9	506.47	158.75	1643.12			
	1327.15	577.85	361.95	2266.95			
	1676.4	506.47	260.35	2443.22			
400	628.5	506.47	506.47	1641.44	685.8 / 787.4 / 914.4 / 1016 / 1117.6	292.1	30
	803.4	506.47	333.5	1643.37			
	977.9	577.85	361.95	1917.7			
	1152.65	577.85	539.75	2270.25			
	1327.15	577.85	361.95	2266.95			
	1676.4	506.47	260.35	2443.22			
600*	803.4	506.47	333.5	1643.37	685.8 / 787.4 / 914.4 / 1016 / 1117.6	292.1	30
	977.9	577.85	361.95	1917.7			
	1152.65	577.85	539.75	2270.25			
	1327.15*	577.85	361.95	2266.95			
	1501.9	577.85	361.95	2441.7			
	1676.4	506.47	260.35	2443.22			
800*	803.4	577.85	539.75	1921	787.4 / 914.4 / 1016 / 1117.6	292.1	20
	977.9	577.85	361.95	1917.7			
	1152.65	577.85	539.75	2270.25			
	1327.15*	577.85	361.95	2266.95			
	1501.9	577.85	361.95	2441.7			
1200	803.4	577.85	539.75	1921	787.4 / 914.4 / 1016 / 1117.6	292.1	20
	977.9	577.85	361.95	1917.7			
	1152.65	577.85	539.75	2270.25			
	1327.15	577.85	361.95	2266.95			
	1501.9	577.85	361.95	2441.7			

*selected power panelboard dimensions for example in Chapter 6.

From Table B.1, 115 power panelboard enclosure box cases can be obtained. However, considering that enclosure and bus bar power losses are given in "watts/ meter", the panelboard enclosure loss cases can be reduced to 21cases given by the panelboard ampere ratings and dimensions as shown in Table B.2. The panelboard bus bar loss cases can be reduced to a total of 6 cases given by the panelboard ampere ratings and bus bar dimensions as shown in Table B.2. The bus bar dimensions were selected according to the standard, UL 67-1993 that establishes that copper bus bars current density shall be limited by 1000 amps/inch² (155 amps/cm²). The bus bar dimensions, width (*a*) and height (*b*) are listed in Table B.2.

The ambient and bus bar operating temperatures were obtained from the standard, UL 891-1992. The maximum operating bus bar temperature was 90˚C conductor temperature (25˚C room temperature + 65˚C bus bar rise temperature). The conductivity of copper for bus bars is 100% IACS (percent conductivity) according to the IEC 60028-1925 standard. However, lower conductivities are used in copper bus bars for panelboards, increasing losses. A copper conductivity of 98.9% and resistivity of copper at 20˚C of 0.01743 μΩ-m were considered for the three phase bus bar model of Chapter 5. In Figure B.1, enclosure and bus bar power panelboard dimensions listed in Table B.1 and B.2 are denoted.

Table B.2: Enclosure and Bus Bar Power Panelboard Dimensions (21 Cases)

Power Panelboard Amper Rating I_{bus}	Bus Bar Current Density Amps/ inch²	Bus Bar and Enclosure Dimensions [mm]						
		b	*a*	*D*	*C*	*p*	*S*	*W*
250	992 (154)	25.4	6.4	1.75	133.4	287.15	44.4	685.8
		25.4	6.4	1.75	133.4	337.95	44.4	787.4
		25.4	6.4	1.75	133.4	401.45	44.4	914.4
400	793 (123)	50.8	6.4	1.75	120.7	236.35	95.2	685.8
		50.8	6.4	1.75	120.7	287.15	95.2	787.4
		50.8	6.4	1.75	120.7	350.65	95.2	914.4
		50.8	6.4	1.75	120.7	401.45	95.2	1016
		50.8	6.4	2.74	120.7	451.25	95.2	1117.6
600	952 (148)	63.5	6.4	1.75	114.3	210.95	120.6	685.8
		63.5	6.4	1.75	114.3	261.75	120.6	787.4
		63.5	6.4	1.75	114.3	325.25	120.6	914.4
		63.5	6.4	1.75	114.3	376.05	120.6	1016
		63.5	6.4	2.74	114.3	425.85	120.6	1117.6
800	907 (141)	88.9	6.4	1.75	101.6	210.95	171.4	787.4
		88.9	6.4	1.75	101.6	274.45	171.4	914.4
		88.9	6.4	1.75	101.6	325.25	171.4	1016
		88.9	6.4	2.74	101.6	375.05	171.4	1117.6
1200	960 (149)	63.5	12.7	1.75	114.3	258.6	114.3	787.4
		63.5	12.7	1.75	114.3	322.1	114.3	914.4
		63.5	12.7	1.75	114.3	372.9	114.3	1016
		63.5	12.7	2.74	114.3	422.71	114.3	1117.6

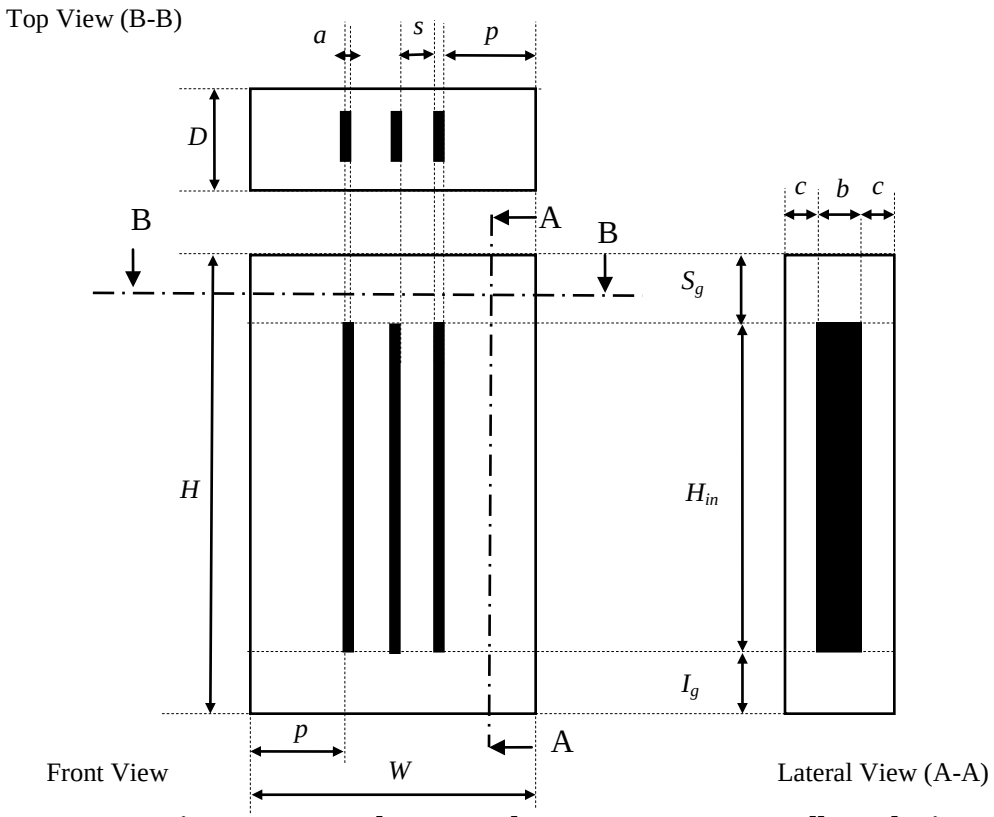

Figure B.1: Enclosure and Bus Bar Power Panelboard Dimensions

Appendix C: Stray Loss

Spreadsheet and Visual Basic Program

The stray losses of the enclosure-bus bar dimension cases pertaining to the different panelboard ampere ratings were estimated using the spreadsheet of Figure D.1. The visual basic program which was part of the spreadsheet was based on the analytical model reported by Del Vecchio (2003).

NONSEGREGATED BUS BARS - STRAY POWER LOSS SPREADSHEET (S.I. Units and Rms Values)

ENCLOSURE

ENTER DATA - ENCLOSURE

Plate Material	Select "1"	FIXED DATA Conductivity (α) Ω/m	Relative Permeability (μr)
Tank steel (TS)	0	4000000	200
Stainless Steel (SS)	1	1333000	1
Aluminum (AL)	0	36000000	1
Copper (CU)	0	50000000	1

You have to choose only one type of plate material

RESULTS - ENCLOSURE

Description	Simbol	Units	Value
Enclosure Material	α	Ω/m	1333000
Air Permeability	μo	……	0.000001256
Enclosure Material Relative Permeability	μr	……	1

BUS BARS

ENTER DATA - BUS BARS

A PhaseCurrent	Ipa	Amps	250
B Phase Current	Ipb	Amps	250
CPhase Current	Ipc	Amps	250
Number of phases	np	…….	3
Conductors per Phase	ncp	……	1
Current Angle	$Phi\ A$	o	0
Current Angle	$Phi\ B$	o	120
Current Angle	$Phi\ C$	o	240
Frequency	f	Hz	60

INTEGRAL

INTEGRATION (FIXED DATA)

Initial limit of the integral	ao	……	0
Number of divisions of the integral	m	……	1000
Step size of the integral	$\Delta x = (1/Hmax)/200$	……	0.03149

The integration stops when the n° of steps is greater than 1000 or the last incremental addition to the integral is less than 1x10^-7

DIMENSIONS

ENTER DATA - ENCLOSURE & BUS BAR DIMENSIONS

CASES — DIMENSIONS

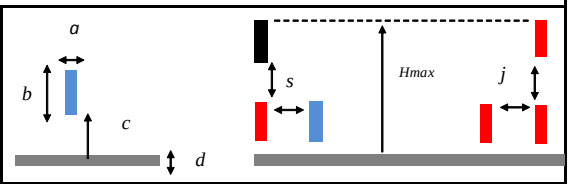

CASES CONFIGURATION	CASE Select "1"	d [m]	c [m]	b [m]	a [m]	s [m]	j [m]	Filament-Plate Maximum Vertical Distance $Hmax$ [m]
1	0	0	0	0	0	0	0	0
2	1	0.00175	0.1334	0.0254	0.0064	0.0444	0	0.1588
3	0	0	0	0	0	0	0	0

RESULTS

2	CAS	Bus Bar Dimensions	0.00175	0.1334	0.0254	0.0064	0.0444	0	0.1588

Reset	To reset all cells click this button	Total Number of Conductors	Filament Current [Amps]
Start	Before starting, click the Reset button	$Numcond = np*ncp$	Phase A / Phase B / Phase C
Omega Factor [$\omega = 2*\prod*f$] [cycle/seg]	376.8	3	$ia = Ipa/ncp*5$ / $ib = Ipb/ncp*5$ / $ic = Ipc/ncp*5$
STRAY POWER LOSS [$P\ stray$] [watts/m]	Final Limit of the Integral [$ao = m*\Delta x$] [meter]		
0.054453737	31.48614693	50	50 / 50

Figure C.1: Stray Power Loss Spreadsheet

VBA Program linked to Stray Power Loss Spreadsheet

Trapezloss Function (Module)

```
Function Trapezloss(ur, Sigma, c, a, b, uo, Omega, Ipa, Ipb, Ipc, PhiA, PhiB, PhiC, d, Numcond, s, CAS, DX)
    % Function to determine the stray loss in metallic enclosures
    % for single and three bus bar phase systems.
    % This calculation follows the procedure developed by Del Vecchio, Robert M.(2003).
    % “Eddy-Current Losses in a Conducting Plate Due to a Collection of Bus Bars Carrying
    % Currents of Different Magnitudes and Phases" which is contained in IEEE Transactions
    % on Magnetics, vol. 39 (1), pp. 549-552.
   ao = 0
   test = 0
   falast = inteval(ao, ur, Sigma, c, a, b, uo, Omega, Ipa, Ipb, Ipc, PhiA, PhiB, PhiC, d, Numcond, s, CAS)
   loss = 0
   Do While test = 0
       ao = ao + DX
       fanext = inteval(ao, ur, Sigma, c, a, b, uo, Omega, Ipa, Ipb, Ipc, PhiA, PhiB, PhiC, d, Numcond, s, CAS)
       dloss = 0.5 * DX * (fanext + falast)
       loss = loss + dloss
       If (Abs(dloss / loss)) < 0.0000001 Then test = 1
       falast = fanext
    Loop
    Trapezloss = loss
End Function

%**************************************************************************
%******* Determine the stray loss for the enclosure, single phase bus bar CAS=1
%******* Determine the stray loss for the enclosure, three phase bus bars CAS=2 (non-flat configuration)
%******* Determine the stray loss for the enclosure, three phase bus bars CAS=3 (flat configuration)
Function inteval(ao, ur, Sigma, c, a, b, uo, Omega, Ipa, Ipb, Ipc, PhiA, PhiB, PhiC, d, Numcond, s, CAS)
    Dim Ic(3), PHI(3), Xc(3), Yc(3), Phase(15), Fc(15), h(15), w(15)
    Pi = 3.14159265358979
       %******* Determine the stray loss for the enclosures, single phase bus bar CAS=1
       If CAS = 1 Then
            Ic(1) = Ipa + Ipb + Ipc
            PHI(1) = 0
            Xc(1) = 0
            Yc(1) = c
            Else
       End If
       %******* Determine the stray loss for the enclosures, three phase bus bars CAS=2 (non-flat configuration)
       If CAS = 2 Then
            Ic(1) = Ipa
            Ic(2) = Ipb
            Ic(3) = Ipc
            PHI(1) = PhiA * Pi / 180
            PHI(2) = PhiB * Pi / 180
            PHI(3) = PhiC * Pi / 180
            Xc(1) = 0
            Xc(2) = a + s
            Xc(3) = Xc(2) + a + s
            Yc(1) = c
            Yc(2) = c
            Yc(3) = c
            Else
       End If
       %******* Determine the stray loss for the enclosures, three phase bus bars CAS=3 (flat configuration)
       If CAS = 3 Then
            Ic(1) = Ipa
            Ic(2) = Ipb
            Ic(3) = Ipc
            PHI(1) = PhiA * Pi / 180
            PHI(2) = PhiB * Pi / 180
            PHI(3) = PhiC * Pi / 180
            Xc(1) = 0
            Xc(2) = 0
            Xc(3) = 0
            Yc(1) = c
            Yc(2) = Yc(1) + b + s
            Yc(3) = Yc(2) + b + s
       End If

    g = 1
    Do While g < Numcond + 1
        J = (g - 1) * 5
        h(1 + J) = Yc(g)
        h(2 + J) = Yc(g)
```

```
        h(3 + J) = Yc(g) + b / 2
        h(4 + J) = Yc(g) + b
        h(5 + J) = Yc(g) + b
        w(1 + J) = Xc(g)
        w(2 + J) = Xc(g) + a
        w(3 + J) = Xc(g) + a / 2
        w(4 + J) = Xc(g)
        w(5 + J) = Xc(g) + a
        Phase(1 + J) = PHI(g)
        Phase(2 + J) = PHI(g)
        Phase(3 + J) = PHI(g)
        Phase(4 + J) = PHI(g)
        Phase(5 + J) = PHI(g)
        Fc(1 + J) = Ic(g) / 5
        Fc(2 + J) = Ic(g) / 5
        Fc(3 + J) = Ic(g) / 5
        Fc(4 + J) = Ic(g) / 5
        Fc(5 + J) = Ic(g) / 5
        g = g + 1
    Loop

    delta = (2 / (Omega * uo * ur * Sigma)) ^ 0.5
    eta = (ao ^ 4 + 4 / delta ^ 4) ^ 0.25
           If ao = 0 Then
                theta = Pi / 4
                Else
                theta = 0.5 * Atn(2 / (ao * delta) ^ 2)
           End If
    Sum = 0
    y = 1
    Do While y < 5 * Numcond + 1
        K = y
        Do While K < 5 * Numcond + 1
            n1 = (ao ^ 2 + 2 * ao * eta * Cos(theta) / ur + (eta / ur) ^ 2)
            n2 = (Exp(2 * eta * d * Cos(theta)) - 1) / (2 * eta * Cos(theta))
            n3 = (ao ^ 2 - 2 * ao * eta * Cos(theta) / ur + (eta / ur) ^ 2)
            n4 = (1 - Exp(-2 * eta * d * Cos(theta))) / (2 * eta * Cos(theta))
            n5 = (ao ^ 2 - (eta / ur) ^ 2) * Sin(2 * eta * d * Sin(theta)) / (eta * Sin(theta))
            n6 = 2 * ao / ur * (Cos(2 * eta * d * Sin(theta)) - 1)
            d1 = (ao ^ 2 + 2 * ao * eta * Cos(theta) / ur + (eta / ur) ^ 2) ^ 2
            d2 = Exp(2 * eta * d * Cos(theta))
            d3 = (ao ^ 2 - 2 * ao * eta * Cos(theta) / ur + (eta / ur) ^ 2) ^ 2
            d4 = Exp(-2 * eta * d * Cos(theta))
            d5 = 2 * ((ao ^ 2 - (eta / ur) ^ 2) ^ 2 - (2 * ao * eta * Sin(theta) / ur) ^ 2)
            d6 = Cos(2 * eta * d * Sin(theta))
            d7 = (8 * ao * eta * Sin(theta) / ur) * (ao ^ 2 - (eta / ur) ^ 2)
            d8 = Sin(2 * eta * d * Sin(theta))
            num = n1 * n2 + n3 * n4 - n5 - n6
            den = d1 * d2 + d3 * d4 - d5 * d6 + d7 * d8
            term = Fc(y)*Fc(K)*Exp(-ao*(h(y)+h(K)))*Cos(ao*(w(y)-w(K)))*num/den*Cos(Phase(y)-Phase(K))
            If y - K < 0 Then term = term * 2
            Sum = Sum + term
            K = K + 1
        Loop
        y = y + 1
    Loop
    Sum = Sum * Sigma / Pi * (Omega * uo) ^ 2
    inteval = Sum

End Function
```

Appendix D: Three Phase Bus Bar Power Loss Effect

Three Phase Bus Bar Power Loss Ratio

An m-file developed by Dr. Warren N. White and based on the method and equations that were reported in White and Piesciorovsky (2009) was used to estimate the power loss ratio (three phase AC power loss / single phase DC power loss) for the three phase bus bar configurations of Chapter 5.

M-file

```
function Rratio = Skin_Effect_Three_Phase(u)

    % Function to determine the ratio of Rac/Rdc for rectangular, solid bus
    % bars of a three phase system.  This calculation follows the procedure
    % developed by PeterSilvester in
    % Modern Electromagnetic Fields, Prentice Hall 1968
    % Library of Congress # 68-11272
    % Better coverage of the calculation is provided by Sergio L. M.
    % Berleze     % and Rene Robert in "Skin and Proximity Effects in
    % Nonmagnetic Conductors" which is contained in IEEE Transactions on
    % Education, Vol. 46, No. 3, August 2003, pp. 368-372.  Particularly
    % notable is that Berleze and Robert cover a constraint on current
    % density that is not mentioned by Silvester.

    h     = u(01);            % h   = conductor height in meters
    w     = u(02);            % w   = conductor width in meters
    rho   = u(03);            % rho = conductor resistivity in ohm - meters
    f     = u(04);            % f   = electrical supply frequency - Hz.
    n     = u(05);            % n   = min. number of small side divisions
    nph   = u(06);            % nph = number of conductors per phase
    Px    = u(07);            % Px  = horizontal separration of bars of the
                              %       same phase - m
    Py    = u(08);            % Py  = vertical separration of bars of the
                              %       same phase - m
    Sx    = u(09);            % Sx  = horizontal separation of phases - m
    Sy    = u(10);            % Sy  = vertical separation of phases - m
    muo   = 4 * pi * 1.0e-7;  % muo = permeability of free space - Henry/m

    % Remove previously used arrays
    clear xmat G IK H J sumH

    % Determine the number of divisions

    ratio = h/w;
    if ratio < 1
        ratio = 1/ratio;
        long  = 'w';
        big   = w;
        small = h;
    else
        long  = 'h';
        big   = h;
        small = w;
    end
    fract = rem(big,small)/small;
    if abs(fract) < 1.0e-3
        ns = n;
        nb = round(ns*ratio);
    else
        ns = round(1/fract);
```

```
        nb = round(ns*ratio);
        while ns < n
            ns = 2 * ns;
            nb = round(ns*ratio);
        end
    end
    if long == 'w'
        nw = nb;
        nh = ns;
    else
        nw = ns;
        nh = nb;
    end
    dh     = h/nh;
    dw     = w/nw;
    % nw = number of vertical divisions
    % nh = number of horizontal divisions
    % Each current element is a square of side = h/nh = w/nw

%**************************************************************************
%   Determine overall dimensions ***************************************
%   Define phaseH = Vertical distance between phases
    phaseH = 0.0;
    if Sy ~= 0.0
        phaseH = h+Sy;
    end
    if Py ~= 0.0
        phaseH = phaseH + (nph-1)*(h+Py);
    end
%   Define condH = Vertical distance between conductors of the same phase
    condH = 0.0;
    if Py ~= 0.0
        condH = h + Py;
    end
%   Define phaseW = Horizontal distance between phases
    phaseW = 0.0;
    if Sx ~= 0.0
        phaseW = w+Sx;
    end
    if Px ~= 0.0
        phaseW = phaseW + (nph-1)*(w+Px);
    end
%   Define condW = Horizontal distance between conductors of the same phase
    condW = 0.0;
    if Px ~= 0.0
        condW = w + Px;
    end
%**************************************************************************

    % Build the X matrix and the G vector
    % The conductor current is chosen as 1 amp
    coef  = 2 * pi * f * muo * dh * dw / (2 * pi * rho);
    matdim = nw*nh*3*nph;
%   nw
%   nh
    count  = 0;
    for iph = 1:3              % loop on the number of phases
        for ic = 1:nph         % loop on the number of conductors per phase
            for i = 1:nh       % loop on the number of horizontal rows
                y = (i-1+0.5)*dh + (ic-1)*condH + (iph-1)*phaseH; %y coord.
                for p = 1:nw   % loop on the number of elements in a row
                    count = count + 1;      % current row of matrix
                    x = (p-1+0.5)*dw+(ic-1)*condW+(iph-1)*phaseW; %x coord.
                    uarg = [dw dh]';
                    xmat(count,count) = coef*log(GMDrs(uarg));
 %                  disp([iph ic i p count]);
                    G(count) = exp(j*(iph-1)*2*pi/3)/(h*w*nph);
                    kount = count-1;
                    for jph = iph:3      % loop on the number of phases
                        jcstart = ic;    % determine starting conductor
                        if jph > iph
                            jcstart = 1;
```

```
                        end
                        for jc = jcstart:nph % loop on # of cond. per phase
                            kstart = 1;
                            if jph == iph
                                if jc == jcstart
                                    kstart = i;
                                end
                            end
                            for k = kstart:nh
                                yn = (k-1+0.5)*dh + (jc-1)*condH +...
                                     (jph-1)*phaseH;
                                qstart = 1;
                                if k == kstart
                                    if jph == iph
                                        if jc == jcstart
                                            qstart = p;
                                        end
                                    end
                                end
                                for q = qstart:nw
                                    kount = kount+1;
                                    xn = (q-1+0.5)*dw + (jc-1)*condW + ...
                                         (jph-1)*phaseW;
                                    if count ~= kount
%                                       disp([jph jc k q count kount]);
                                        U  = [dw dh x y dw dh xn yn]';
                                        xmat(count,kount)=...
                                                          coef*log(GMD2r(U));
                                        xmat(kount,count)=...
                                                           xmat(count,kount);
                                    end
                                end
                            end
                        end
                    end
                end
            end
        end
    end

    % Impose the constraint that the current densities add up to the total
    % current.
    ncd    = nw*nh;
    IK     = eye(matdim)-j*xmat;
    H      = inv(IK);
%   xmat
%   G
    for iph = 1:3
        iref = (iph-1) * nph * ncd;
        for ic = 1:nph
            iref = iref + (ic-1)*ncd;
            for jph = 1:3
                jref = (jph-1) * nph * ncd;
                for jc = 1:nph
                    jref = jref + (jc-1)*ncd;
                    sum    = 0 + j*0;
                    for p  = 1:ncd
                        for q = 1:ncd
                            sum = sum + H(p+iref,q+jref);
                        end
                    end
                    sumH((iph-1)*nph+ic,(jph-1)*nph+jc) = sum;
                end
            end
            IT((iph-1)*nph+ic) = 1/nph*exp(j*(iph-1)*2*pi/3);
        end
    end
%   sumH
    for iph = 1:3
        iref = (iph-1)*nph;
        for jph = 1:3
            jref = (jph-1)*nph;
```

```
            sum  = 0 + j*0;
            sumI = 0 + j*0;
            for p = 1:nph
                for q = 1:nph
                    sum = sum + sumH(iref+p,jref+q);
                end
                sumI = sumI + IT(iref+p);
            end
            HT(iph,jph) = sum;
        end
        Isum(iph) = sumI;
    end
    C = inv(HT)*Isum'/(dw*dh);
    for iph = 1:3
        iref = (iph-1) * nph * ncd;
        for ic = 1:nph
            iref = iref + (ic-1)*ncd;
            for p = 1:ncd
%               G(iref+p) = G(iref+p)*C((iph-1)*nph+ic)*h*w;
                G(iref+p) = C(iph);
            end
        end
    end
    % Determine the real and imaginary parts of the current density
    J      = H*G';
    % Determine the losses per unit length of conductor
    % Because current = 1 amp, the losses per unit length are numerically
    % equal to the AC resistance.
    Losses = 0.0;
    dArea  = dh  * dw;
    coef1  = rho * dArea;
    for i = 1:matdim
        Losses = Losses + coef1 * (real(J(i))^2 + imag(J(i))^2);
    end
    rDC = rho/(h*w*nph);        % DC resistance - ohms/meter

    Rratio = Losses / rDC;
end

%*************************************************************************

function gmdr =GMD2r(u)
    % function to compute the GMD between two rectangles
    % The formula comes from "Formulas for the Geometric Mean Distances
    % of Rectangular Areas and of Line Segments," by Thomas James Higgins
    % Journal of Applied Physics, Vol. 14, April, 1943 pp. 188 - 195
    r    = u(1);    % width of first rectangle
    s    = u(2);    % height of first rectangle
    x1   = u(3);    % x coordinate (horizontal) of first rectangle center
    y1   = u(4);    % y coordinate (vertical) of first rectangle center
    R    = u(5);    % width of second rectangle
    S    = u(6);    % height of second rectangle
    x2   = u(7);    % x coordinate (horizontal) of second rectangle center
    y2   = u(8);    % y coordinate (vertical) of second rectangle center
    if x1 == x2
        D = -(r+R)/2;
      else
        if x2 > x1
            D = x2-R/2-x1-r/2;
          else
%           D = x2+R/2-x1-r/2;
            D = x1-r/2-x2-R/2;
        end
    end
    if y1 == y2
        P = -(s+S)/2;
      else
        if y2 > y1
            P = y2-S/2-y1-s/2;
          else
%           P = y2+S/2-y1-s/2;
            P = y1-s/2-y2-S/2;
```

```
        end
    end

%     D    = x2 - R/2 - x1 - r/2; % distance from first conductor right side
%                                 % to second conductor left side along the x
%                                 % axis
%     P    = y2 - S/2 - y1 - s/2; % distance from first conductor top side
%                                 % to second conductor bottom side along the
%                                 % y axis
    A    = [abs(D+R+r) abs(D+R) abs(D) abs(D+r)];   % array needed for calc
    B    = [abs(P+S+s) abs(P+S) abs(P) abs(P+s)];   % array needed for calc
    sum  = 0;
    for i = 1:4
        for j = 1:4
            sum = sum + (-1)^(i+j)*Kcrunch(A(i),B(j));
        end
    end
    logr = (-(25/12)*R*S*r*s - sum/24)/(R*S*r*s);
    gmdr = exp(logr);
end

%*************************************************************************

function r = GMDrs(u)
    % Function to compute the geometric mean distance (GMD) of a rectangle
    % with itself
    % Formula comes from page 302 of "The Theory and Practice of Absolute
    % Measurements in Electricity and Magnetism," Volume II,
    % Macmillian and Co., 1893
    w    = u(1);        % width of rectangle
    h    = u(2);        % height of rectangle
    logr = log(w^2 + h^2)/2 -(h^2/w^2*log(1+w^2/h^2)+...
           w^2/h^2*log(1+h^2/w^2))/12 + 2*(h/w*atan(w/h)+...
           w/h*atan(h/w))/3 -25/12;
    r    = exp(logr);   % r = geometric mean distance (w and h units)
end
```